



University of Kentucky
UKnowledge

University of Kentucky Doctoral Dissertations

Graduate School

2008

ZINC DEFICIENCY AND MECHANISMS OF ENDOTHELIAL CELL DYSFUNCTION

Huiyun Shen

University of Kentucky, huiyun@gmail.com

[Right click to open a feedback form in a new tab to let us know how this document benefits you.](#)

Recommended Citation

Shen, Huiyun, "ZINC DEFICIENCY AND MECHANISMS OF ENDOTHELIAL CELL DYSFUNCTION" (2008).
University of Kentucky Doctoral Dissertations. 610.
https://uknowledge.uky.edu/gradschool_diss/610

This Dissertation is brought to you for free and open access by the Graduate School at UKnowledge. It has been accepted for inclusion in University of Kentucky Doctoral Dissertations by an authorized administrator of UKnowledge. For more information, please contact UKnowledge@lsv.uky.edu.

ABSTRACT OF DISSERTATION

Huiyun Shen, MS

The Graduate School
University of Kentucky
2008

ZINC DEFICIENCY AND MECHANISMS OF ENDOTHELIAL CELL
DYSFUNCTION

ABSTRACT OF DISSERTATION

A dissertation submitted in partial fulfillment of the requirements for
the degree of Doctor of Philosophy at the Graduate Center for
Toxicology at the University of Kentucky

By
Huiyun Shen, MS
Lexington, Kentucky

Advisor: Dr. Bernhard Hennig, Professor of Nutrition and Toxicology
Lexington, Kentucky
2008

Copyright © Huiyun Shen 2008

ABSTRACT OF DISSERTATION

ZINC DEFICIENCY AND MECHANISMS OF ENDOTHELIAL CELL DYSFUNCTION

Atherosclerosis is a chronic inflammatory disease thought to be initiated by endothelial cell dysfunction. Research described in this dissertation is focused on the role of zinc deficiency in endothelial cell activation with an emphasis on the function of the transcription factors nuclear factor- κ B (NF- κ B), peroxisome proliferator activated receptor (PPAR), and the aryl hydrocarbon receptor (AhR), which all play critical roles in the early pathology of atherosclerosis. Cultured porcine aortic vascular endothelial cells were deprived of zinc by the zinc chelator TPEN and/or treated with the NF- κ B inhibitor CAPE or the PPAR γ agonist rosiglitazone, followed by measurements of PPAR α expression, cellular oxidative stress, NF- κ B and PPAR DNA binding, COX-2 and E-selectin expression, and monocyte adhesion. Cellular labile zinc deficiency increased oxidative stress and NF- κ B DNA binding activity, and induced COX-2 and E-selectin gene expression, as well as monocyte adhesion in endothelial cells. CAPE significantly reduced the zinc deficiency-induced COX-2 expression, suggesting regulation through NF- κ B signaling. PPAR can inhibit NF- κ B signaling. Zinc deficiency down-regulated PPAR α expression and PPAR DNA binding activity in endothelial cells. Zinc deficiency compromised PPAR γ transactivation activity in PPAR γ and PPARE co-transfected rat aortic vascular smooth muscle cells. Furthermore, rosiglitazone was unable to inhibit the adhesion of monocytes to endothelial cells during zinc deficiency. Most of these effects of zinc deficiency could be reversed by zinc supplementation. An *in vivo* study utilizing the atherogenic LDL-R^{-/-} mouse model generally supported the importance of PPAR dysregulation during zinc deficiency. LDL-R^{-/-} mice were maintained for four weeks on either zinc deficient or zinc adequate diets. Half of the mice within each zinc group were gavaged daily with rosiglitazone during the last stage of the study. Selected inflammation and lipid parameters were measured. The anti-inflammatory properties of rosiglitazone were compromised during zinc deficiency. Specifically, rosiglitazone induced inflammatory genes (MCP-1) in abdominal aorta only during zinc deficiency, and adequate zinc was required for rosiglitazone to down-regulate pro-inflammatory markers such as iNOS in abdominal aorta of the mice. Rosiglitazone significantly up-regulated liver I κ B α protein expression only in zinc adequate mice.

Plasma data also suggest an overall pro-inflammatory environment during zinc deficiency and support the concept that zinc is required for proper anti-inflammatory or protective functions of PPAR. Zinc deficiency also altered PPAR-regulated lipid metabolism in LDL-R^{-/-} mice. Specifically, zinc deficiency increased plasma total cholesterol, and non-HDL (VLDL, IDL and LDL)-cholesterol. Plasma total fatty acids tended to be increased during zinc deficiency, and rosiglitazone treatment resulted in similar changes in fatty acid profile in zinc deficient mice. FAT/CD36 expression in abdominal aorta was upregulated by rosiglitazone only in zinc-deficient mice. In contrast, rosiglitazone treatment markedly increased LPL expression only in zinc-adequate mice. These data suggest that in this atherogenic mouse model treated with rosiglitazone, lipid metabolism can be compromised during zinc deficiency. AhR is another transcription factor involved in the development and homeostasis of the cardiovascular system. Cultured porcine aortic endothelial cells were exposed to the AhR ligands PCB77 or beta-naphthoflavone (β -NF) alone or in combination with the zinc chelator TPEN, followed by measurements of the AhR responsive cytochrome P450 enzymes CYP1A1 and 1B1. Zinc deficiency significantly reduced PCB77- induced CYP1A1 activity and mRNA expression, as well as PCB77 or β -NF-induced CYP1A1 protein expression, which could be restored by zinc supplementation. These data suggest that adequate zinc is required for the activation of the AhR-CYP1A1 pathway. Impairment of the AhR pathway presents an additional mechanism by which zinc deficiency negatively affects transcription factor function and homeostasis of the vascular system. Taken together, zinc nutrition can markedly modulate the pathogenesis of inflammatory diseases such as atherosclerosis.

KEYWORDS: atherosclerosis, zinc deficiency, NF- κ B, PPAR, AhR

Huiyun Shen

Student's Signature

04-22-2008

Date

ZINC DEFICIENCY AND MECHANISMS OF ENDOTHELIAL CELL
DYSFUNCTION

By

Huiyun Shen, MS

Bernhard Hennig

Director of Dissertation

David Orren

Director of Graduate Studies

04-22-2008

Date

DISSERTATION

Huiyun Shen, MS

The Graduate School
University of Kentucky
2008

ZINC DEFICIENCY AND MECHANISMS OF ENDOTHELIAL CELL
DYSFUNCTION

DISSERTATION

A dissertation submitted in partial fulfillment of the requirements for
the degree of Doctor of Philosophy at the Graduate Center for
Toxicology at the University of Kentucky

By
Huiyun Shen, MS
Lexington, Kentucky

Advisor: Dr. Bernhard Hennig, Professor of Nutrition and Toxicology
Lexington, Kentucky
2008

Copyright © Huiyun Shen 2008

TO MY MOTHER

ACKNOWLEDGEMENTS

I would like to thank the key figures that guided me throughout my last five years as a graduate student at the University of Kentucky. Most of all, I thank my advisor, Dr. Bernhard Hennig, who provided me with a great environment for completing and enjoying my training as a Ph.D. student. He not only gave advice and support in research and academic matters but was also considerate and supportive in “extramural” issues.

I would also like to express my gratitude to all my Ph.D. committee members, Dr. Lisa Cassis, Dr. Michael Kilgore, Dr. Michal Toborek, Dr. Mary Vore, and Dr. Haining Zhu, who were all very generous in sharing their expertise and providing support to any research related issue I had during my time as a graduate student.

Special thanks also go to Dr. Ruth MacDonald at Iowa State University. She is our collaborator in the project investigating the effect of zinc deficiency on PPAR function and early events of atherosclerosis in mice.

In addition, I would like to thank those individuals who contributed to the research projects I have been working on. Most of them are represented as coauthors or acknowledged in my research publications: Dr. Dennis Bruemmer, Dr. Arnold Stromberg, Dr. Alan Daugherty, Dr. Xiang-an Li, Dr. Thomas Mawhinney, Dr. Xabier Arzuaga, Elizabeth Heywood, Jessica Moorleghen, Elizabeth Oesterling, Joseph Przybyszewski, Dr. Sandor Sipka, Jason Stevens, and Dr. Lei Wang. Many thanks go to Dr. Zhongwen Xie, Dr. Hong Pu, Dr. SungYong Eum, and my other laboratory coworkers as well.

Last but not least I would like to acknowledge the support of my family, in particular my mother Yanfang as well as my fiancé Jiukun Dai. Despite the long distance they played an important and very valuable part in my time at the University of Kentucky.

The research reported in this dissertation was supported in part by grants from NIEHS/NIH (P42ES 07380, P20RR 16481), USDA/NRI (2001-01054), National Cattlemen’s Beef Association, Kentucky Cattlemen’s Association and the Kentucky Agricultural Experimental Station.

TABLE OF CONTENTS

Acknowledgements.....	iii
Table of Contents.....	iv
List of Tables.....	vi
List of Figures.....	vii
Chaper 1. Introduction.....	1
1.1 Background.....	1
1.2 General Hypothesis and Specific Aims.....	11
Chaper 2. Compromised Anti-inflammatory Responses and Intensified Pro-inflammatory Responses in Vascular Endothelial Cells during Zn Deficiency.....	13
2.1 Synopsis.....	13
2.2 Introduction.....	14
2.3 Materials and Methods.....	15
2.4 Results.....	19
2.5 Discussion.....	21
Chaper 3. Zinc Deficiency Alters Pro-inflammatory and Anti-inflammatory Responses in LDL-Receptor-Deficient Mice Treated with Rosiglitazone.....	35
3.1 Synopsis.....	35
3.2 Introduction.....	36
3.3 Materials and Methods.....	37
3.4 Results.....	41
3.5 Discussion.....	43
Chaper 4. Zinc Deficiency Alters Lipid Metabolism in LDL-Receptor-Deficient Mice Treated with Rosiglitazone.....	60
4.1 Synopsis.....	60
4.2 Introduction.....	60
4.3 Materials and Methods.....	62
4.4 Results.....	64
4.5 Discussion.....	65
Chaper 5. Zinc Nutritional Status Modulates Expression of AhR-Responsive P450 Enzymes in Vascular Endothelial Cells.....	75

5.1	Synopsis	75
5.2	Introduction.....	75
5.3	Materials and Methods.....	77
5.4	Results.....	79
5.5	Discussion.....	80
Chaper 6. Conclusion.....		86
Appendix.....		94
Methods.....		94
Additional data.....		110
References.....		117
Vita.....		131

LIST OF TABLES

Table 3.1. Experimental diets	48
Table 3.2. Effects of dietary zinc status and rosiglitazone on selected plasma anti-inflammatory cytokine concentrations in LDL-R ^{-/-} mice	49
Table 3.3. Effects of dietary zinc status and rosiglitazone on selected plasma pro-inflammatory cytokine/chemokine concentrations in LDL-R ^{-/-} mice	50
Table 4.1. Effects of dietary zinc status and rosiglitazone on plasma glucose, insulin, and adiponectin concentrations in LDL-R ^{-/-} mice	69
Table 4.2. Effects of dietary zinc status and rosiglitazone on plasma total and individual fatty acid concentrations in LDL-R ^{-/-} mice	70

LIST OF FIGURES

Figure 1.1. The anti-inflammatory properties of PPAR α and γ	12
Figure 2.1. Zinc deficiency increases cellular oxidative stress in endothelial cells.	25
Figure 2.2. Zinc deficiency increases NF- κ B DNA binding activity in endothelial cells. 26	
Figure 2.3. Zn deficiency induces COX-2 (A) and E-selectin (B) mRNA expression in endothelial cells.	27
Figure 2.4. Zinc deficiency-induced COX-2 protein expression in endothelial cells is partially reduced during inhibition of NF- κ B activation.	29
Figure 2.5. Zn deficiency decreases PPAR α expression in endothelial cells.	30
Figure 2.6. Zn deficiency decreases PPAR DNA binding activity in endothelial cells.	32
Figure 2.7. Zinc deficiency increases monocyte adhesion to endothelial cells and blocks the inhibitory effect of rosiglitazone on monocyte adhesion.	33
Figure 2.8. Effect of zinc status on rosiglitazone-induced PPAR γ transactivation in PPAR γ and PPRE co-transfected RAVSMC.	34
Figure 3.1. Treatment of the LDL-R ^{-/-} mice.	51
Figure 3.2. Body weight changes of the LDL-R ^{-/-} mice.	52
Figure 3.3. Effects of dietary zinc status and rosiglitazone on plasma and liver zinc levels in LDL-R ^{-/-} mice.	53
Figure 3.4. Effects of dietary zinc status and rosiglitazone on iNOS (A) and MCP-1 (B) gene expression in LDL-R ^{-/-} mice.	54
Figure 3.5. Effects of dietary zinc status and rosiglitazone on I κ B α protein expression in LDL-R ^{-/-} mice	56
Figure 3.6. Effects of dietary zinc status and rosiglitazone on NF- κ B (A) and PPAR (B) DNA binding activities in LDL-R ^{-/-} mice.	57
Figure 3.7. Proposed mechanism of pro-inflammatory environment and endothelial cell activation during zinc deficiency.	59
Figure 4.1. Effects of dietary zinc status and rosiglitazone on plasma total cholesterol concentration in LDL-R ^{-/-} mice.	71
Figure 4.2. Effects of dietary zinc status and rosiglitazone on cholesterol distribution in different lipoprotein fractions in LDL-R ^{-/-} mice.	72

Figure 4.3. Effects of dietary zinc status and rosiglitazone on LPL and CD36 gene expression in LDL-R ^{-/-} mice.	74
Figure 5.1. Zinc deficiency reduces PCB77-induced CYP1A activity and CYP1A1 mRNA expression in vascular endothelial cells.	83
Figure 5.2. Zinc deficiency compromises PCB77-induced CYP1A1 and CYP1B1 protein expression in vascular endothelial cells.....	84
Figure 5.3. Zinc deficiency compromises β-naphthoflavone-induced CYP1A1 protein expression in vascular endothelial cells.....	85
Figure 6.1. Crosstalk between the NF-κB, PPAR, and AhR pathways during zinc deficiency.....	93

Chaper 1. Introduction

1.1 Background

1.1.1 Atherosclerosis/Inflammation

Atherosclerosis, a progressive disease of large arteries, is one of the most common underlying causes of death in western countries, accounting for about 50 % of all deaths [1, 2]. Atherosclerosis is a chronic inflammatory condition that results from interaction between modified lipoproteins, monocyte/macrophages, T lymphocytes, and the normal cellular components of the arterial wall such as endothelial cells, and smooth muscle cells. This inflammatory process can lead to the development of complex lesions, or fibrous plaques, which protrude into the arterial lumen and narrow the vessel. Plaque rupture results in the formation of thrombus and the subsequent acute clinical events of myocardial infarction and stroke [1, 2]. Atherosclerosis is associated with endothelial cell dysfunction and apoptosis [3]. The vascular endothelium, with its intercellular tight junctions, functions as a selectively permeable barrier between blood and tissues. It also plays important roles in the physiological and pathological processes of vessels via both sensory and executive functions. By generating effector molecules, the endothelium regulates vascular tone, inflammation, thrombosis, and vascular remodeling [2]. Epidemiological studies have revealed multiple risk factors for atherosclerosis, including factors with a strong genetic component, and environmental factors, such as lifestyle and nutritional factors [1-3].

1.1.2 Zinc deficiency

Zinc deficiency has been identified as a risk factor for atherosclerosis [3, 4]. As a frequent condition in human populations, zinc deficiency affects about one third of the world's population and contributes to 1.4 % of all deaths worldwide [3, 4]. Although acute zinc deficiency is rare nowadays in industrialized countries, marginal zinc deficiency is still relatively common [3]. Zinc deficiency can happen when zinc intake is inadequate or zinc is poorly absorbed, when zinc loss from the body is increased, or when the body's requirement for zinc increases [4]. Some dietary factors, which are present

mainly in vegetable products, such as phytates (including inositol hexaphosphates and pentaphosphates), can strongly inhibit zinc absorption [5]. Certain disease states, like diabetes and alcoholism, can increase urinary loss of zinc and are thus responsible for the total body zinc decrease [4, 6]. Other physiological and pathological conditions, such as reproduction, rapid growth, and acute inflammation, all increase the organism's demand for zinc and will lead to zinc deficiency if the demand is not fulfilled [4, 7]. Symptoms of zinc deficiency include growth retardation, delayed sexual maturation, immune dysfunction, delayed wound healing, diarrhea, dermatitis, pregnancy complications, behavioral abnormalities and eye lesions [4, 8].

1.1.3 Zinc physiology

Zinc plays multiple important functions in biological systems. As a component of biomembrane, zinc is distributed among the major membrane protein fractions and is critical for membrane structural integrity and stability [9, 10]. Membrane-bound zinc can regulate activities of membrane-bound enzymes, protect biomembrane against lipid peroxidation, and constitute a pool of rapidly available zinc [4, 9]. Zinc is also necessary for maintaining normal cytoskeletal structure [4]. Furthermore, zinc plays structural and catalytical roles in hundreds of enzymes and thousands of "zinc-finger" protein domains [11]. Zinc has antioxidant functions in that it 1) stabilizes macromolecules against radical-induced oxidation; 2) competes with pro-oxidant metals (iron and copper) for binding sites, thus decreasing their ability to form free radicals; 3) inhibits excess production of free radicals by biological systems; 4) is an essential part of the intracellular and extracellular antioxidant enzyme superoxide dismutase (SOD), and 5) induces the potent antioxidant metallothionein, which is an efficient hydroxyl radical scavenger [4, 11-13]. In addition, zinc-protein interactions have been found to regulate signal transduction [4, 11].

Most intracellular zinc is bound to structural and/or regulatory proteins such as metallothionein, resulting in very low concentrations of metabolic active (labile) zinc, estimated at picomolar to nanomolar range [14]. Cellular zinc homeostasis is tightly regulated by the levels of zinc uptake, cellular storage, trafficking, and elimination [11,

14]. There are basically two categories of membrane zinc transporters involved in zinc uptake and elimination: Zip (Zrt- and Irt-like proteins (SLC39A)) and ZnT (solute-linked carrier 30 (SLC30A)). Zip transporters mediate extracellular zinc uptake and intracellular vesicle zinc release into the cytoplasm, therefore increasing intracellular zinc, while ZnT transporters promote zinc efflux from cells to extracellular space or into intracellular vesicles, thereby lowering intracellular zinc [15, 16]. The mechanisms of Zip and ZnT mediated zinc transport are not well understood. Zip-mediated zinc uptake could be a process of facilitated diffusion driven by a zinc concentration gradient. ZnT transporters could function as secondary active transporters or antiporters since cellular extrusion of zinc and vesicular zinc deposition occur against a zinc concentration gradient [16]. Coordination of intracellular zinc storage and trafficking mainly depends on the cysteine-rich protein metallothionein. Metallothionein is an intracellular transition metal binding protein that is critical for regulation of homeostasis of essential metals such as zinc and copper, and detoxification of heavy metals such as cadmium [17]. Metallothioneins provide intracellular zinc binding sites with one metallothionein molecule capable of binding totally seven Zn^{2+} atoms, with the metal detoxification related α domain binding four Zn^{2+} atoms via 11 cysteines and the physiologically relevant β domain binding three Zn^{2+} atoms via 9 cysteines [16, 18]. Behaving as zinc chaperones, metallothioneins play a donor/acceptor role for zinc-binding motifs in metalloproteins, such as various metalloenzymes and transcription factors, thereby can activate or deactivate them [14, 16]. Furthermore, metallothioneins play an important role in protecting against cellular stressors, such as carbon-centered radicals, reactive oxygen species (ROS), and reactive nitrogen species (RNS) [16]. As free radical scavengers, metallothioneins can efficiently scavenge most types of ROS, including hydroxyl radical ($\cdot OH$), superoxide ($O_2^{\cdot -}$), hydrogen peroxide (H_2O_2), peroxyxynitrite ($ONOO^-$) and nitric oxide (NO) [19, 20]. Despite the high affinity of metallothionein for zinc, the metal can be released from and rebind to the protein, which is regulated by cellular redox state (the so called “metallothionein redox cycle”). Specifically, oxidation of the thiolate cluster of metallothionein by various cellular oxidants can release zinc from metallothionein, forming metallothionein-disulfide, which in turn can be reduced by cellular reducing agents, such as glutathione, thereby restoring zinc binding to the protein

and reconstitute metallothionein. In general, the thermodynamically stable zinc binding makes metallothionein an ideal intracellular zinc reservoir, and the redox regulation of zinc mobilization enables metallothionein to maintain cellular zinc homeostasis [17].

1.1.4 Zinc and redox signaling

The unique chemical nature of zinc determines its central position in the cellular redox signaling network. Zinc by itself is redox inert but it can create a redox active environment when binding to a sulfur ligand. Oxidation of the sulfur ligand mobilizes zinc, while reduction of the oxidized ligand promotes zinc binding. Thus the reversible oxidation of the sulfur ligand is coupled to the reversible zinc release from the protein, providing redox control over zinc availability. These cysteine-rich zinc binding proteins are thereby called “redox zinc switches” that are controlled by concentrations of both oxidants and zinc [14, 18]. Some of these protein “redox zinc switches” are redox sensors, in which zinc release is coupled to protein conformational changes that affect enzymatic activity, molecular chaperone activity, and binding interactions, with no known function of the released zinc. Other protein “redox zinc switches” are redox transducers, in which redox signals are converted to zinc signals via binding of the released zinc to other proteins and modulating signal transduction, metabolic energy generation, mitochondrial function, and gene expression. Metallothionein is one example of such redox transducers, which, together with its apoprotein, thionein, functions to control zinc availability, redistribute cellular zinc, and interconvert redox and zinc signals [18]. To maintain redox homeostasis, it is essential to keep tight control of zinc availability, because both inadequate and excessive cellular zinc will elicit oxidative stress [18].

Cellular labile zinc deficiency leads to a condition of oxidative stress [4]. A low zinc status alters the expression and activity of anti-oxidant enzymes and other components of the biological oxidant defense system. In addition, zinc deficiency rapidly increases cellular global oxidants, including ROS and RNS, which will lead to tissue oxidative damage, increasing DNA, protein, and lipid oxidation. The mechanisms of zinc deficiency-induced oxidative stress are not clear. Possible mechanisms could be 1)

compromised roles of zinc as a physiological antioxidant, 2) impaired mitochondrial function that increases ROS formation, possibly by altered expression of certain respiratory chain components, and 3) altered expression and/or activity of ROS/RNS metabolizing enzymes [4]. On the other hand, excessive zinc that overwhelms the buffering capacity of the cellular zinc homeostasis system also induces oxidative stress by increasing mitochondrial ROS generation, etc. [18]. Therefore, zinc exhibits antioxidant properties only in an intermediate range of physiological and possibly also pharmacological concentrations [18].

1.1.5 Zinc deficiency and cell signaling

Zinc deficiency-induced oxidative stress affects cell signaling, including zinc finger transcription factors, such as peroxisome proliferator activated receptors (PPARs), and other oxidative stress sensitive transcription factors, such as activator protein-1 (AP-1) and nuclear factor- κ B (NF- κ B) [4, 18]. Oxidative stress impairs the DNA-binding activity of zinc finger transcription factors by oxidizing the thiol groups in cysteine residues, which coordinate zinc in the reduced form, followed by alteration of the secondary structure of the transcription factor proteins. In this way, oxidative stress can reduce transcription of genes regulated by zinc finger transcription factors [4]. The PPARs are ligand-activated transcription factors belonging to the steroid/thyroid hormone nuclear receptor superfamily [21, 22]. PPARs regulate the expression of genes involved in lipid and glucose homeostasis, inflammatory response, and cell differentiation [21, 23]. There are three isotypes of PPAR: PPAR α , PPAR β/δ , and PPAR γ [21]. Upon ligand binding, PPAR heterodimerizes with another nuclear receptor retinoid X receptor (RXR) and binds to peroxisome proliferators response elements (PPREs) located in the promoter regions of PPAR regulated genes and transactivates these genes [21, 23]. Since both PPAR and RXR have two zinc fingers in their DNA binding domains [22, 24], zinc deficiency could impair the DNA binding and transactivation activities of the PPAR:RXR transcription factor complex. There is evidence that zinc deficiency can compromise PPAR α and γ signaling in vascular endothelial cells [25, 26].

Zinc deficiency-induced oxidative stress activates AP-1, mainly through activation of the stress-responsive mitogen-activated protein kinases (MAPKs) JNK and p38 [4]. The effect of zinc-deficiency on NF- κ B activation is cell line specific. Earlier work in our lab has shown that zinc-deficiency can increase NF- κ B DNA binding activity in porcine vascular endothelial cells compared to zinc-adequate cells [10]. Similar observations were obtained in mast cells and mononuclear cells as well [27, 28]. However, in some other cell types, such as rat glioma C6 cells, human T-helper type-0 (Th₀) malignant lymphoblastoid HUT-78 cells, human neuroblastoma IMR-32 cells, and 3T3 fibroblasts, zinc deficiency has been described to decrease NF- κ B DNA binding activity [29-32]. Although the cytosolic events in NF- κ B signaling, i.e., I κ B α phosphorylation and subsequent ubiquitination and degradation, are activated by increased oxidative stress in the zinc deficient cells, zinc deficiency-induced tubulin depolymerization impairs translocation of the activated NF- κ B into the nucleus. This can result in inhibition of transactivation of NF- κ B regulated genes and thus may explain in part the inhibitory effects of zinc deficiency on NF- κ B activation [4, 30]. The reason for the cell specific effects of zinc deficiency on NF- κ B activity is not clear [3]. Since NF- κ B is the major transcription factor responsible for up-regulating pro-inflammatory genes, such as vascular adhesion molecules [33], it is necessary to investigate the influence of endothelial zinc status on the expression of adhesion molecules and other NF- κ B target genes. This type of study has not been reported so far and thereby becomes one focus of the current *in vitro* study utilizing vascular endothelial cells as the research model.

1.1.6 PPAR/TZD

PPARs have anti-inflammatory properties by negative cross-talk with major inflammatory pathways including NF- κ B, AP-1, nuclear factor of activated T cells (NFAT), signal transducer and activator of transcription-1 (STAT-1), and CAAT/enhancer binding protein β (C/EBP β) (Fig. 1.1) [21]. PPAR α can repress NF- κ B and AP-1 pathways via interactions with p65 subunit of NF- κ B and c-Jun of AP-1, respectively [34]. Similarly, PPAR γ can inhibit the NF- κ B pathway by physically

interacting with p50 and p65 subunits of NF- κ B [35]. PPAR α agonists, such as fibrates, induce I κ B α (an inhibitor of NF- κ B) expression, providing an additional mechanism for the inhibition of NF- κ B by PPAR α and the anti-inflammatory properties of PPAR α agonists [36]. PPAR γ agonists, such as troglitazone, a member of the thiazolidinedione (TZD) class, inhibit c-fos induction, which constitutes an additional mechanism for the inhibition of AP-1 by PPAR γ [37].

TZDs are synthetic PPAR γ ligands that have been clinically used to treat type II diabetes [38-40]. In addition to their metabolic effects of improving insulin sensitivity and glycemic control, TZDs have direct anti-atherogenic effects of increasing NO bioavailability, inhibiting leukocyte/endothelial cell interaction, repressing vascular smooth muscle cell proliferation and migration, and promoting macrophage cholesterol efflux [39]. Animal studies have shown that TZDs can decrease blood pressure, repress left ventricular hypertrophy and atherosclerotic lesion development, and protect the myocardium from ischemia/reperfusion injury [38]. TZDs have also been shown to affect surrogate markers of vascular disease, such as dyslipidemia, hypertension, microalbuminuria, visceral fat, levels of adiponectin, C-reactive protein (CRP), plasminogen activator inhibitor type I (PAI-I), and matrix metalloproteinases (MMPs), carotid intima-media thickness, coronary stent restenosis, and delay progression of atherosclerosis in different patient groups, including type II diabetic patients [39, 40]. The anti-atherogenic effects of TZDs can be due to their insulin-sensitizing anti-diabetic effects. Because TZDs decrease insulin resistance, they may also improve other insulin resistance associated abnormalities, thereby decrease the morbidity and mortality of cardiovascular diseases [38, 40]. On the other hand, by modulating gene expression in a wide variety of cells, TZDs can also benefit the cardiovascular system by means independent of their anti-diabetic effects [38]. Despite the favorable effects of TZDs on cardiovascular surrogate markers, adverse effects of TZDs, including weight gain, fluid retention (edema), and the potential to exacerbate or precipitate heart failure can considerably limit the use of TZDs, especially in heart failure patients [41]. Recent clinical trials suggest that treatment with TZDs increased the risk for development of congestive heart failure in prediabetic and type II diabetic patients [41, 42]. The effects of TZDs on overall cardiovascular outcome still await better-designed future study. The

effects of zinc nutritional status on the anti-inflammatory and anti-atherogenic properties of TZDs in an atherogenic animal model have not been studied. These questions are of particular interest to us and led to the current *in vivo* study utilizing the atherosclerosis prone LDL-receptor deficient (LDL-R^{-/-}) mouse model treated with the PPAR γ specific agonist rosiglitazone.

1.1.7 AhR/PCB

The effect of endothelial zinc status on the aryl hydrocarbon receptor (AhR) pathway is another focus of the research presented in this dissertation. AhR is a ligand-activated transcription factor which belongs to the Per-ARNT-Sim (PAS) family of basic-helix-loop-helix (bHLH) transcription factors [43]. AhR ligands include planar polycyclic and halogenated aromatic hydrocarbons, such as polychlorinated biphenyls (PCBs), and various classes of plant-derived chemicals [44, 45]. Prior to activation, AhR exists in the cytoplasm in association with heat shock protein (HSP)90, HSP90 accessory proteins, and immunophilin-like proteins such as XAP2/ARA9/AIP and p23 [45]. Ligand binding to the AhR promotes its dissociation from this chaperone complex and exposure of its nuclear localization signals, and its subsequent translocation to the nucleus where the ligand-activated AhR heterodimerizes with the aryl hydrocarbon nuclear translocator (ARNT) [46, 47]. The AhR:ARNT complexes then bind to the aryl hydrocarbon, xenobiotic, or dioxin response elements (AhREs, XREs, DREs) located in the promoter regions of target genes and transactivate the expression of a battery of genes involved in the metabolism (activation or detoxification) of endogenous and foreign compounds, oxidative stress response, cell cycle control, and apoptosis. These AhR-regulated genes are collectively called the AhR gene battery [44, 47, 48]. AhR-generated cellular oxidative stress responses can elicit metabolic events ranging from physiological to adaptive, and to toxicological processes. The mechanisms involved include 1) induction of genes associated with inflammation, such as tumor necrosis factor α (TNF α) and cyclooxygenase-2 (COX-2); 2) regulation of prooxidant and antioxidant enzymes that generate or detoxify ROS, such as xanthine oxidase/xanthine dehydrogenase (XO/XDH) and SOD; and 3) induction of cytochrome P450 enzymes, such as the CYP1

family [44]. P450s catalyze the monooxygenation of various endogenous and exogenous compounds and normally reduce diatomic oxygen to water efficiently with little release of ROS. However, when uncoupling of the P450-substrate complex with the NADPH-P450 oxidoreductase and/or cytochrome b₅ happens, the activated oxygen is released from the enzyme as either O₂^{•-}, or H₂O₂, or other forms of ROS without substrate modification [44, 48, 49]. In addition to the well characterized roles of the AhR in inducing Phase I and Phase II metabolizing enzymes and mediating xenobiotic signaling [45, 50], the AhR has recently been shown to be involved in multiple molecular cascades leading to the modulation of cell proliferation, differentiation, and apoptosis, thereby playing important regulatory roles in the development and homeostasis of various organ systems including the cardiovascular system [45, 47, 51, 52]. Although the DNA binding activity of AhR does not seem to require zinc [53], zinc deficiency can inhibit the DNA binding activity of SP1 [53], a zinc finger transcription factor that cooperates with AhR:ARNT in regulating CYP1A1 gene expression [54]. Since zinc plays multiple roles in maintaining homeostasis of the cardiovascular system [55] and is also required for normal cardiovascular development [56], it is intriguing to find out how zinc status could influence the AhR pathway. Little is known on how zinc nutritional status could modulate certain AhR ligands, such as the toxic environmental contaminants polychlorinated biphenyls (PCBs), and thus modulate a biological outcome in the cardiovascular system.

PCBs, a class of halogenated aromatic hydrocarbons with different numbers and positions of chlorine substitution on the biphenyl moiety, are widespread persistent organic environmental contaminants because of their chemical stability and previous extensive industrial use [57]. The use of PCBs has been banned in most countries since the late 1970s and the PCB levels in environmental samples are beginning to decline [57, 58]. PCBs are resistant to degradation by metabolism. Being lipophilic, they tend to bioaccumulate and biomagnify, and can be found at all levels of the food chain [57, 58]. PCBs have systemic toxicity in laboratory animals, wildlife species, and the human beings through activation of the AhR [59]. The major source of human exposure to PCBs is food [60]. The toxicological effects of PCBs on human health include endocrine disruption, immune dysfunction, defects in reproduction and neurological development,

as well as carcinogenesis [60]. PCBs can also contribute to the development of inflammatory diseases, such as atherosclerosis [61]. Coplanar PCBs, such as PCB 77, can cause endothelial cell dysfunction by disrupting endothelial barrier function, increasing cellular oxidative stress, activating NF- κ B, and mediating production of the inflammatory cytokine IL-6. As an AhR agonist, PCB 77 induces these inflammatory responses mostly via the AhR-CYP1A pathway [62].

In general, zinc has potent anti-inflammatory and anti-atherogenic properties. As an anti-oxidant, zinc can prevent the oxidative modifications of LDL thereby inhibit one of the main mechanisms of atherosclerosis [63]. Zinc can also modulate the activity of lipase. Zinc deficiency reduces the activity of lipoprotein lipase, which plays an important role in clearance of triglyceride-rich lipoproteins, and is correlated with increased serum triglycerides concentrations [64], which is a risk factor of atherosclerosis [65]. In addition, zinc participates in the regulation of blood pressure and in the pathogenesis of hypertension, and loss of zinc homeostasis can be the cause of high blood pressure. [66]. Zinc deficiency could thus constitute a risk factor for atherosclerosis by increasing LDL oxidation, elevating plasma triglycerides levels, and inducing hypertension [3, 4, 63]. Epidemiological studies have shown that low dietary zinc intake and low serum zinc levels are associated with an increased prevalence of coronary artery disease and its associated risk factors, such as hypertriglyceridemia and hypertension, in certain populations [67, 68]. Furthermore, significantly lower than control (normal aortas from subjects died in accidents or from causes other than atherosclerosis) concentrations of zinc were also found in atherosclerotic plaques of abdominal aorta in patients deceased with ischemic heart disease and acute myocardial infarction [69]. So far only a few molecular and cellular mechanisms have been proposed on how zinc deficiency could contribute to the pathogenesis of atherosclerosis, including activation of NF- κ B and related inflammatory responses, activation of caspase-mediated apoptosis, and changes in NO signaling [3]. It is important to further explore the mechanisms involved in zinc deficiency induced pro-inflammatory events in endothelial cells and the vascular system as well, and to clarify how these events can contribute to the development of atherosclerosis. The new findings described in this dissertation will add to the existing

knowledge of the micronutrient zinc and zinc-deficiency-related adverse effects on biological systems, especially the cardiovascular system, and will contribute to provide a scientific basis for the prevention of atherosclerosis by zinc nutritional intervention.

1.2 General Hypothesis and Specific Aims

The general hypothesis of the research described in this dissertation is that zinc deficiency can lead to endothelial cell inflammatory responses as well as pro-inflammatory events in whole animal through modulation of the NF- κ B, PPAR, and AhR signaling pathways. To test this hypothesis, the following specific aims were proposed:

Specific Aim 1: To test the hypothesis that zinc deficiency induces endothelial cell inflammation by activating the NF- κ B pathway and inhibiting the PPAR pathway.

Specific Aim 2: To test *in vivo* the hypotheses that zinc deficiency compromises proper PPAR γ function and alters PPAR γ -regulated inflammatory responses and lipid metabolism. The LDL-R^{-/-} mouse model was used to demonstrate the zinc-dependent anti-inflammatory properties and favorable lipid effects of rosiglitazone in early stages of atherosclerosis.

Specific Aim 3: To test the hypothesis that zinc deficiency can modulate PCB77-induced endothelial cell inflammation.

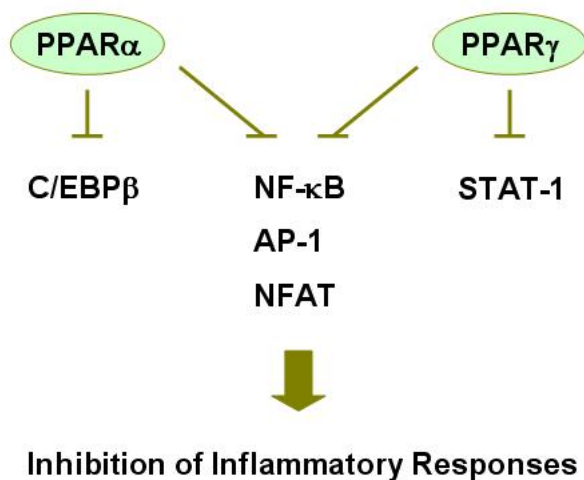


Figure 1.1. The anti-inflammatory properties of PPAR α and γ

By interfering with the major inflammatory pathways, such as NF- κ B, AP-1, NFAT, C/EBP β , and STAT-1, PPAR α and γ can inhibit the inflammatory responses. NF- κ B, nuclear factor- κ B; AP-1, activator protein-1; NFAT, nuclear factor of activated T cells; C/EBP β , CAAT/enhancer binding protein β ; STAT-1, signal transducer and activator of transcription-1 (adapted from Blanquart C, *J Steroid Biochem Mol Bio*, 2003. 85: 267-73).

Chaper 2. Compromised Anti-inflammatory Responses and Intensified Pro-inflammatory Responses in Vascular Endothelial Cells during Zn Deficiency

2.1 Synopsis

Zinc has anti-inflammatory properties and is crucial for the integrity of vascular endothelial cells. We have shown that zinc deficiency can increase cellular oxidative stress and subsequently activate NF- κ B. Mechanisms of endothelial cell inflammation during zinc deficiency are not well defined. The current study focuses on the hypothesis that during zinc deficiency, pro-inflammatory signaling pathways, such as NF- κ B, are activated; meanwhile anti-inflammatory signaling pathways, such as PPAR, are compromised. Porcine vascular endothelial cells were made zinc deficient by chelation with the membrane permeable zinc chelator TPEN. Zinc deficiency increased oxidative stress and NF- κ B DNA binding activity, and induced COX-2 and E-selectin gene expression, as well as monocyte adhesion in cultured endothelial cells. These changes were reversed by zinc supplementation to the endothelial cell cultures. The NF- κ B inhibitor caffeic acid phenethyl ester (CAPE) significantly reduced the zinc deficiency-induced COX-2 protein expression, suggesting regulation through NF- κ B signaling. PPAR can inhibit NF- κ B signaling. Zinc deficiency down-regulated PPAR α expression in cultured endothelial cells. PPAR DNA binding activity was also compromised during zinc deficiency. Furthermore, the PPAR γ agonist rosiglitazone was unable to inhibit the adhesion of monocytes to endothelial cells during zinc deficiency, an event which could be reversed by zinc supplementation. A transient transfection-luciferase assay confirmed that adequate zinc is required for rosiglitazone-induced PPAR γ activation to transactivate target genes. These data demonstrate the importance of zinc in proper PPAR function and the requirement of zinc to prevent inflammatory responses, suggesting that zinc deficiency might be involved in the pathogenesis of atherosclerosis.

2.2 Introduction

The development of atherosclerosis is of multiple causes and involves the interaction of genetics, lifestyle, nutrition and other environmental risk factors [1]. Atherosclerosis is believed to begin with endothelial cell activation or dysfunction, which is associated with a series of early changes that lead to fatty streak lesion formation. The changes include oxidative modifications of low density lipoprotein (LDL), up-regulation of endothelial adhesion molecules, recruitment of monocytes to the activated endothelium, accelerated migration of monocytes into the arterial wall, and differentiation of monocytes into macrophages; all events can lead to accelerated lesion progression and ultimately to plaque rupture and thrombosis [1]. There is evidence that zinc nutrition can modulate early phases of atherosclerosis [70].

As an essential trace element, zinc plays multiple roles in biological systems, including structural, catalytic, and regulatory functions [71, 72]. Zinc is required for the maintenance of the normal structure of membrane and cytoskeleton [4]. Zinc also plays both catalytic and structural roles in hundreds of enzymes and thousands of “zinc finger” protein domains. Through zinc/protein interactions, zinc also plays regulatory functions in cellular signaling, in the architecture of protein complexes, and in redox control [4, 11]. Cellular zinc homeostasis is maintained largely by membrane zinc transporters and by the intracellular zinc storage and trafficking protein metallothionein [11, 15, 16].

There is evidence showing that zinc deficiency is related to the pathogenesis of atherosclerosis. For example, low dietary zinc intake and low serum zinc levels were found to be associated with increased prevalence of coronary artery disease and its associated risk factors, such as hypertension and hypertriglyceridemia, in certain populations [67, 68]. In addition, lower concentrations of zinc were found in atherosclerotic plaques of abdominal aortas in deceased patients with ischemic heart disease and acute myocardial infarction compared with normal aortas [69]. The mechanisms of zinc deficiency in the development of atherosclerosis remain to be elucidated. Zinc may play a critical role as a potent antioxidant and anti-inflammatory agent [10, 28]. For example, zinc deficiency increases cellular oxidative stress [10, 31], and in turn activates oxidative stress-sensitive transcription factors such as NF- κ B and AP-1 in endothelial cells [10] and 3T3 cells [31], respectively.

Zinc has also been shown to modulate the function of PPARs [25, 26, 73]. PPARs are ligand-activated transcription factors that heterodimerize with RXR and bind to PPRE to regulate expression of genes involved in lipid and glucose metabolism, inflammatory response, and cellular differentiation [21]. There are three PPAR isoforms, i.e. PPAR α , PPAR β/δ , and PPAR γ and they are expressed in all major cell types of atherosclerotic lesions [74]. PPARs possess anti-inflammatory properties by inhibiting major pro-inflammatory pathways, such as NF- κ B and AP-1. In this way, PPARs modulate the expression of adhesion molecules as well as cytokines/chemokines and their receptors, which in turn inhibits inflammatory responses [21]. Since the DNA binding domains of both PPAR and RXR have two zinc fingers [22, 24], zinc deficiency could impair the function of this transcription factor complex and thus lead to inflammation.

The present study utilized the porcine vascular endothelial cell model to further investigate the effects of zinc deficiency on endothelial cell dysfunction with a focus on NF- κ B and PPAR pathways. In order to demonstrate the requirement of zinc for PPAR transactivation function, transient transfection-luciferase assays were performed in rat aortic vascular smooth muscle cells. We hypothesize that zinc deficiency, by activating NF- κ B and inhibiting PPAR signaling, induces endothelial cell activation.

2.3 Materials and Methods

Cell culture and experimental media

Endothelial cells were isolated from porcine pulmonary arteries and subcultured in Medium 199 (M-199) (Invitrogen Corporation, Carlsbad, CA) containing 10% (v/v) fetal bovine serum (FBS) (HyClone, Logan, UT) as previously described [75, 76]. The experimental media were composed of M-199 enriched with 1 % (v/v) FBS. Zinc (20 μ M) was added as zinc acetate from a stock solution in water. *N, N, N', N'*-Tetrakis (2-pyridylmethyl) ethylene diamine (TPEN, 1.5 or 1.0 μ M) was added from a stock solution in ethanol. Caffeic acid phenethyl ester (CAPE, 1.0 μ g/mL) and rosiglitazone (RSG, 10 μ M) were added from stock solutions in DMSO. When 90 % confluent, the cells were synchronized with M-199 containing 0 % (v/v) FBS overnight and then treated with zinc and/or TPEN and/or CAPE and/or rosiglitazone for 24 h.

Measurement of cellular oxidative stress

Oxidative stress was measured as previously described [77] with minor modifications. Endothelial cells in 24-well plate were treated with vehicle control (ethanol, 0.05 %), TPEN (1.0 μ M), TPEN (1.0 μ M) plus Zn (20 μ M), or Zn (20 μ M) alone for 24 h, and washed twice with HEPES buffered salt solution (HBSS, pH 7.4) containing 25 mM HEPES, 120 mM NaCl, 5.4 mM KCl, 1.8 mM CaCl₂, 25 mM NaHCO₃, and 15 mM glucose. After an incubation with 10 μ M of 2',7'-dichlorodihydrofluorescein diacetate (H₂DCF-DA) for 30 minutes at 37°C in the dark, cells were washed twice with HBSS and replaced with 1 ml of HBSS. DCF fluorescence (relative fluorescence intensity) was measured using a SpectraMax® M2 microplate reader (Molecular Devices Corporation, Sunnyvale, CA) with excitation and emission wavelengths of 485 nm and 530 nm, respectively.

Measurement of PPAR α , cyclooxygenase-2 (COX-2) and endothelial cell selectin (E-selectin) gene expression

Total RNA was extracted with Trizol reagent (Invitrogen, Carlsbad, CA) according to the manufacturer's directions. cDNA was generated using the Reverse Transcription System (Promega, Madison, WI). Gene expression of PPAR α was determined by real-time PCR (RT-PCR) using the ABI Prism 7300 Real Time PCR System (Applied Biosystems, Branchburg, NJ) and SYBR® GREEN PCR Master Mix (Applied Biosystems, Branchburg, NJ). The primers used were: PPAR α , forward, 5'-CAT GCC TGT GAA GGT TGC AA -3', and reverse, 5'-CAG CTC CGA TCA CAT TTG TCA T -3'; β -actin, forward, 5'-TCA TCA CCA TCG GCA ACG -3', and reverse, 5'-TTC CTG ATG TCC ACG TCG C -3'. Gene expression of COX-2 and E-selectin was determined by RT-PCR. Specific primer sequences were synthesized by IDT Technologies, Inc, San Jose, CA. The primers used were: COX-2, forward, 5'-GGA GAG ACA GCA TAA ACT GC -3', and reverse, 5'-GTG TGT TAA ACT CAG CAG CA -3'; E-selectin, forward, 5'-GAC TCG GGC AAG TGG AAT GAT GAG -3', and reverse, 5'-CAT CAC CAT TCT GAG GAT GGC GGA C -3'; β -actin, forward, 5'-GGG ACC TGA CCG ACT ACC TC-3', and reverse, 5'-GGG CGA TGA TCT TGA

TCT TC-3'. β -actin was used as an endogenous control for normalizing the expression of genes of interest.

Measurement of PPAR α and COX-2 protein expression

Cellular protein was extracted as previously described [62]. Cellular protein extracts (25 μ g) were electrophoresed on 8-10% SDS-polyacrylamide gels followed by transfer to nitrocellulose membranes (Bio-Rad Laboratories, Hercules, CA). The membranes were incubated in blocking buffer [5% nonfat milk in tris-buffered saline (pH 7.6) containing 0.05 % tween 20 (TBST)] for 1 hour followed by incubation with a 1:1000 dilution of PPAR α rabbit polyclonal IgG (Cayman Chemical Company, Ann Arbor, MI) or COX-2 goat polyclonal IgG (Santa Cruz Biotechnology, Santa Cruz, CA) or a 1:4000 dilution of β -actin rabbit polyclonal antibody (Sigma, St. Louis, MO) in blocking buffer overnight at 4°C. β -actin was used as an endogenous control to normalize the expression of proteins of interest. The membranes were then incubated with a goat anti-rabbit (Cell Signaling Technology, Inc., Danvers, MA) or mouse anti-goat (Santa Cruz Biotechnology, Santa Cruz, CA) secondary antibody conjugated to horseradish peroxidase. Signals of the blots were measured using the enhanced chemiluminescence (ECL) detection system (GE Healthcare, Piscataway, NJ).

Monocyte Adhesion Assay

The monocyte adhesion assay was performed with modifications as described previously [77]. Endothelial cells were treated with vehicle control (ethanol, 0.05 % and DMSO, 0.1 %), TPEN (1.0 μ M), TPEN (1.0 μ M) plus zinc (20 μ M), zinc (20 μ M) alone, rosiglitazone (10 μ M) alone, rosiglitazone (10 μ M) plus TPEN (1.0 μ M), rosiglitazone (10 μ M) plus TPEN (1.0 μ M) and zinc (20 μ M), or rosiglitazone (10 μ M) plus zinc (20 μ M) for 24 h in 6-well plates. Human THP-1 monocytes (50,000 cells/well) were activated with 10 ng/mL of TNF α for 10 min, then labeled with 3 μ g/mL of the fluorescent probe calcein (Molecular Probes, Carlsbad, CA) by incubation at 37 °C for 15 min. After two times of washing with 1 % FBS/M199, THP-1 monocytes were resuspended in 1% FBS/M199, added to the treated endothelial cell monolayers (50 μ L/

well) and incubated at 37 °C for 30 min to allow for monocyte adhesion. Nonadherent monocytes were washed away with 1% FBS/M199, and the monolayers were fixed with 500 µL/well of 1% glutaraldehyde at room temperature for 30 minutes. Attached fluorescent monocytes were counted using an Olympus IX70-S1F2 microscope (Olympus Optical Co., Ltd., Japan). The monocyte adhesion assays were performed by Elizabeth Oesterling at the University of Kentucky Molecular and Cell Nutrition Laboratory (Hennig's laboratory).

Transcription factor (NF-κB and PPAR): DNA interaction studies: electrophoretic mobility shift assay (EMSA)

Endothelial cells were treated with vehicle control (ethanol, 0.05 %), TPEN (1.0 µM), TPEN (1.0 µM) plus Zn (20 µM), or Zn (20 µM) alone for 24 h. Nuclear proteins were extracted as previously described [78]. EMSA assays were performed using LightShift® Chemiluminescent EMSA Kit (PIERCE, Rockford, IL). Nuclear extracts were incubated for 25 min at room temperature with 5'-biotin-labeled oligonucleotide probes containing the specific DNA binding consensus sequences for NF-κB (Promega, Madison, WI) or PPAR (Santa Cruz, Santa Cruz, CA). Incubation was performed in the presence of nonspecific competitor DNA (Poly dI-dC). Following binding, the transcription factor complexed DNA and free probe in the mixture were resolved by electrophoresis in a 6.0 % (w/v) non-denaturing polyacrylamide gel followed by transfer to nylon membranes (Thermo Scientific, Rockford, IL), and visualized by autoradiography. Control reactions using supershift assay were performed to demonstrate the specificity of the shifted DNA-protein complexes for NF-κB and PPAR, respectively. Antibodies for NF-κB p65 and PPARα were obtained from Santa Cruz (Santa Cruz Biotechnology, Santa Cruz, CA) and Cayman (Cayman Chemical Company, Ann Arbor, MI), respectively.

Transient transfection and luciferase assay

Rat aortic vascular smooth muscle cells (RAVSMC) were grown in 6-well plates in DMEM (Invitrogen Corporation, Carlsbad, CA) containing 10 % FBS (Invitrogen

Corporation, Carlsbad, CA). Media were changed to DMEM containing 2 % FBS without antibiotics, in which the cells were treated with 600 nM of the zinc chelator diethylenetriaminepentaacetic acid (DTPA) (Sigma-Aldrich, Saint Louis, MO) with or without 600 nM ZnSO₄ for 24 h. Subsequently, 400 ng DNA of the acyl-CoA oxidase PPRE-Tk-luciferase reporter construct and 200 ng of the full-length PPAR γ 1 expression vector were co-transfected using Lipofectamine 2000 (Invitrogen Corporation, Carlsbad, CA) and OPTI-MEM[®]I (Invitrogen Corporation, Carlsbad, CA) [79]. After transfection for 6-8 h, cells were stimulated with 10 μ mol/L of rosiglitazone for 24 h. Luciferase activity was measured using a Dual-Luciferase Reporter Assay System (Promega, Madison, MA) according to the manufacturer's instructions. Transfection efficiency was adjusted by normalizing firefly luciferase activities to the renilla luciferase activities generated by co-transfection with 10 ng pGL4.74 [hRluc/TK] (Promega, Madison, MA).

Statistical analysis

Statistical analysis was performed with SPSS 12.0 (SPSS, Inc., Chicago, IL). Data were analyzed using one way ANOVA with post hoc comparisons of the means by least significance difference (LSD) procedure. Differences were considered significant at $P < 0.05$. Data are means \pm standard error of the mean (SEM).

2.4 Results

Zinc deficiency increases cellular oxidative stress in vascular endothelial cells

Zinc deficiency caused by TPEN markedly increased cellular oxidative stress ($P < 0.05$, Fig. 2.1), which was reduced by zinc supplementation to the chelator-containing media ($P < 0.05$, Fig. 2.1). Zinc supplementation alone caused a similar level of cellular oxidative stress to that in zinc supplemented TPEN treated cells (Fig. 2.1).

Zinc deficiency increases NF- κ B DNA binding activity in vascular endothelial cells

Similar results were observed with NF- κ B DNA binding activity (Fig. 2.2), which was markedly increased during zinc deficiency ($P < 0.01$, Fig. 2.2) and significantly

reduced during zinc supplementation ($P < 0.01$, Fig. 2.2). Zinc supplementation alone did not affect NF- κ B DNA binding activity (Fig. 2.2).

Zinc deficiency induces gene expression of COX-2 and E-selectin in vascular endothelial cells

To test the effect of zinc deficiency on pro-inflammatory genes down-stream of NF- κ B, gene expression of COX-2 and E-selectin was assessed by RT-PCR analysis. Both COX-2 (Fig. 2.3A) and E-selectin (Fig. 2.3B) mRNAs were markedly up-regulated during zinc deficiency and restored to control levels following zinc supplementation (Fig. 2.3). Zinc supplementation alone had no effect on the expression of either COX-2 or E-selectin mRNA (Fig. 2.3).

Inhibition of NF- κ B reduces the up-regulation of COX-2 protein by zinc deficiency in vascular endothelial cells

Consistent with the COX-2 gene expression data, TPEN-induced zinc deficiency led to a significant increase in COX-2 protein level in endothelial cells ($P < 0.001$, Fig. 2.4). CAPE, a specific NF- κ B inhibitor, at the concentration of 1.0 μ g/mL, did not have any effect on COX-2 protein expression. However, when cells were co-treated with TPEN and CAPE, the induction of COX-2 by TPEN was partially blocked ($P < 0.001$, Fig. 2.4), suggesting that NF- κ B activation is involved in the induction of COX-2 protein by TPEN.

Zinc deficiency decreases PPAR α mRNA and protein expression in vascular endothelial cells

Zinc deficiency greatly decreased PPAR α mRNA expression in vascular endothelial cells ($P < 0.05$, Fig. 2.5A), which was partially restored by zinc supplementation to TPEN-containing media ($P < 0.05$, Fig. 2.5A). Zinc supplementation alone caused a similar level of PPAR α mRNA expression to that in zinc supplemented TPEN treated cells (Fig. 2.5A). Similar results were obtained with PPAR α protein

expression, which was also decreased by zinc chelation and restored by zinc supplementation ($P < 0.05$, Fig. 2.5B).

Zinc deficiency decreases PPAR DNA binding activity in vascular endothelial cells

Zinc deficiency significantly decreased PPAR DNA binding activity in vascular endothelial cells ($P < 0.05$, Fig. 2.6). Zinc supplementation tended to restore the PPAR DNA binding activity to the control level (Fig. 2.6).

Zinc deficiency increases monocyte adhesion to vascular endothelial cells and blocks the inhibitory effect of rosiglitazone on monocyte adhesion

Zinc deficiency significantly increased monocyte adhesion to vascular endothelial cells ($P < 0.001$, Fig. 2.7). Zinc supplementation ameliorated the monocyte adhesion observed during zinc deficiency. Rosiglitazone was unable to block adhesion of monocytes to endothelial cells during zinc deficiency ($P < 0.001$); however, inhibition of monocyte adhesion by rosiglitazone was observed following zinc supplementation (Fig. 2.7).

Adequate zinc is required for functional activity of PPAR γ

PPAR γ transactivation activity in PPAR γ and PPRE co-transfected RAVSMC was induced by rosiglitazone in zinc adequate cells ($P < 0.001$, Fig. 2.8). Zinc deficiency caused by DPTA inhibited PPAR γ transactivation activity induced by rosiglitazone ($P < 0.05$, Fig. 2.8), which could be reversed by zinc supplementation ($P < 0.05$, Fig. 2.8).

2.5 Discussion

Evidence indicates that major chronic or age-related diseases, such as atherosclerosis, arthritis, dementia, osteoporosis, and cardiovascular diseases, are inflammation-related, and that a balance between NF- κ B and PPAR signaling is a critical regulator of inflammation-related diseases [80]. Furthermore, zinc deficiency or a disturbance in zinc homeostasis in individuals genetically predisposed to a dysregulation

of the inflammatory and/or immune response may contribute to adverse effects associated with age-related diseases [81]. Zinc plays an important role in reactions related to cell-mediated immunology and also functions as an antioxidant and anti-inflammatory nutrient [82]. The results from the studies described above suggest that zinc deficiency activates vascular endothelial cells through activation of NF- κ B and inhibition of PPAR pathways.

NF- κ B is well known to be a key signaling pathway to up-regulate adhesion molecules [3], but the effect of endothelial cellular zinc status on adhesion molecule and other NF- κ B regulated gene expression has rarely been reported. The anti-inflammatory and anti-atherogenic roles of PPAR in endothelial cells have aroused interest only in recent years with the findings that adequate zinc is required for proper PPAR signaling in these cells [25, 26].

The present study looked at the influence of endothelial zinc status on adhesion molecule and other NF- κ B regulated gene expression and further investigated the molecular mechanisms involved in zinc deficiency-induced endothelial cell activation. Oxidative stress is believed to play a fundamental role in the etiology of cardiovascular diseases, including atherosclerosis [83, 84]. The finding that zinc deficiency induced by TPEN chelation increased cellular oxidative stress is consistent with our previous finding that zinc deficiency induced by endothelial cell culture in low serum media for eight days can cause an increase in oxidative stress [10]. NF- κ B is an oxidative stress sensitive transcription factor and critical in the regulation of an inflammatory response [85]. Furthermore, activated NF- κ B has been found in human atherosclerotic plaques [86], suggesting its importance in the etiology of atherosclerosis. In the current study, zinc deficiency significantly increased NF- κ B DNA binding activity. However, our previous studies using long term (8-10 day) culture of endothelial cells in low serum (zinc-deficient) media have shown that zinc deficiency by itself, without additional oxidative stress, does not increase [87] or only slightly increases NF- κ B DNA binding [10]. The different observations of the effect of zinc deficiency on NF- κ B DNA binding may be due to the different ways of making endothelial cells zinc-deficient, and possibly the extent of zinc deficiency as well. Both COX-2 and E-selectin are NF- κ B regulated genes

[88, 89]. COX-2 catalyzes production of the pro-inflammatory prostaglandin E2 (PGE2) and is highly induced and active at sites of inflammation [90]. E-selectin is an adhesion molecule expressed on the surface of activated vascular endothelial cells that mediates adhesion of neutrophils, monocytes, and memory T-cells to endothelial cells [89, 91]. In the current study, as a consequence of zinc deficiency-induced NF- κ B activation, both COX-2 and E-selectin genes were significantly up-regulated, with the latter contributing to the observed increased adhesion of THP-1 monocytes to the activated endothelial cells. CAPE is a potent and specific inhibitor of NF- κ B activation that acts by preventing the translocation of p65 subunit of NF- κ B to the nucleus, thus inhibiting NF- κ B DNA binding [92]. In our study, COX-2 protein expression induced during zinc deficiency was partially blocked by CAPE, again suggesting that NF- κ B activation is involved in the up-regulation of inflammatory markers by zinc deficiency in vascular endothelial cells.

PPARs, and especially PPAR α and PPAR γ , are inhibitors of NF- κ B [21]; therefore dysfunctional PPAR signaling will lead to activation of NF- κ B. PPAR α can repress the NF- κ B pathway via interactions with the p65 subunit of NF- κ B [34]. Similarly, PPAR γ can inhibit the NF- κ B pathway by physically interacting with p50 and p65 subunits of NF- κ B [35]. PPAR α agonists, such as fibrates, induce I κ B α (an inhibitor of NF- κ B) expression, providing an additional mechanism for the inhibition of NF- κ B by PPAR α [36]. In the present study, PPAR α expression at both the mRNA and protein levels was decreased due to zinc deficiency and this effect was reversible by zinc supplementation. Similar effects of zinc deficiency and zinc supplementation were observed on PPAR γ expression in vascular endothelial cells [25]. Furthermore, our previous study has shown that both PPAR α and PPAR γ agonists can induce PPAR DNA binding activity, which was compromised during zinc deficiency [26]. In this study, zinc deficiency consistently decreased PPAR DNA binding activity in endothelial cells. The present transfection-luciferase assay demonstrated that zinc deficiency can inhibit rosiglitazone-induced PPAR γ transactivation activity and that this effect can also be reversed by zinc supplementation. As expected, compromised PPAR γ function was observed in the current study during zinc deficiency. This was reflected by the requirement of adequate zinc for rosiglitazone to inhibit monocyte-endothelial cell

adhesion. Taken together, these findings clearly demonstrate that zinc deficiency compromises PPAR function.

In conclusion, our present *in vitro* studies suggest that zinc deficiency intensifies pro-inflammatory and impairs anti-inflammatory responses in vascular endothelial cells through activation of NF- κ B and inhibition of PPAR pathways. Zinc adequacy therefore has important implications in preventing endothelial cell dysfunction and subsequent cardiovascular diseases such as atherosclerosis.

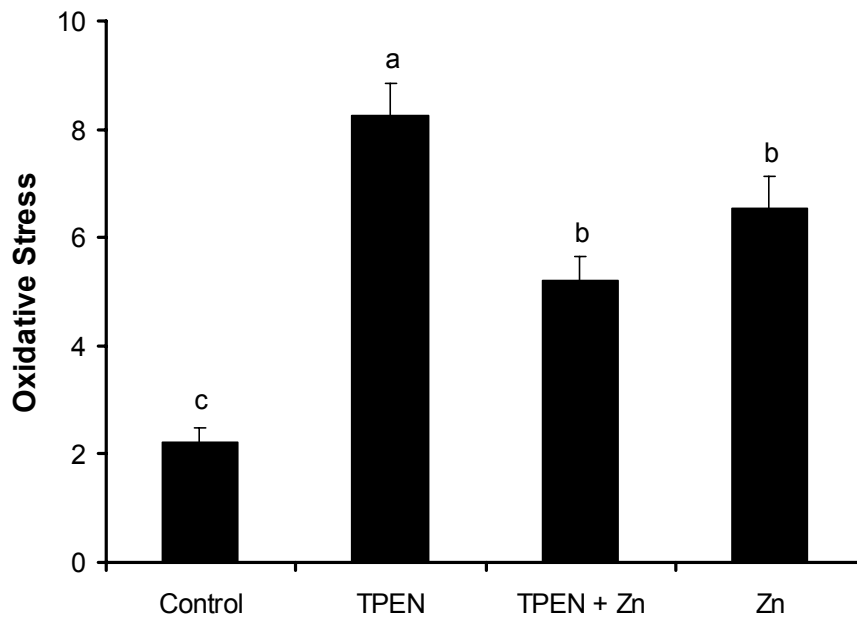


Figure 2.1. Zinc deficiency increases cellular oxidative stress in endothelial cells.

Endothelial cells were exposed to vehicle control (ethanol, 0.05 %), TPEN (1.0 μ M), TPEN (1.0 μ M) plus Zn (20 μ M), or Zn (20 μ M) for 24 h. Oxidative stress was measured by DCF fluorescence (relative fluorescence units). Values are means \pm SEM, n = 4-6. Means without a common letter differ (a > b > c), P < 0.05.

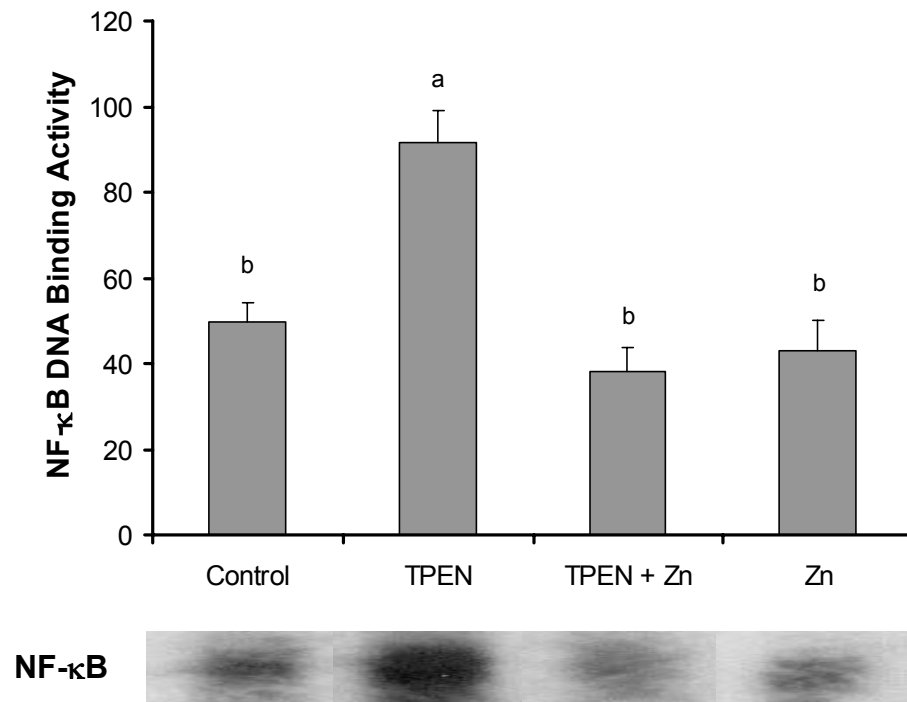


Figure 2.2. Zinc deficiency increases NF-κB DNA binding activity in endothelial cells.

Endothelial cells were exposed to vehicle control (ethanol, 0.05 %), TPEN (1.0 μM), TPEN (1.0 μM) plus Zn (20 μM), or Zn (20 μM) for 24 h. The vertical axis represents densitometric units. Values are means ± SEM, n = 3. Means without a common letter differ (a > b), P < 0.01. The gel data are a representative of the typical outcome of three repeated EMSA experiments.

A

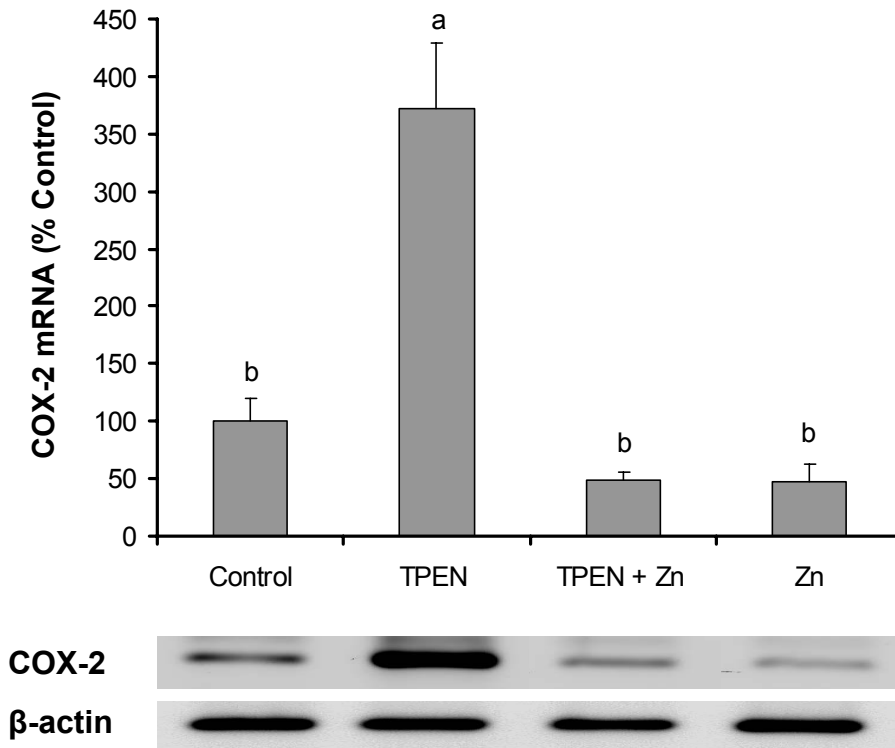


Figure 2.3. Zn deficiency induces COX-2 (A) and E-selectin (B) mRNA expression in endothelial cells.

A. COX-2 mRNA expression measured by RT-PCR. B. E-selectin mRNA expression measured by RT-PCR. Endothelial cells were exposed to vehicle control (ethanol, 0.075 %), TPEN (1.5 μ M), TPEN (1.5 μ M) plus Zn (20 μ M), or Zn (20 μ M) for 24 h. The vertical axes represent ratios of the densitometric units of COX-2 or E-selectin mRNA over those of β -actin mRNA, respectively, expressed as percentage of control. Values are means \pm SEM, n = 4. Means without a common letter differ (a > b), P < 0.01(A) or 0.05 (B). The gel data are a representative of the typical outcome of four repeated RT-PCR experiments.

B

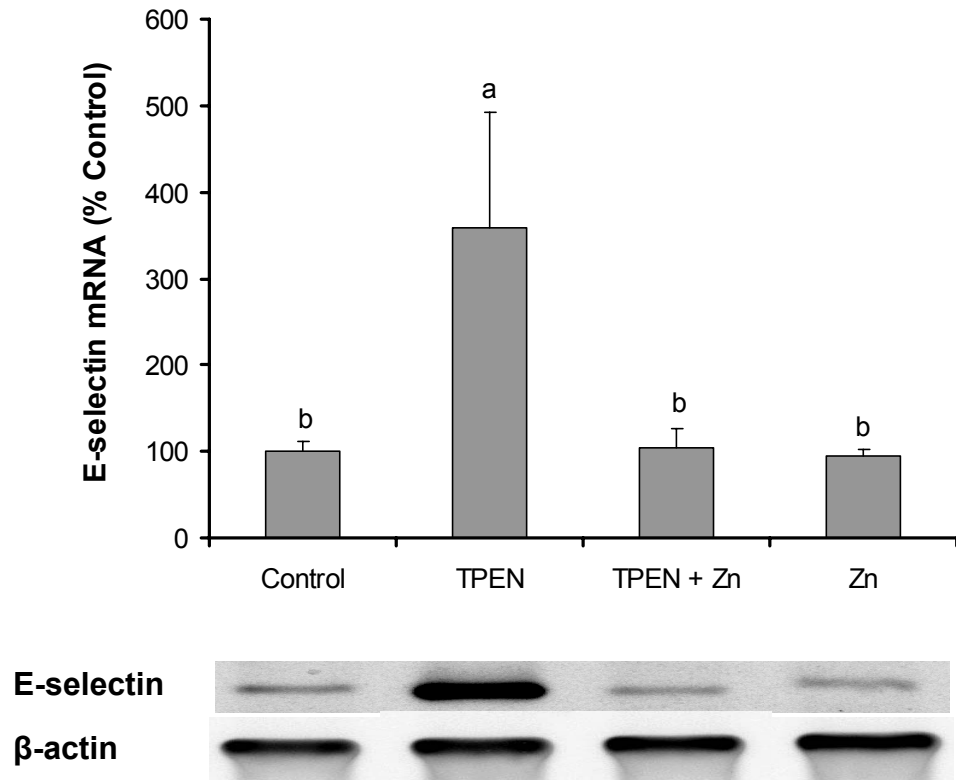


Figure 2.3 (Continued)

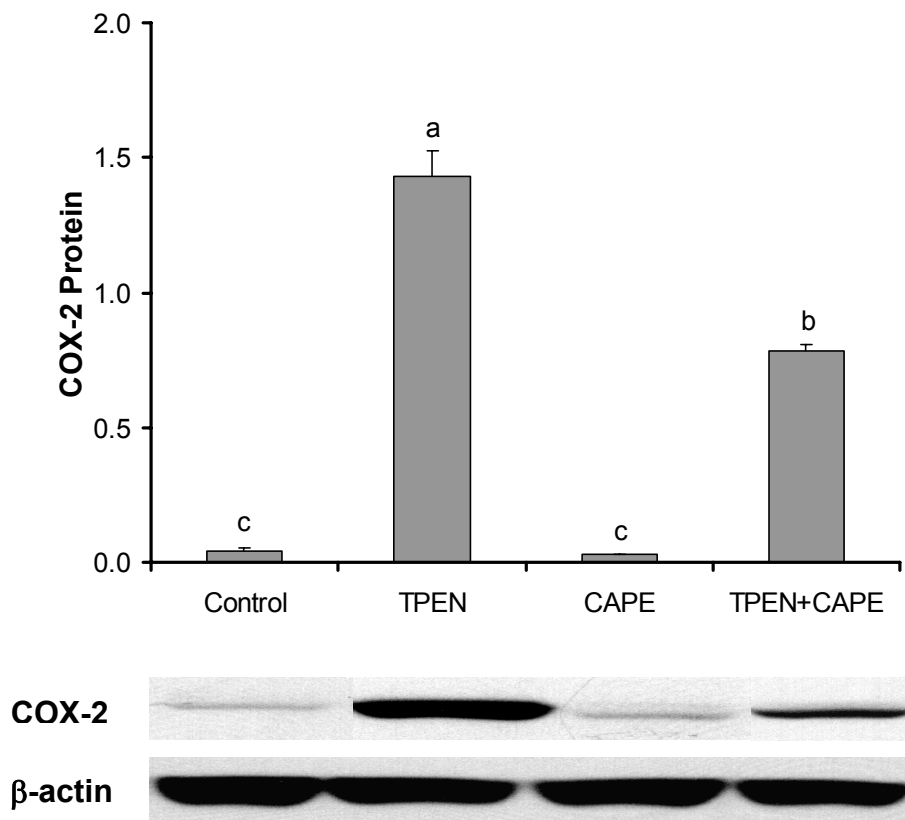


Figure 2.4. Zinc deficiency-induced COX-2 protein expression in endothelial cells is partially reduced during inhibition of NF- κ B activation.

Endothelial cells were exposed to vehicle control (ethanol, 0.05 % and DMSO, 0.04 %), TPEN (1.0 μ M), CAPE (1.0 μ g/mL), or TPEN (1.0 μ M) plus CAPE (1.0 μ g/mL) for 24 h. The values are ratios of the densitometric units of COX-2 over those of β -actin. Values are means \pm SEM, n = 3. Means without a common letter differ (a > b > c), P < 0.001. The gel data are a representative of the typical outcome of three repeated Western Blot experiments.

A

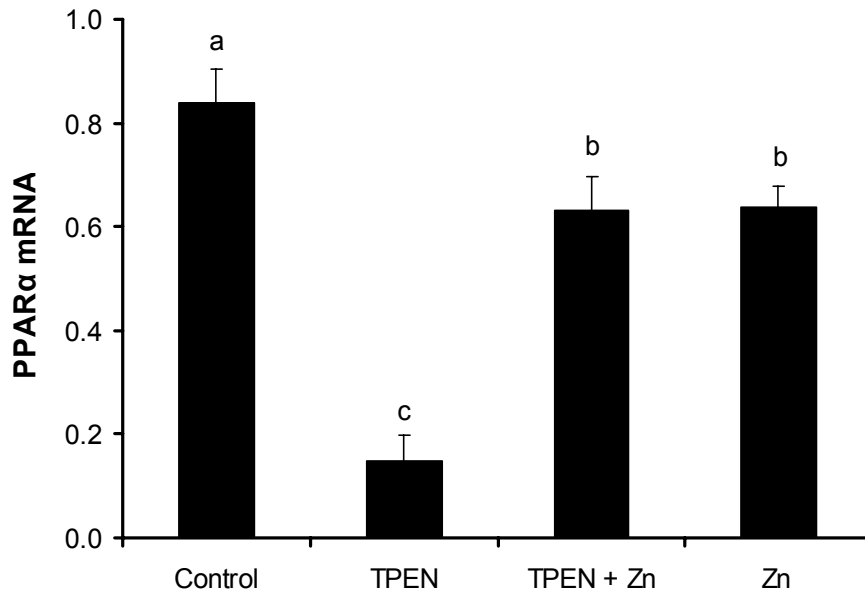


Figure 2.5. Zn deficiency decreases PPAR α expression in endothelial cells.

Endothelial cells were exposed to vehicle control (ethanol, 0.075 %), TPEN (1.5 μ M), TPEN (1.5 μ M) plus Zn (20 μ M), or Zn (20 μ M) for 24 h. A. PPAR α mRNA expression measured by real-time PCR. The vertical axis represents relative units, calculated as the ratio of the copy number of PPAR α over the copy number of β -actin, the endogenous control. Values are means \pm SEM, n = 4. Means without a common letter differ (a > b > c), P < 0.05. B. PPAR α protein expression measured by Western blot. The values are ratios of the densitometric units of PPAR α over those of β -actin, expressed as percentage of control. Values are means \pm SEM, n = 4. Means without a common letter differ (a > b), P < 0.05. The gel data are a representative of the typical outcome of four repeated Western Blot experiments.

B

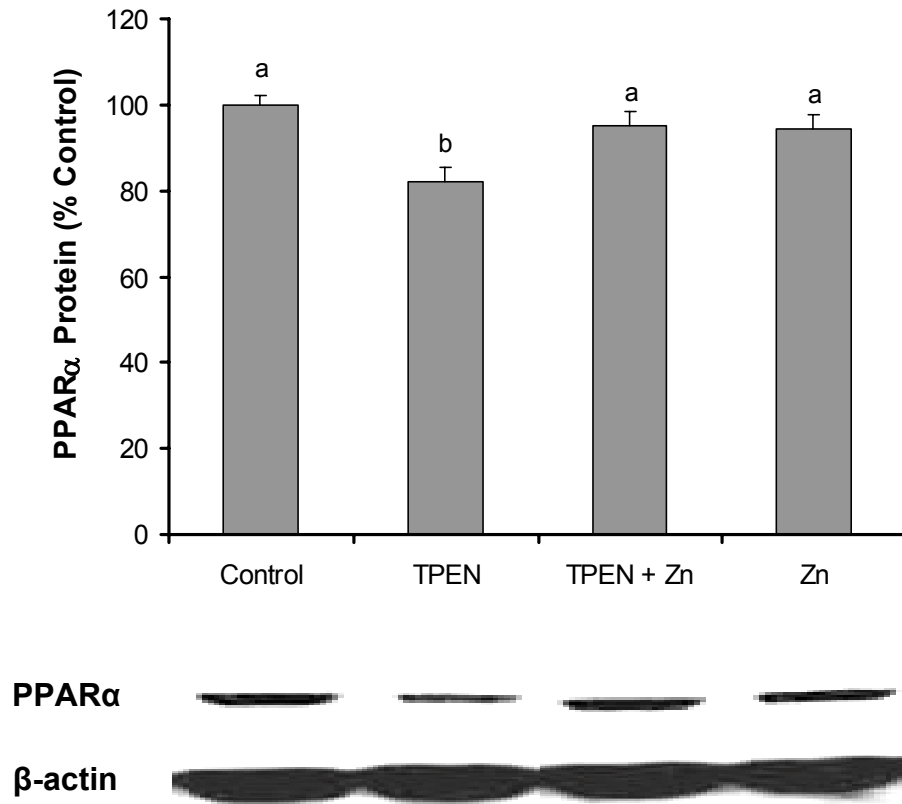


Figure 2.5 (Continued)

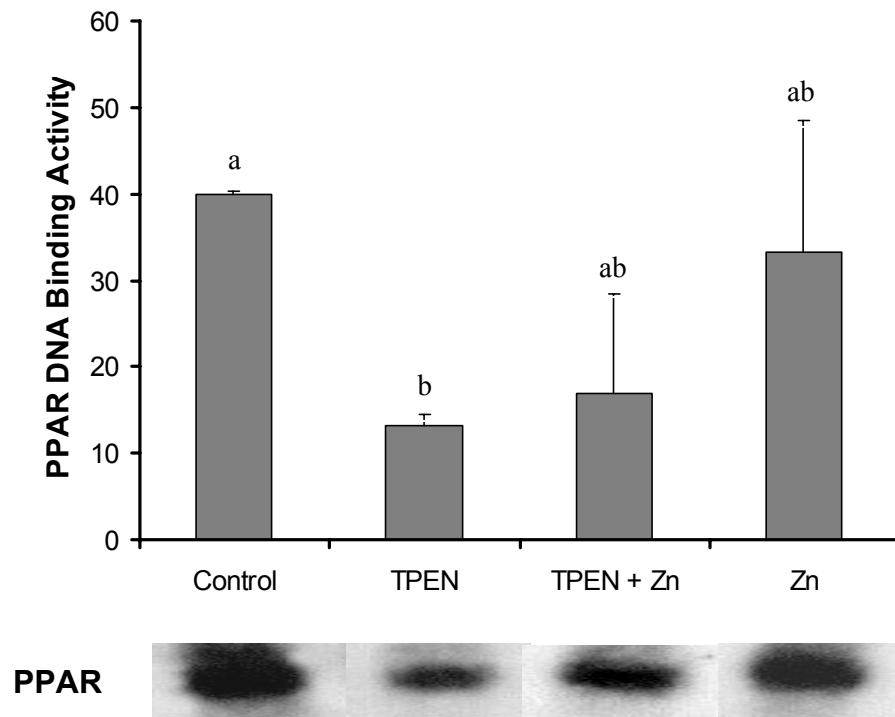


Figure 2.6. Zn deficiency decreases PPAR DNA binding activity in endothelial cells. Endothelial cells were exposed to vehicle control (ethanol, 0.05 %), TPEN (1.0 μ M), TPEN (1.0 μ M) plus Zn (20 μ M), or Zn (20 μ M) for 24 h. Values are means \pm SEM, n = 3. Means without a common letter differ (a > b), P < 0.05. The gel data are a representative of the typical outcome of three repeated EMSA experiments.

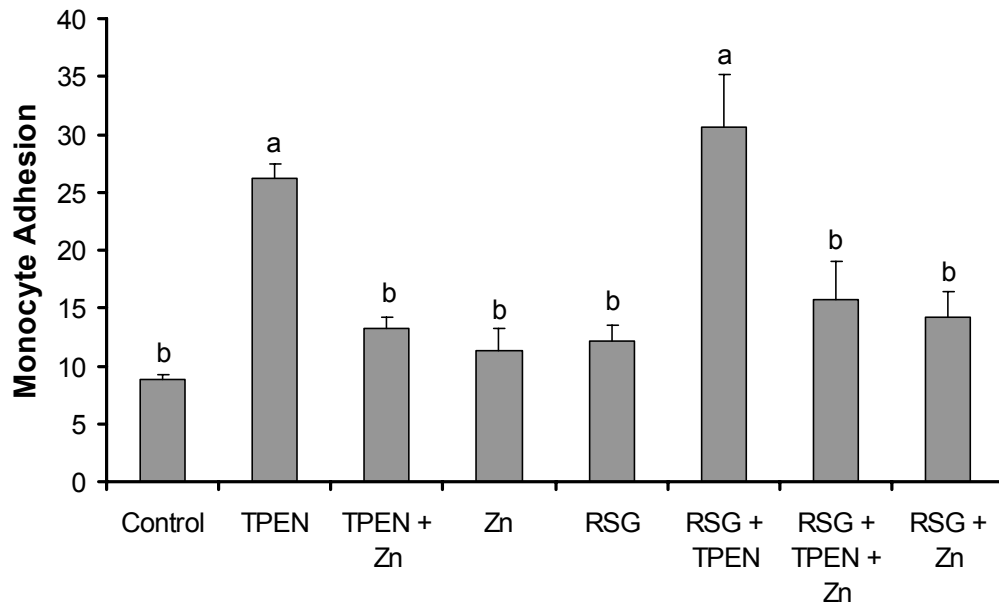


Figure 2.7. Zinc deficiency increases monocyte adhesion to endothelial cells and blocks the inhibitory effect of rosiglitazone on monocyte adhesion.

Endothelial cells were exposed to vehicle control (ethanol, 0.05 % and DMSO, 0.1 %), TPEN (1.0 μ M), TPEN (1.0 μ M) plus Zn (20 μ M), Zn (20 μ M), rosiglitazone (RSG, 10 μ M), RSG (10 μ M) plus TPEN (1.0 μ M), RSG (10 μ M) plus TPEN (1.0 μ M) and Zn (20 μ M), or RSG (10 μ M) plus Zn (20 μ M) for 24 h followed by incubation with human THP-1 monocytes for 30 min. Monocyte adhesion is expressed as numbers of monocyte adhered per microscopic high power field, with 5 ~ 7 fields examined per well. Values are means \pm SEM, n = 3. Means without a common letter differ (a > b), P < 0.01.

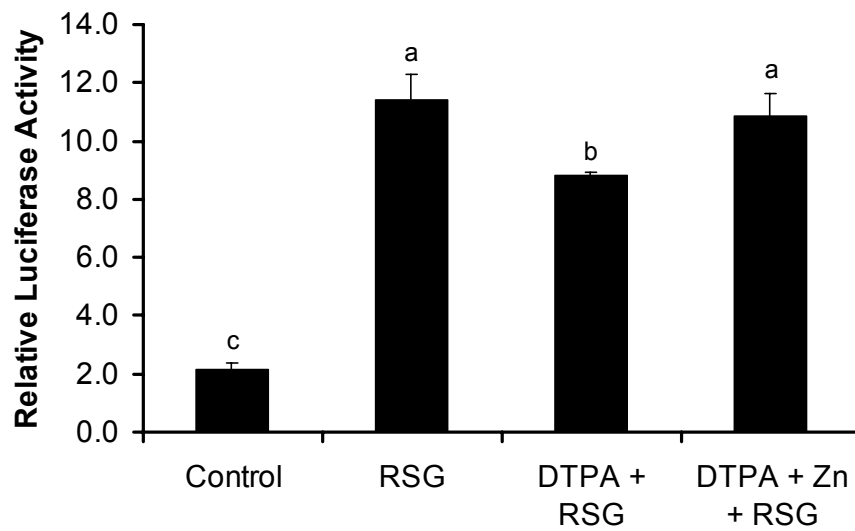


Figure 2.8. Effect of zinc status on rosiglitazone-induced PPAR γ transactivation in PPAR γ and PPRE co-transfected RAVSMC.

PPAR γ transactivation activity was measured as relative luciferase activity (firefly luciferase activity: renilla luciferase activity). Means without a common letter differ ($a > b > c$), $P < 0.05$. Values are means \pm SEM, $n = 3$. The results represent the outcome of three repeated experiments.

Chaper 3. Zinc Deficiency Alters Pro-inflammatory and Anti-inflammatory Responses in LDL-Receptor-Deficient Mice Treated with Rosiglitazone

3.1 Synopsis

Marginal intake of dietary zinc can be associated with increased risk of cardiovascular diseases. Zinc has potent antioxidant and anti-inflammatory properties. Zinc is also a structural and functional component of PPAR. Numerous studies indicate that rosiglitazone, a selective and potent PPAR γ agonist, has antioxidant and anti-inflammatory effects and would be beneficial in inflammatory conditions, such as atherosclerosis. The present study focused on the hypothesis that PPAR γ signaling, and especially its anti-inflammatory properties, are dysfunctional during zinc-deficiency and that adequate dietary zinc is critical for anti-inflammatory properties of PPAR γ agonists such as rosiglitazone. LDL-R deficient (LDL-R^{-/-}) mice were maintained for three weeks on low-fat (7g/100g) diets that were either zinc deficient or zinc adequate. Subsequently, the low-fat regimen was switched to a high-fat (15g/100g) regimen for one week to induce a biological environment of mild oxidative and inflammatory stress. Half of the mice within each zinc group were gavaged with rosiglitazone two days prior to the high fat feeding. Subsequently, expression of selected pro-inflammatory genes was measured in abdominal aorta. I κ B α protein expression and DNA binding activities of NF- κ B and PPAR in liver were also assayed. Furthermore, concentrations of pro- and anti-inflammatory cytokines/chemokines were determined in plasma. Rosiglitazone induced inflammatory genes (e.g., MCP-1) only during zinc deficiency, and adequate zinc was required for rosiglitazone to down-regulate pro-inflammatory markers such as iNOS. In addition, rosiglitazone increased I κ B α protein expression only in zinc adequate mice. Finally, plasma cytokine profiles suggest an overall pro-inflammatory environment during zinc deficiency and support the concept that zinc is required for proper anti-inflammatory or protective functions of PPAR. These data suggest that in this atherosclerotic mouse model the proper anti-inflammatory function of PPAR γ was compromised during zinc deficiency and that adequate dietary zinc is critical for anti-inflammatory properties of the PPAR γ agonist rosiglitazone.

3.2 Introduction

Atherosclerosis and its complications are the main causes of morbidity and mortality of coronary heart disease [2, 93]. Atherosclerosis is a chronic inflammatory disease that may progress over many decades and is characterized by the accumulation of lipids and fibrous elements in large arteries [2]. Atherosclerotic lesions are thought to be initiated by vascular endothelial cell dysfunction followed by monocyte adhesion, invasion and macrophage foam cell formation [1, 94]. Interaction between modified lipoproteins, macrophage foam cells, T cells, and the normal cellular elements of the arterial wall, such as smooth muscle cells [94], results in the formation and progression of atherosclerotic lesions [1]. In addition to genetic risk factors, such as high LDL and VLDL levels and low HDL levels, the development of atherosclerosis is greatly influenced by lifestyle as well as nutritional factors, such as zinc deficiency [1-3], which has been suggested to be associated with coronary artery disease by epidemiological studies [67]. Several molecular and cellular mechanisms on how zinc deficiency could contribute to the pathogenesis of atherosclerosis have been found. For example, zinc deficiency can enhance oxidative stress-related signaling in endothelial cells, including activation of NF- κ B, which is a key transcription factor leading to adhesion molecule up-regulation and inflammatory response, induction of caspase-mediated apoptosis of endothelial cells, which is also a characteristic of atherosclerosis, and changes in NO signaling, which is linked to the development of atherosclerosis [3]. The anti-atherogenic properties of zinc with a focus on endothelial cell metabolism have been previously reviewed [95].

Zinc is an essential trace element required in biological systems for many physiological functions. Zinc is recognized as a growth factor, membrane and cytoskeleton stabilizer, anti-inflammatory and antioxidant agent, and anti-apoptotic agent [4, 28, 70]. Zinc is a structural component of numerous zinc-finger proteins and plays functional roles in these proteins [4, 11]. PPAR is a ligand-activated transcription factor which has anti-inflammatory properties by interfering with major inflammatory pathways such as NF- κ B and AP-1, and inhibiting inflammatory responses with decreased inflammatory cytokine and deactivated inflammatory mediators [21]. Since the DNA binding domains of PPAR and its DNA binding partner RXR both have two zinc fingers

[22, 24], zinc deficiency may affect proper function of the PPAR:RXR transcription factor complex and compromise the anti-inflammatory properties of PPAR.

The synthetic PPAR γ agonist, rosiglitazone, one member of thiazolidinediones (TZDs), is clinically used to treat type II diabetes [96]. In addition to its insulin-sensitizing anti-diabetic effects [96], rosiglitazone has potent anti-inflammatory and anti-atherosclerotic properties [97, 98] and is able to inhibit the development of atherosclerosis in LDL-R^{-/-} [99] and apolipoprotein E deficient (ApoE^{-/-}) mice [100]. Rosiglitazone has also been shown to attenuate vascular inflammation in both type II diabetic [101] and non-diabetic patients [102, 103]. Substantial experimental and clinical studies have provided evidence that chronic administration of TZDs, including rosiglitazone, is beneficial on cardiovascular system [38].

Some *in vitro* studies using porcine vascular endothelial cells have shown that zinc can modulate PPAR function [25] and that adequate zinc is important for anti-inflammatory properties of PPAR α and γ [26]. The next question is whether the requirement of zinc for PPAR to exert its anti-inflammatory effect is also the case *in vivo*. To answer this question we carried out the current animal study utilizing an atherogenic mouse model (LDL-R^{-/-} mice). We hypothesize that rosiglitazone, by activating PPAR γ , is able to decrease high-fat diet induced inflammatory responses in LDL-R^{-/-} mice, and that this protective effect of rosiglitazone is dependent on adequate zinc intake.

3.3 Materials and Methods

Animals and diets

The atherosclerosis-prone animal model used in this study was the homozygous LDL-R null strain of mouse with a C57BL6/J Background. These mice develop marked hypercholesterolemia and early to intermediate atherosclerotic lesions after 6 to 8 weeks on a high-fat, high-cholesterol diet [104]. The mice were obtained from The Jackson Laboratory (Bar Harbor, ME; Stock Number: 002207) and housed 4 per cage in plastic cages with wire mesh floors over wood chip bedding. Cellulose pads were provided to the mice for nesting and a 12 h light/dark cycle was maintained. Mice were given ad

libitum access to distilled water provided through plastic bottles with plastic stoppers to reduce zinc contamination. All procedures were in compliance with and approved by the Iowa State University Animal Care and Use Committee. LDL-R^{-/-} mice were obtained at 5 wk of age, weighed 16.3 g on average, and were fed a low-fat (LF) diet with either 0.4 mg/kg of zinc (0 Zn, zinc-deficient diet) or 33.1 mg/kg of zinc (30 Zn, zinc-adequate diet). After 21 d of feeding the LF diet, all mice were assigned to a high-fat (HF) diet, without changing the original zinc nutritional status. Mice were fed the HF diet for one week. Diets were prepared based on AIN-93 standards [105] but used egg white rather than casein as the protein source in order to provide a low zinc diet [106] (Table 3.1). The diets were of similar caloric value, 18.17 kJ/g for the HF and 16.50 kJ/g for the LF diets, respectively. Rosiglitazone (RSG, 20 mg · kg⁻¹ · d⁻¹) [99] or the vehicle (0.25% of methylcellulose) were administered for 9 d by oral gavage. RSG treatment was initiated 2 d prior to the start of the HF dietary regimen. Body weights of all mice were determined every 2 d throughout the study. After completion of the study (4 wk), the mice were euthanized by intraperitoneal phenobarbital injection (Fig. 3.1).

Food intake was measured over a 3 day period within the first week of the study. Mean food intake was not statistically different in zinc deficient vs. zinc adequate mice at this time. In a preliminary study we observed that mice fed the zinc-deficient diet cycle their food intake between 100 % and 75 % of that of the zinc-adequate animals during this time period with a net overall decrease of about 16% of food intake in zinc-deficient mice.

Zinc quantification

Blood was drawn from exposed hearts using heparinized syringes. Plasma samples were prepared by centrifugation at 14,000 × g at room temperature for 10 min. Livers were flash frozen in liquid nitrogen after excision. Both plasma and liver samples were stored at -80° C prior to analysis. Zinc concentrations in plasma, liver and RSG solution were analyzed by inductively coupled plasma (ICP) mass spectrometry by Dr. Thomas Mawhinney at the University of Missouri-Columbia Agricultural Experiment Station Chemical Laboratory (Columbia, MO) [107].

Measurement of plasma cytokines and chemokines

Concentrations of plasma IL-1 α , IL-2, IL-4, IL-6, IL-10, IL-12, IL-13, IL-17, TNF α , and MCP-1 were measured using Mouse Cytokine/Chemokine LINCOplex kit (LINKO Research Inc., St. Louis, MO). Luminex 100 (Luminex Corporation, Austin, TX) and Multiplex Data Analysis Software 1.0 (Upstate USA, Inc., Chicago, IL) were utilized for signal detection and data analysis, respectively, by Jason Stevens at the University of Kentucky Center for Oral Health Research.

Gene expression analysis

Abdominal aortas were excised from the mice, immersed in RNAlater (Qiagen, Valencia, CA) and stored at -80° C until analysis. Total RNA was isolated from abdominal aorta using RNeasy Fibrous Tissue Mini Kit (Qiagen, Valencia, CA) after surrounding adipose and connective tissues were removed. cDNA was generated using the Reverse Transcription System (Promega, Madison, WI). Gene expression was determined by real-time PCR using the ABI Prism 7300 Real Time PCR System (Applied Biosystems, Branchburg, NJ) and TaqMan® Universal PCR Master Mix, No AmpErase® UNG (Applied Biosystems, Branchburg, NJ). TaqMan® gene expression assays were used for mouse iNOS and MCP-1 (Applied Biosystems, Branchburg, NJ). Each assay consisted of a specific pair of unlabeled PCR primers and a specific TaqMan® MGB probe that was 5' end labeled with a FAM™ reporter dye and 3' end labeled with a minor groove binder/non-fluorescent quencher (MGBNFQ). Detection of 18S rRNA, or β -actin as endogenous control, utilized pre-developed Taqman assay reagents, i.e. Eukaryotic 18S rRNA Endogenous Control or Mouse ACTB Endogenous Control (Applied Biosystems, Branchburg, NJ).

Measurement of I κ B α protein expression

Liver tissues were flash frozen and stored at -80 °C until analysis. Frozen tissue was cut on ice into approximately 2 mm³ pieces with scalpel and submerged into ice cold lysis buffer containing 50 mM Tris, 150 mM NaCl, 1 mM EDTA, 1 mM EGTA, 2 mM DTT, 1 mM Na₃VO₄, 0.1 mg/mL phenylmethanesulfonyl fluoride (PMSF), 2.5 μ g/mL

leupeptin, 10 µg/mL pepstatin A, 10 µg/mL aprotinin, 0.5 % nonidet P-40, and 0.5 % Triton X-100. The liver tissue was homogenized on ice for 10 min and the homogenate was kept on ice for another 30 min followed by centrifugation at 14,000 rpm at 4 °C for 30 min. Cellular protein extract was obtained by collecting the supernatant. 25 µg of cellular protein extracts were electrophoresed on 8 % SDS-polyacrylamide gels followed by transfer to nitrocellulose membranes. The membranes were blocked with blocking buffer [5% nonfat milk in tris-buffered saline (pH 7.6) containing 0.05 % tween 20 (TBST)] for 1 h followed by incubation with a 1:1000 dilution of rabbit anti-IκBα, C-terminal polyclonal antibody (Millipore, Billerica, MA) or a 1:4000 dilution of rabbit anti-actin polyclonal antibody (Sigma, St. Louis, MO) in blocking buffer overnight at 4°C. β-actin was used as an endogenous control to normalize the expression of IκBα. The membranes were then incubated with a goat anti-rabbit secondary antibody conjugated to horseradish peroxidase (Cell Signaling Technology, Inc., Danvers, MA). Signals of the blots were measured using the enhanced chemiluminescence (ECL) detection system (GE Healthcare, Piscataway, NJ).

Transcription factor (NF-κB and PPAR):DNA interaction studies: electrophoretic mobility shift assay (EMSA)

Liver tissues were flash frozen and stored at -80 °C until analysis. Nuclear proteins were extracted using CellLytic™ NuCLEAR™ Extraction Kit (Sigma-Aldrich, St. Louis, MO) according to the manufacturer's instruction. EMSA assays were performed using LightShift® Chemiluminescent EMSA Kit (PIERCE, Rockford, IL). Nuclear extracts were incubated for 25 min at room temperature with 5'-biotin-labeled oligonucleotide probes containing the specific DNA binding consensus sequences for NF-κB (Promega, Madison, WI) or PPAR (Santa Cruz, Santa Cruz, CA). Incubation was performed in the presence of nonspecific competitor DNA (Poly dI-dC). Following binding, the transcription factor complexed DNA and free probe in the mixture were separated by electrophoresis in a 6.0 % (w/v) non-denaturing polyacrylamide gel followed by transfer to nylon membranes (Thermo Scientific, Rockford, IL), and visualized by autoradiography. Control reactions using supershift assay were performed

to demonstrate the specificity of the shifted DNA-protein complexes for NF- κ B and PPAR, respectively. Antibodies for NF- κ B p65 and PPAR α were obtained from Santa Cruz (Santa Cruz Biotechnology, Santa Cruz, CA) and Cayman (Cayman Chemical Company, Ann Arbor, MI), respectively.

Statistical analyses

Data were expressed as means \pm SEM and analyzed using SPSS 12.0 (SPSS, Inc., Chicago, IL) and JMP 7.0 (SAS, Inc., Cary, NC). Zinc and RSG were used as explanatory variables in two-way ANOVA models. Non significant interactions were removed from the models. Post hoc comparisons were conducted using LSD method only when there were significant interactions in the two-way model. A statistical probability of $P < 0.05$ was considered significant. Actual P values were reported when less than 0.1.

3.4 Results

Body weight was unchanged until day 9, but subsequently only increased in zinc-adequate mice (Fig. 3.2). Rosiglitazone treatment had no effect on body weight within either zinc adequate or deficient groups, respectively (Fig. 3.2). Body weights in each group at the end of the feeding study were (mean \pm SEM): 0 Zn, 16.43 \pm 1.20 g; 0 Zn + RSG, 15.12 \pm 0.52 g; 30 Zn, 19.56 \pm 0.26 g; 30 Zn + RSG, 19.29 \pm 0.48 g.

Plasma zinc concentrations were not different in the LDL-R^{-/-} mice fed the zinc-deficient diet compared to the zinc-adequate diet regardless of rosiglitazone treatment (Fig. 3.3). Treatment with rosiglitazone resulted in increased plasma zinc concentrations in both dietary groups ($P < 0.001$, Fig. 3.3). Liver zinc concentration was lower in untreated mice fed the zinc-deficient diet compared to the zinc-adequate diet ($P < 0.001$, Fig. 3.3). In mice fed the zinc-adequate diet only, rosiglitazone treatment resulted in reduced liver zinc concentration ($P < 0.01$, Fig. 3.3).

The effects of rosiglitazone on expression of pro-inflammatory genes in LDL-R^{-/-} mice are regulated by zinc status

Rosiglitazone treatment resulted in lower levels of iNOS mRNA expression in abdominal aortas compared with untreated mice ($P < 0.01$, Fig. 3.4A). The zinc adequate untreated mice had a higher level of iNOS mRNA expression in abdominal aorta than the zinc deficient untreated mice ($P < 0.05$, Fig. 3.4A). Rosiglitazone treatment significantly reduced iNOS mRNA expression in abdominal aorta only in zinc adequate mice ($P < 0.05$, Fig. 3.4A) but not in zinc deficient mice.

Zinc deficiency alone did not increase MCP-1 mRNA expression (Fig. 3.4B). Rosiglitazone treatment had a significant interaction with zinc status by tending to increase MCP-1 mRNA expression in zinc deficient mice and decrease MCP-1 mRNA expression in zinc adequate mice ($P < 0.05$, Fig. 3.4B). During zinc deficiency, rosiglitazone treatment significantly up-regulated MCP-1 mRNA in abdominal aorta compared to rosiglitazone treated zinc adequate mice ($P < 0.05$, Fig. 3.4B).

The effects of rosiglitazone on I κ B α protein expression in LDL-R^{-/-} mice are regulated by zinc status

The zinc deficient LDL-R^{-/-} mice had lower levels of liver I κ B α protein expression than the zinc adequate mice ($P < 0.01$, Fig. 3.5). Regulation of liver I κ B α protein expression was affected by both treatments with rosiglitazone and zinc, and the treatment interaction was statistically significant. Specifically, I κ B α protein expression in liver of LDL-R^{-/-} mice was up-regulated by rosiglitazone in zinc adequate mice but not in zinc deficient mice ($P < 0.05$, Fig. 3.5).

Zinc deficiency and rosiglitazone increase PPAR DNA binding activity in LDL-R^{-/-} mice

NF- κ B DNA binding activity in LDL-R^{-/-} mice liver was unaffected by either zinc intake or rosiglitazone treatment (Fig. 3.6A). However, rosiglitazone tended to increase NF- κ B DNA binding activity during zinc deficiency and decrease it during zinc adequacy (Fig. 3.6A). Zinc deficiency resulted in higher PPAR DNA binding activity in mice liver

($P < 0.05$, Fig. 3.6B). Rosiglitazone treatment also increased PPAR DNA binding activity in mice liver ($P < 0.05$, Fig. 3.6B).

The effects of rosiglitazone on concentrations of plasma anti- and pro-inflammatory cytokines in LDL-R^{-/-} mice are regulated by zinc status

Zinc deficiency resulted in lower plasma IL-10 concentrations in LDL-R^{-/-} mice ($P < 0.01$, Table 3.2). Although statistically not significant, treatment with rosiglitazone tended to increase circulating anti-inflammatory cytokine (IL-4, IL-10, IL-13) concentrations during zinc adequacy and tended to decrease them during zinc deficiency (Table 3.2).

Zinc deficiency resulted in lower plasma IL-1 α concentrations ($P < 0.001$, Table 3.3) and higher plasma IL-6 concentrations ($P < 0.05$, Table 3.3) in LDL-R^{-/-} mice. Rosiglitazone tended to further increase IL-6 concentrations in zinc deficient mice and slightly decrease them in zinc adequate mice ($P = 0.095$, Table 3.3). Zinc and rosiglitazone had a significant interaction in affecting plasma IL-12 concentrations ($P < 0.01$, Table 3.3). Specifically, rosiglitazone treatment decreased plasma IL-12 concentrations during zinc adequacy ($P < 0.01$, Table 3.3), but tended to increase IL-12 concentrations during zinc deficiency (Table 3.3).

3.5 Discussion

This study was designed to investigate the interaction of a modest zinc depletion and dietary fat intake on the response to rosiglitazone in mice lacking LDL-R. To our knowledge, this is the first study to investigate the effect of rosiglitazone and dietary zinc depletion in this strain of mice.

Growth retardation is well known to be one of the major symptoms of zinc deficiency in the human being [4]. In the current study, the mice were on either a zinc-deficient or a zinc-adequate diet in powder form. Apparently it took some time for the mice to adjust themselves to the powder-formed experimental diets, which could explain why the body weight was generally not changed until day 9. After that, only mice on the

zinc-adequate diet gained weight, contrasting the almost unchanged body weight of the zinc-deficient mice.

Based on our preliminary study with LDL-R normal mice and the short duration of the study, we did not expect plasma zinc concentrations to be significantly affected. And in fact, plasma zinc levels were not different between mice fed the zinc depleted compared to the zinc adequate diets regardless of rosiglitazone treatment. However, within the dietary zinc groups (0 zinc or 30 zinc) rosiglitazone treatment increased plasma zinc levels. We verified that the rosiglitazone solution was zinc-free, therefore this repartitioning of plasma zinc by rosiglitazone appears to be a specific effect of the drug. Liver zinc concentration is considered to be more responsive to dietary zinc intake than plasma zinc [108] and indeed we observed lower liver zinc concentrations in mice fed the low compared to the adequate zinc diet. However, with rosiglitazone treatment liver zinc was reduced only in the mice fed the zinc adequate diet. The observation that rosiglitazone increased plasma zinc in both dietary groups suggests that other body zinc stores besides liver may be mobilized by rosiglitazone, and this observation is worthy of further study.

The present *in vivo* study generally supports the *in vitro* finding of PPAR dysregulation during zinc deficiency. For example, rosiglitazone treatment significantly down-regulated iNOS gene expression in abdominal aorta only in zinc adequate mice, indicating that only under zinc adequate condition is PPAR γ functioning properly to inhibit NF- κ B activity. The pro-inflammatory gene iNOS is regulated by NF- κ B [88]. During inflammation, smooth muscle cells and macrophages express iNOS thus causing an increase in NO generation. NO can react with O₂^{•-} to produce the strong oxidant ONOO⁻, which in turn can increase lipid peroxidation, protein nitration, and LDL oxidation, contributing to the pathogenesis of atherosclerosis [83]. Interestingly, in the current study, the zinc adequate mice had unexpected higher basal levels of iNOS mRNA expression in abdominal aorta, which could be due to the high-fat feeding. In our preliminary work using the same mouse model with low-fat diet feeding, iNOS mRNA expression in abdominal aorta were higher in the zinc-deficient mice than in the zinc-adequate mice (see Appendix, Fig. I). In the present study, MCP-1 mRNA expression was also observed to be higher in rosiglitazone treated zinc deficient mice than in

rosiglitazone treated zinc adequate mice. This “adverse” effect of rosiglitazone during zinc deficiency again suggests that proper anti-inflammatory properties of PPAR γ are compromised during zinc deficiency. MCP-1 is a potent chemoattractant for monocytes and plays an important role in monocyte recruitment and endothelium activation. The expression of MCP-1 by endothelial cells is NF- κ B regulated [109].

Both zinc and metallothioneins (MT) can protect cells against redox stress [110]. MT are intracellular cysteine-rich transition metal binding proteins critical in maintaining cellular zinc homeostasis [17]. MT have zinc-buffering and anti-oxidant properties [17, 18, 110] and might prevent diabetic cardiovascular complications [111]. In the current *in vivo* study, zinc deficiency tended to down-regulate liver MT1 mRNA expression compared to zinc adequate mice (see Appendix, Fig. II). Furthermore, rosiglitazone significantly up-regulated liver MT1 mRNA expression in mice regardless of the zinc status (see Appendix, Fig. II), suggesting that the anti-inflammatory and anti-atherogenic properties of rosiglitazone could be in part due to its induction of MT.

Another critical element in the etiology of atherosclerosis is via regulation by cytokines [112]. There are basically two categories of cytokines, i.e. pro-inflammatory cytokines, which promote inflammation, such as IL-1, TNF, and IL-6; and anti-inflammatory cytokines, which inhibit the activity of pro-inflammatory cytokines, such as IL-4, IL-10, and IL-13 [113, 114]. Epidemiological studies have shown that plasma IL-6 level is a potent independent predictor of risk of future cardiovascular events [93]. IL-6 exhibits its main inflammatory properties in the acute phase response by promoting the production of a variety of hepatic acute phase proteins [93, 115]. Elevated levels of IL-6 also have been found in both human and mice atherosclerotic lesions and can act in a pro-inflammatory and pro-coagulant way, thus contributing to lesion progression and thrombotic complications [93]. On the other hand, IL-10 is an important anti-inflammatory cytokine which inhibits the production of pro-inflammatory monocyte/macrophage and neutrophil cytokines, and pro-atherogenic T-helper 1 (Th1) lymphocyte cytokines [114, 116]. By deactivating pro-inflammatory cytokines and iNOS, IL-10 has anti-inflammatory properties on cardiovascular tissues [117]. In the present study, zinc deficiency significantly elevated the pro-inflammatory IL-6 and decreased the anti-inflammatory IL-10 levels in plasma. IL-12 is an immunoregulatory

cytokine that favors Th1 cell phenotype and induces Th1 cytokines, such as $\text{INF}\gamma$ and IL-2. By regulating cell mediated immunity and activating macrophages, the Th1 cytokines contribute to the development of atherosclerosis [114, 116]. In the current study, rosiglitazone had a significant interaction with zinc status to regulate plasma IL-12 levels by decreasing it during zinc adequacy and increasing it during zinc deficiency, which indicates that the proper anti-inflammatory effect of the $\text{PPAR}\gamma$ agonist rosiglitazone requires zinc.

An earlier research in our lab utilizing the same mouse model (i.e. $\text{LDL-R}^{-/-}$ mice) has revealed that zinc deficiency can increase pro-atherosclerotic markers, such as $\text{NF-}\kappa\text{B}$ DNA binding and vascular cell adhesion molecule-1 (VCAM-1) expression, and decrease $\text{PPAR}\gamma$ DNA binding in these animals [118]. In the current study, the expression of $\text{I}\kappa\text{B}\alpha$ protein in liver tissue was elevated by rosiglitazone only in zinc adequate mice but not in zinc deficient mice, suggesting that rosiglitazone exerts its anti-inflammatory effect by up-regulating $\text{I}\kappa\text{B}\alpha$ only during zinc adequacy. $\text{I}\kappa\text{B}\alpha$ is a natural inhibitor of $\text{NF-}\kappa\text{B}$. By interacting with and shielding the nuclear localization signal of $\text{NF-}\kappa\text{B}$, $\text{I}\kappa\text{B}\alpha$ prevents the translocation of $\text{NF-}\kappa\text{B}$ to the nucleus and its DNA binding [119, 120]. $\text{I}\kappa\text{B}\alpha$ is also able to dissociate prebound $\text{NF-}\kappa\text{B}$ from its cognate DNA binding sites [119]. In the current study, $\text{NF-}\kappa\text{B}$ DNA binding activity in liver tissue was not significantly affected by either zinc status or rosiglitazone. However, rosiglitazone tended to decrease $\text{NF-}\kappa\text{B}$ DNA binding during zinc adequacy, a trend that was reversed during zinc deficiency. The $\text{NF-}\kappa\text{B}$ DNA binding activity data seem to be consistent with the $\text{I}\kappa\text{B}\alpha$ protein expression data. Together they can partially explain the observed iNOS and MCP-1 gene expression patterns in these $\text{LDL-R}^{-/-}$ mice. In the present study, interestingly, both $\text{PPAR}\gamma$ mRNA expression in abdominal aorta (see Appendix, Fig. III) and PPAR DNA binding activity in liver were higher in zinc deficient mice, suggesting a compensatory process in these mice, i.e. up-regulation of the anti-inflammatory transcription factor PPAR and its DNA binding activity against decreased PPAR signaling. A similar phenomenon of increased $\text{PPAR}\gamma$ mRNA level in thoracic aorta during zinc deficiency was observed earlier in a study using the same mouse model [118]. Taken together, these *in vivo* studies suggest that adequate zinc is crucial in

providing an overall anti-inflammatory environment by inhibiting NF- κ B and by activating protective PPAR signaling.

In conclusion, our present *in vivo* study suggests that zinc deficiency intensifies pro-inflammatory and impairs anti-inflammatory events in the atherogenic LDL-R^{-/-} mouse model by activating NF- κ B pathway and compromising PPAR function. The *in vivo* data are generally in accordance with the *in vitro* findings made in endothelial cells as has been described in Chapter Two (Fig. 3.7). Adequate dietary zinc intake is therefore recommended in patients treated with rosiglitazone to ameliorate inflammatory and atherosclerotic events.

Table 3.1. Experimental diets¹

Ingredient	LF / 0 Zn	HF / 0 Zn	LF /30 Zn	HF /30 Zn
	<i>g/kg</i>			
Egg white	200	200	200	200
DL-Methionine	3	3	3	3
Choline bitartrate	2.5	2.5	2.5	2.5
Corn starch	397.5	397.5	397.5	397.5
Sucrose	100	100	100	100
Dyetrose	131	51	121	41
Cellulose	35	35	35	35
Corn oil	50	130	50	130
Safflower oil	20	20	20	20
Mineral Mix ²	50	50	50	50
Zinc Mix ^{3,4}	0	0	10	10
Vitamin Mix AIN-93	10	10	10	10
Biotin mix ⁵	1	1	1	1

¹ Diet ingredients were purchased from MP Biomedicals, Salon, OH except for dyetrose which was purchased from Dyets Inc., Bethlehem, PA, and corn starch, sucrose, and corn oil which were purchased from a local food supply warehouse.

² A mineral mix was prepared using elemental compounds in cornstarch to provide a zinc depleted mixture [105, 106].

³ Zinc carbonate was mixed with dyetrose and added to provide the desired final concentrations in the diets.

⁴ Actual zinc concentrations of the zinc-deficient and zinc-adequate diets determined by atomic absorption were 0.4 ± 0.1 and 33.1 ± 0.3 mg/kg, respectively.

⁵ Biotin was mixed with dyetrose and added to provide 0.005 g biotin/g egg white protein.

Table 3.2. Effects of dietary zinc status and rosiglitazone on selected plasma anti-inflammatory cytokine concentrations in LDL-R^{-/-} mice¹

Cytokine	0 Zn	0 Zn + RSG	30 Zn	30 Zn + RSG	<i>P</i> -values ²		
					Overall	Zn	RSG
	<i>pg/mL</i>						
IL-4 ³	7.1 ± 0.3	6.6 ± 0.3	6.7 ± 0.3	7.0 ± 0.3	0.602	0.955	0.622
IL-10 ⁴	53.9 ± 8.3	51.4 ± 7.3	67.3 ± 8.0	85.3 ± 7.6	0.012	0.004	0.323
IL-13 ⁴	179.5 ± 9.3	166.2 ± 8.2	163.3 ± 8.9	173.3 ± 8.9	0.675	0.730	0.718

¹ Values are means ± SEM.

² *P*-values from two-way ANOVA. Zn × RSG interactions were not significant, *P* > 0.05.

³ n = 10-14.

⁴ n = 10-13.

Table 3.3. Effects of dietary zinc status and rosiglitazone on selected plasma pro-inflammatory cytokine/chemokine concentrations in LDL-R^{-/-} mice¹

Cytokine/ Chemokine	0 Zn	0 Zn + RSG	30 Zn	30 Zn + RSG	P-values ²			
					Overall	Zn	RSG	Zn×RSG
	<i>pg/mL</i>							
IL -1 α ³	12.1±3.0	16.0±2.5	26.6±2.8	25.5±2.7	0.001	<0.001	0.604	*
IL -2 ³	25.8±4.1	24.2±3.4	20.6±3.7	23.2±3.7	0.801	0.406	0.891	*
IL -6 ⁴	60.6±5.5	76.7±4.9	57.3±4.5	56.6±4.7	0.018	0.023	0.124	0.095
IL -12 ⁵	105.0±15.9 ^b	130.6±12.3 ^b	184.2±15.0 ^a	104.6±15.0 ^b	0.002	0.076	0.072	0.001
IL -17 ⁶	20.3±2.0	16.7±1.7	18.5±1.8	16.2±1.9	0.428	0.537	0.116	*
TNF α ⁶	15.0±2.6	16.0±2.1	13.2±2.3	10.7±2.5	0.419	0.146	0.752	*
MCP-1 ⁵	85.3±44.4	145.2±34.4	98.1±36.9	110.8±40.1	0.700	0.784	0.359	*

¹ Values are means \pm SEM.

² P-values from two-way ANOVA. Means without a common letter differ ($a > b$), $P < 0.01$. * Zn \times RSG interactions were not significant, $P > 0.05$.

³ n = 10-14.

⁴ n = 9-13.

⁵ n = 9-15.

⁶ n = 10-15.

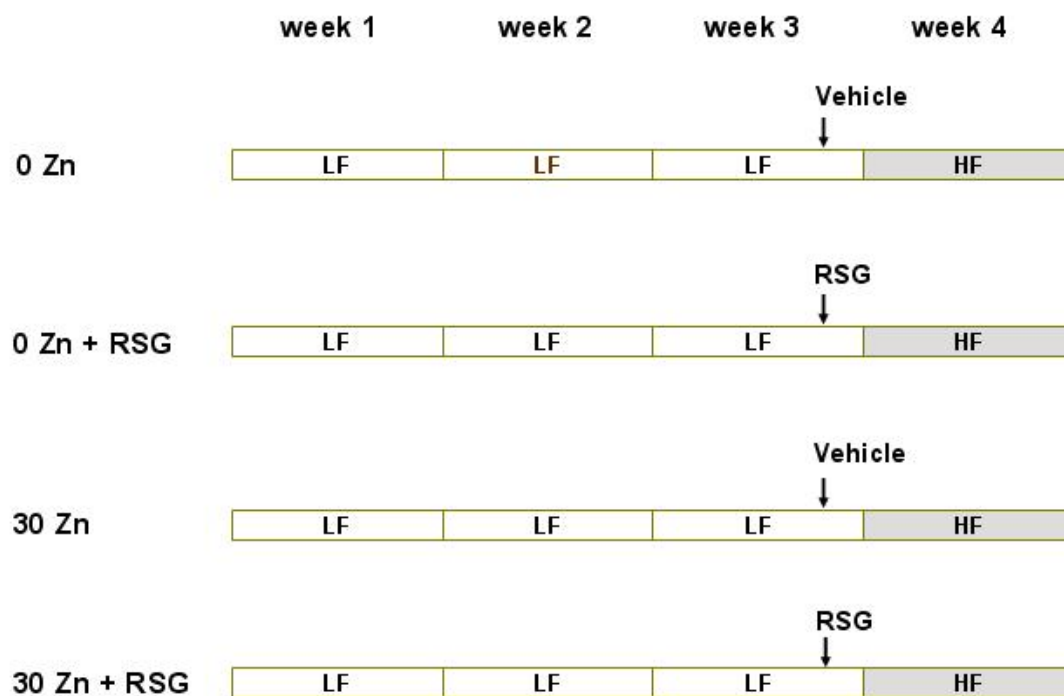


Figure 3.1. Treatment of the LDL-R^{-/-} mice.

LDL-R^{-/-} mice were fed a low-fat diet with either 0 or 30 mg/kg of zinc. After 3 wk of feeding the low-fat diet, all mice were fed a high-fat diet for 1 wk, without changing the original zinc nutritional status. Rosiglitazone (20 mg/kg/d) or the vehicle (0.25% of methylcellulose) was administered by gavage once per day for 9 d, which was initiated 2 d prior to the start of the high-fat regimen. LF, low-fat; HF, high-fat. 0 Zn, 0.4 mg/kg of zinc; 30 Zn, 33.1 mg/kg of zinc. RSG, rosiglitazone.

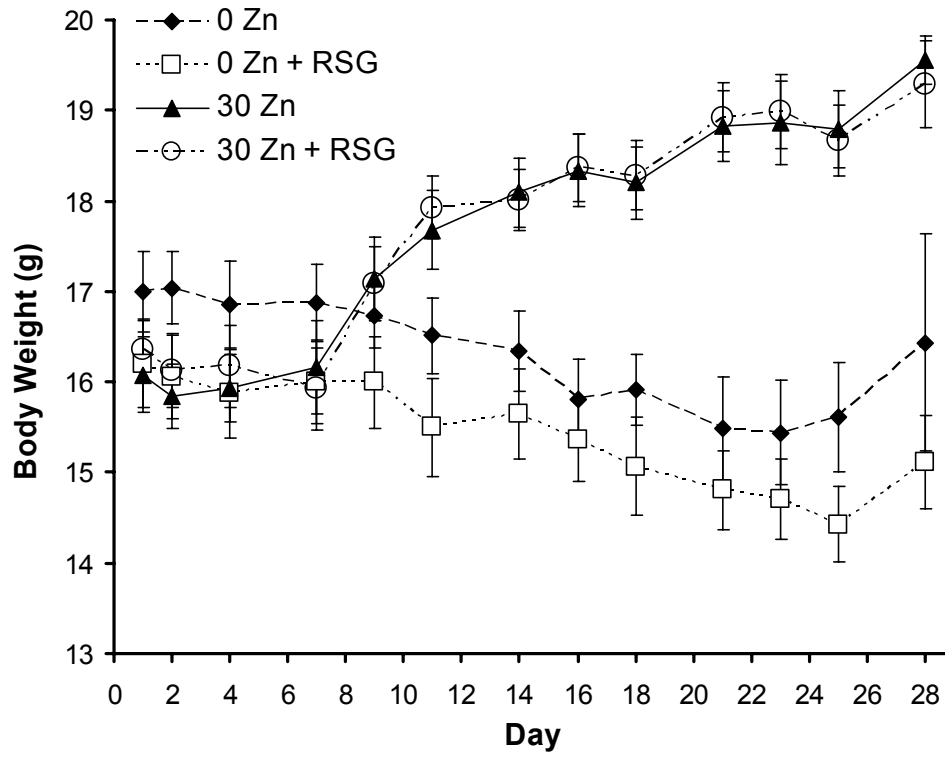


Figure 3.2. Body weight changes of the LDL-R^{-/-} mice.

Values are means \pm SEM, n = 10-15.

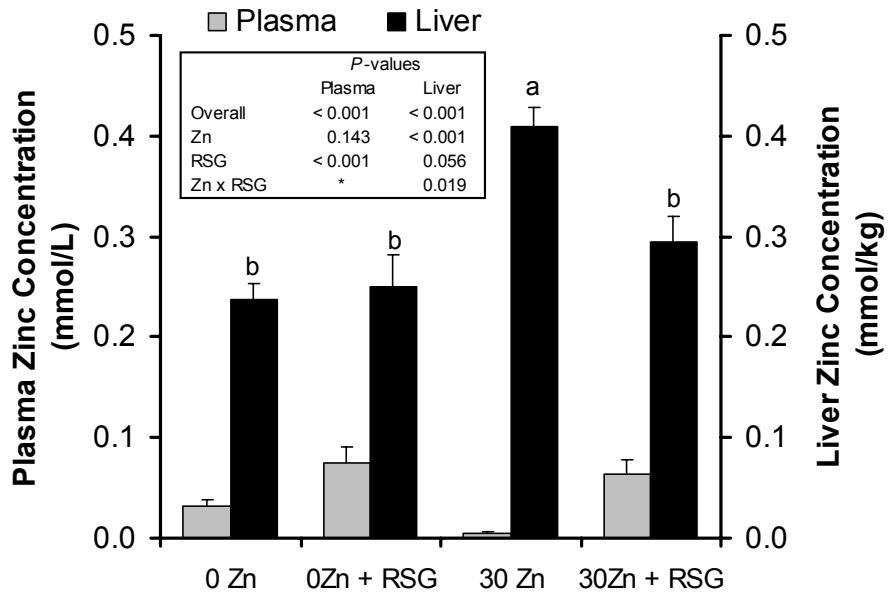


Figure 3.3. Effects of dietary zinc status and rosiglitazone on plasma and liver zinc levels in LDL-R^{-/-} mice.

Values are means \pm SEM, n = 9-15. Means without a common letter differ (a > b), P < 0.01. * Zn \times RSG interaction was not significant (P > 0.05).

A

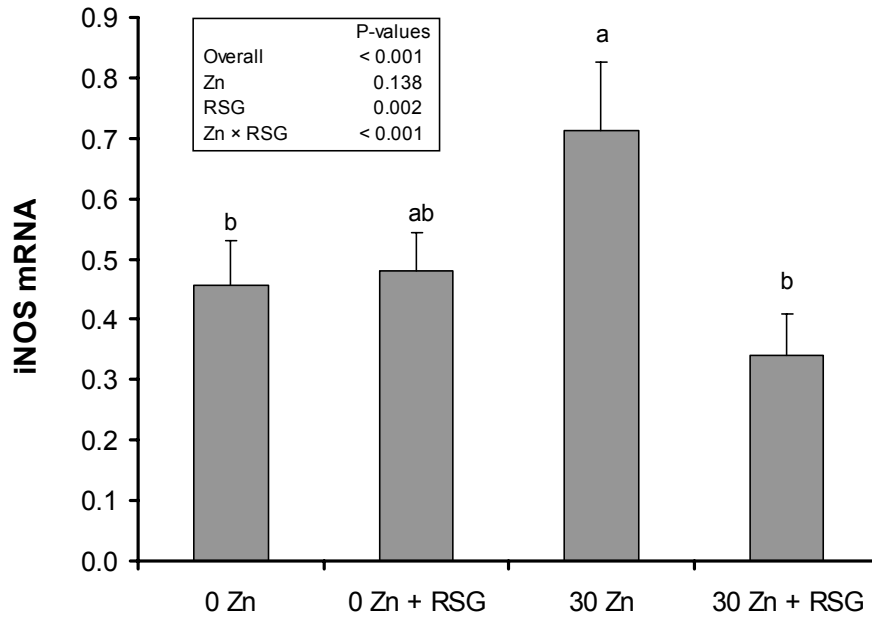


Figure 3.4. Effects of dietary zinc status and rosiglitazone on iNOS (A) and MCP-1 (B) gene expression in LDL-R^{-/-} mice.

The vertical axis in each graph represents relative units, calculated as the ratio of the copy number of the target gene over the copy number of the endogenous control (18S rRNA and β -actin, respectively). Values are means \pm SEM, n = 7-9. Means without a common letter differ (a > b), P < 0.05.

B

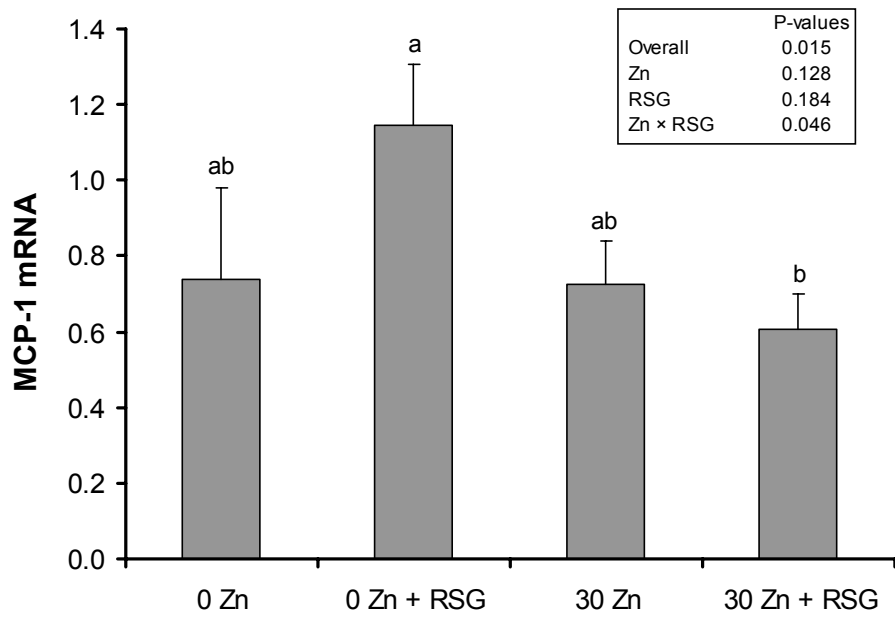


Figure 3.4 (Continued)

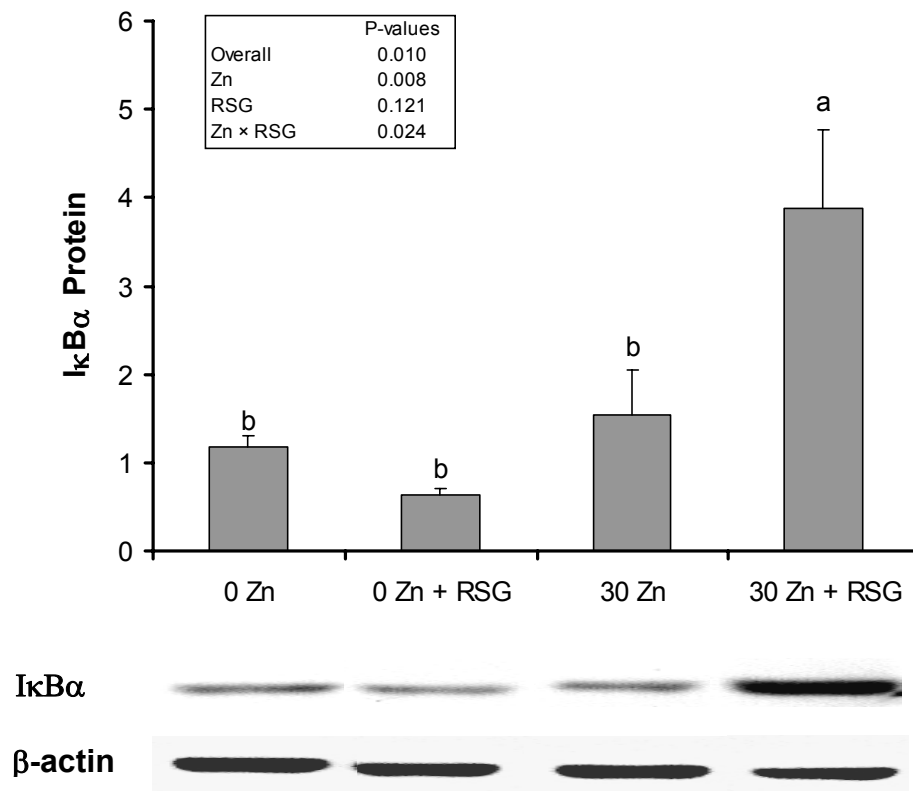


Figure 3.5. Effects of dietary zinc status and rosiglitazone on IκBα protein expression in LDL-R^{-/-} mice

The values are ratios of the densitometric units of IκBα over those of β-actin. Values are means ± SEM, n = 3. Means without a common letter differ (a > b), P < 0.05. The gel data are a representative of the typical outcome of three repeated Western blot experiments.

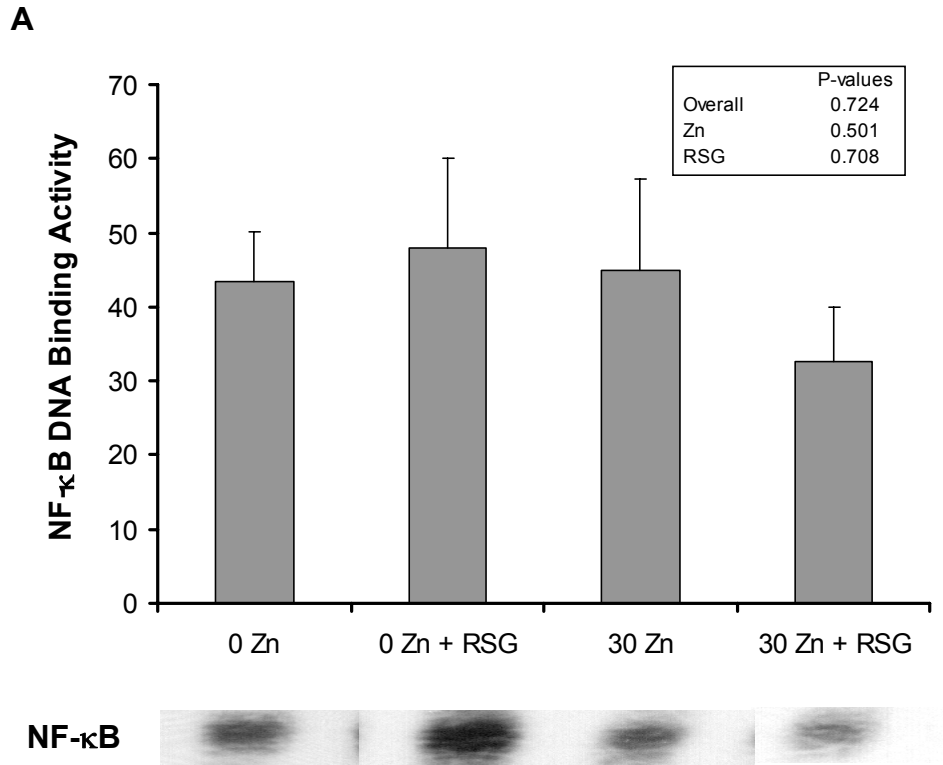


Figure 3.6. Effects of dietary zinc status and rosiglitazone on NF-κB (A) and PPAR (B) DNA binding activities in LDL-R^{-/-} mice.

The vertical axis in each graph represents densitometric units. Values are means \pm SEM, n = 3. The gel data are representatives of the typical outcome of three repeated EMSA experiments for NF-κB and PPAR, respectively.

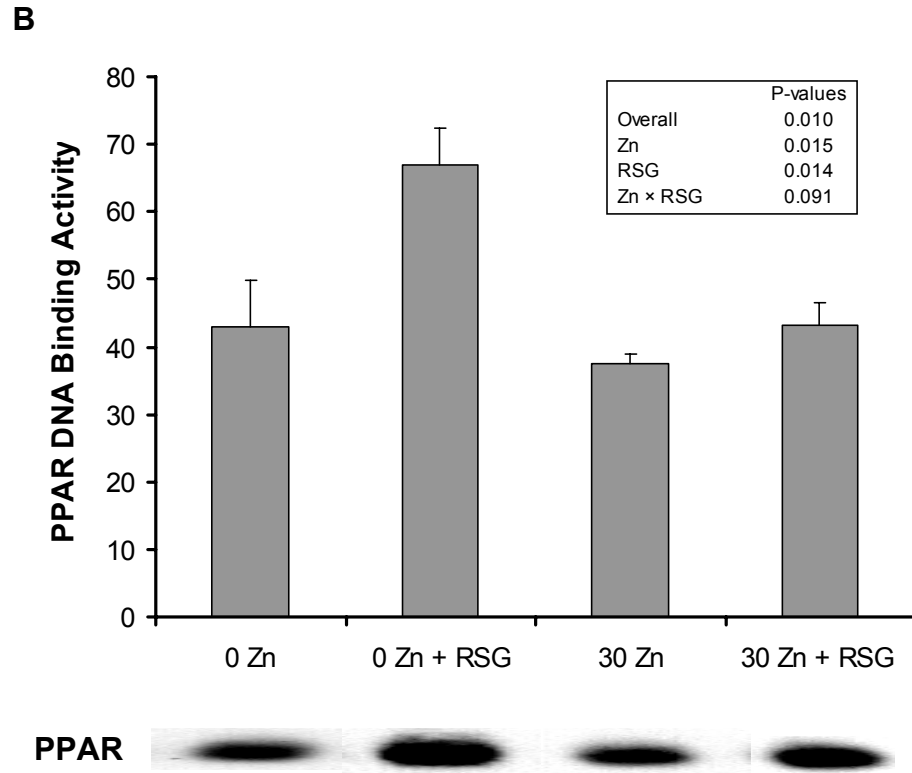


Figure 3.6 (Continued)

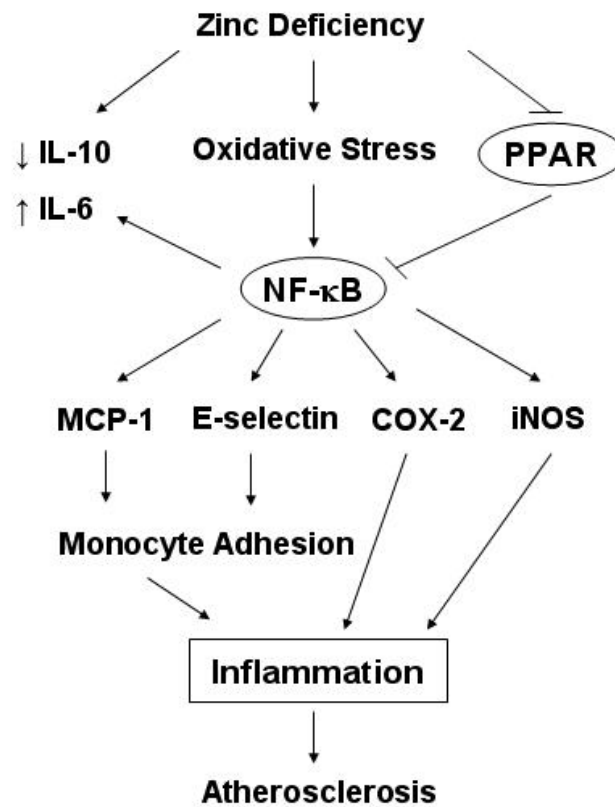


Figure 3.7. Proposed mechanism of pro-inflammatory environment and endothelial cell activation during zinc deficiency.

Zinc deficiency induces an increase in cellular oxidative stress, activation of NF- κ B and induction of inflammatory cytokines and adhesion molecules. The anti-inflammatory properties of PPARs are blocked in part by zinc deficiency, further contributing to inflammation and monocyte adhesion to activated endothelial cell. The apparent imbalance of NF- κ B and PPAR signaling during zinc deficiency may be a major risk factor of atherosclerosis.

Chaper 4. Zinc Deficiency Alters Lipid Metabolism in LDL-Receptor-Deficient Mice Treated with Rosiglitazone

4.1 Synopsis

Zinc is a structural and functional component of PPAR and zinc deficiency may be associated with an increased risk for cardiovascular diseases. We tested the hypothesis that zinc deficiency compromises lipid metabolism in rosiglitazone-treated mice lacking the functional LDL-R gene. LDL-R deficient (LDL-R^{-/-}) mice were maintained for three weeks on low-fat (7g/100g) diets that were either zinc deficient or zinc adequate. Subsequently, diets were adjusted to a high-fat (15g/100g) regimen for one week to produce a biological environment of mild oxidative and inflammatory stress. Half of the mice within each zinc group were gavaged daily with the PPAR γ agonist rosiglitazone, starting two days prior to the high-fat feeding. Selected lipid parameters were studied. Zinc deficiency increased plasma total cholesterol, which was also elevated by rosiglitazone. Zinc deficiency also caused an increased lipoprotein-cholesterol distribution towards the non-HDL fraction (VLDL, intermediate density lipoprotein, LDL). Plasma total fatty acids tended to be increased during zinc deficiency, and rosiglitazone treatment resulted in similar changes in the fatty acid profile in zinc deficient mice. Fatty acid translocase (FAT/CD36) expression in abdominal aorta was up-regulated by rosiglitazone only in zinc-deficient mice. In contrast, rosiglitazone treatment markedly increased lipoprotein lipase (LPL) expression only in zinc-adequate mice. These data suggest that in this atherogenic mouse model treated with rosiglitazone, lipid metabolism can be compromised during zinc deficiency, and that adequate dietary zinc may be considered during therapy with the anti-diabetic medicine rosiglitazone.

4.2 Introduction

Cardiovascular diseases are a major health problem in industrialized countries and have a rising incidence in the non-industrialized part of the world as well. Causes for the development of atherosclerosis are usually of multiple nature. Lifestyle and nutrition can be closely linked to the onset and the pace of progression of atherosclerotic events [121,

122]. Hyperlipidemia, central obesity, impaired glucose tolerance and overall insulin resistance are among the many risk factors associated with accelerated pathology of atherosclerosis [123].

Studies in rodent models suggest that zinc supplementation is effective for reducing the incidence of both Type I and Type II diabetes [124], and that zinc deficiency can activate stress pathways resulting in loss of insulin sensitivity [125]. Evidence also suggests that Type II diabetic patients experience zinc malabsorption and increased excretion of urinary zinc [6].

Synthetic PPAR γ agonists, such as thiazolidinediones (including rosiglitazone and pioglitazone), improve insulin sensitivity and glycemic control in type II diabetes and may reduce atherosclerosis progression in patients with diabetes [126, 127]. Protective mechanisms of PPAR γ agonists may include favorable changes in plasma lipoprotein profiles and inflammatory markers. For example, rosiglitazone can raise HDL-cholesterol levels and lower C-reactive protein levels in patients with type II diabetes [96, 101, 128]. Rosiglitazone also is able to lower postprandial triglyceride levels in patients with type II diabetes, without changes in fasting plasma triglycerides [129]. However, favorable lipid effects of rosiglitazone may not be as apparent in nondiabetic patients. Even though rosiglitazone can lower plasma concentrations of C-reactive protein and IL-6, it also can increase total cholesterol [103], as well as LDL cholesterol and triglyceride levels [130] in nondiabetic patients. Other endogenous or exogenous factors, such as the overall nutritional status of a patient, may play a role in the effectiveness of PPAR agonists as a broad antiatherogenic agent [131].

There is evidence that zinc can modulate PPAR signaling [25]. The DNA-binding domain (DBD) of PPAR has two sets of zinc fingers [22]. The specificity and polarity of PPAR-DNA binding seems to be at least in part due to features in the zinc finger domains of PPAR [132]. The DNA binding partner of PPAR, retinoid X receptor (RXR), also has a DBD with two zinc fingers involved [24]. Upon ligand activation, PPAR heterodimerizes with RXR and binds to PPAR response elements (PPRE) within the promoter region of target genes, thereby regulating or transactivating their expression [133]. As zinc is an essential constituent of the DBD of both PPAR and RXR, zinc deficiency could impair the function of this transcription factor complex.

Zinc fingers also have been described to mediate protein-lipid interactions. Zinc-containing FYVE domains are specific in recognizing and binding phosphatidylinositol-3-phosphate (PtdIns3P), a component of cell membrane [134]. It is thus very likely that zinc plays a critical role in PPAR signaling and associated regulation of cellular lipid metabolism. Thus, the objective of the present study was to explore the role of zinc in the antiatherogenic properties of the PPAR γ ligand rosiglitazone, with a focus on selected lipid parameters in an atherogenic mouse model. We hypothesize that PPAR signaling and associated lipid metabolism are compromised during zinc deficiency and that adequate dietary zinc may be critical to maintain favorable lipid effects of the anti-diabetic medicine rosiglitazone.

4.3 Materials and Methods

Animals and diets (See Chapter Three)

Sufficient plasma samples were not available from all animals for glucose analysis, resulting in variations in sample size as outlined.

Zinc quantification (See Chapter Three)

Measurement of plasma cholesterol and lipoprotein-cholesterol distribution

Plasma total cholesterol content was determined enzymatically using a commercially available kit, Wako Cholesterol E (Wako Chemicals USA, Inc., Richmond, VA). Plasma cholesterol distribution in different lipoprotein fractions was measured by Jessica Moorleghen at the University of Kentucky Cardiovascular Research Center using fast-performance liquid chromatography (FPLC) utilizing a Biologic DuoFlow System (Bio-Rad Laboratories, Hercules, CA) equipped with a SuperoseTM 6HR 10/30 column (Amersham Pharmacia Biotech AB, Uppsala, Sweden) [135].

Analysis of plasma fatty acids

Plasma total lipids were extracted with chloroform [136] followed by methyl esterification of total fatty acids with BF₃/Methanol (Supelco, Bellefonte, PA). Analysis of fatty acids was performed by Dr. Xiang-an Li at the University of Kentucky Department of Pediatrics using a gas chromatography system, Agilent 6890 GC G2579A system (Agilent, Palo Alto, CA) equipped with an OMEGAWAX™ 250 capillary column (Supelco, Bellefonte, PA) and a flame ionization detector. An Agilent 5973 network mass selective detector (Agilent, Palo Alto, CA) was used to identify target peaks. Heptadecanoic acid (17:0) was used as an internal standard for data analysis.

Real-time RT-PCR

Abdominal aorta and liver were excised from the mice, immersed in RNAlater (Qiagen, Valencia, CA) and stored at -80° C until analysis. Total RNA was isolated from abdominal aorta using RNeasy Fibrous Tissue Mini Kit (Qiagen, Valencia, CA) after surrounding adipose and connective tissues were removed, and total RNA was isolated from liver using RNeasy Mini Kit (Qiagen, Valencia, CA). cDNA was generated using the Reverse Transcription System (Promega, Madison, WI). Gene expression was determined by real-time PCR using the ABI Prism 7300 Real Time PCR System (Applied Biosystems, Branchburg, NJ) and TaqMan® Universal PCR Master Mix, No AmpErase® UNG (Applied Biosystems, Branchburg, NJ). TaqMan® gene expression assays were used for mouse fatty acid translocase (FAT/CD36), and lipoprotein lipase (LPL) (Mm00432403_m1, and Mm 00434764_m1, Applied Biosystems, Branchburg, NJ). Each assay consisted of a specific pair of unlabeled PCR primers and a specific TaqMan® MGB probe which was 5' end labeled with a FAM™ reporter dye and 3' end labeled with a minor groove binder/non-fluorescent quencher (MGBNFQ). Detection of 18S rRNA, or β -actin as endogenous control, utilized pre-developed Taqman® assay reagents, i.e. Eukaryotic 18S rRNA Endogenous Control, or Mouse ACTB Endogenous Control (Applied Biosystems, Branchburg, NJ).

Measurement of plasma glucose

Plasma glucose concentration was determined using glucose oxidase/peroxidase (PGO enzymes) (Sigma-Aldrich, Saint Louis, MO) and o-dianisidine dihydrochloride (Sigma-Aldrich, Saint Louis, MO) according to the manufacturer's instruction. The amount of glucose in the test sample was determined by measurement of the absorbance at 450 nm using a SpectraMax® M2 microplate reader (Molecular Devices Corporation, Sunnyvale, CA).

Statistical analysis (See Chapter Three)

4.4 Results

Rosiglitazone treatment contributed to a predictable biological outcome by affecting plasma insulin and adiponectin concentrations. Administration of rosiglitazone resulted in a 36 % decrease in plasma insulin concentrations and a 2-fold increase in adiponectin concentrations (Table 4.1).

Zinc deficiency elevates plasma total cholesterol in LDL-R^{-/-} mice

The zinc-deficient diet led to higher concentrations of plasma total cholesterol in LDL-R^{-/-} mice compared with the zinc-adequate diet (Fig. 4.1). Treatment with rosiglitazone increased the concentration of plasma total cholesterol (Fig. 4.1).

Zinc deficiency increases non-HDL cholesterol distribution in LDL-R^{-/-} mice

Consistent with the data on plasma total cholesterol, zinc deficiency increased concentrations of plasma cholesterol contained in the non-HDL fraction [VLDL, intermediate density lipoprotein (IDL), LDL] as compared with zinc-adequate mice (area under the curves; $P < 0.001$, Fig. 4.2). In contrast, levels of HDL cholesterol were similar in all mice independent of the dietary zinc intake (Fig. 4.2). Rosiglitazone treatment had no effect on lipoprotein-cholesterol profile under either zinc-adequate or zinc-deficient conditions (Fig. 4.2).

Zinc deficiency elevates plasma fatty acid concentrations in LDL-R^{-/-} mice

The major plasma fatty acids are palmitic acid (16:0), stearic acid (18:0), oleic acid (18:1), linoleic acid (18:2), and arachidonic acid (20:4), which add up to about 90% of total plasma fatty acids [137]. Plasma total fatty acids in LDL-R^{-/-} mice tended to be increased during zinc deficiency (P = 0.080, Table 4.2). Detailed analysis of the fatty acid profile revealed that the patterns of fatty acid changes due to rosiglitazone treatment (except for 20:4) were similar and that elevated levels of 18:0 and 18:1 in zinc-deficient LDL-R^{-/-} mice were mostly responsible for the increased total fatty acid levels (Table 4.2).

The effects of rosiglitazone on expression of genes associated with lipid uptake and metabolism in LDL-R^{-/-} mice are regulated by zinc status

LPL is an enzyme which hydrolyses triglyceride-rich lipoproteins and CD36 mediates cellular uptake of free fatty acids. Zinc status did not affect the baseline LPL and CD36 mRNA expression (Fig. 4.3). Treatment with rosiglitazone up-regulated LPL mRNA expression in livers (P < 0.05, Fig. 4.3).

The effects of rosiglitazone on CD36 gene expression in abdominal aortas were also regulated by zinc status. Specifically, CD36 mRNA levels were significantly increased (1.75 fold) in zinc-deficient LDL-R^{-/-} mice which received rosiglitazone treatment (P < 0.05, Fig. 4.3). These effects were not observed in zinc-adequate mice (Fig. 4.3).

4.5 Discussion

Zinc is critical for normal function of numerous proteins. Thus, a change in cellular zinc status can affect multiple cellular events. Because PPARs play a role in lipid transport and metabolism [138], lack of zinc appears to result in dysfunctional PPAR signaling with a subsequent detrimental lipid metabolism. PPAR γ activation by its endogenous or exogenous ligands, such as TZDs, up-regulates the expression of adiponectin, a PPAR γ target gene [139], which promotes insulin sensitivity and down-

regulates inflammatory cytokines and thus decreases insulin resistance [131, 140]. Most of all, PPAR γ activates numerous genes involved in lipid storage and lipogenesis [131] and in particular in the cellular assimilation of lipids via anabolic pathways [141]. Whether or not the overall antiatherogenic properties of PPAR γ agonists are due to favorable lipid changes or anti-inflammatory properties is not clear. However, protection against cardiovascular complications by PPAR γ agonists is well accepted. For example, rosiglitazone, a PPAR γ agonist, strongly inhibited the development of atherosclerosis in LDL-R^{-/-} mice [99].

The role of zinc deficiency in atherosclerosis is not well defined; however, epidemiological studies suggest that in some population groups, low serum concentrations of zinc are associated with coronary artery disease [67]. Although controversy still exists about the effect of zinc on human lipoprotein metabolism, some studies confirmed the lipid lowering effects of zinc in humans. Oral zinc supplementation decreased total and LDL cholesterol, while HDL cholesterol increased in both normal and diabetic humans [142, 143]. Other studies, however, found that zinc supplementation had little effect on lipoprotein profiles [144] or decreased HDL cholesterol [145, 146].

In the present *in vivo* study, we provide evidence that PPAR γ -regulated gene expression and associated lipid metabolism are compromised during zinc deficiency and that adequate dietary zinc may be critical to maintain favorable lipid effects of rosiglitazone. Treatment with rosiglitazone tended to increase plasma total cholesterol more in zinc-deficient mice. Such lipid change is atherogenic and suggests that any possible favorable lipid profile induced by rosiglitazone treatment may be compromised during zinc deficiency. Furthermore, zinc deficiency alone caused a shift of lipoprotein-cholesterol distribution to the non-HDL (VLDL, IDL, and LDL) fraction. This is consistent with our previous findings that zinc deficiency can increase plasma lipids and atherosclerotic markers in LDL-R^{-/-} mice [118].

Although many studies suggest that treatment with PPAR γ agonists such as rosiglitazone stabilizes or improves plasma lipid parameters, especially in diabetic patients [102, 147, 148], other studies reported significantly increased triglycerides following treatment with rosiglitazone [130, 149, 150]. In the LDL-R^{-/-} mouse model, we

observed an elevation of total plasma fatty acids in zinc-deficient mice treated with rosiglitazone. All major plasma fatty acids appeared to be elevated in the zinc-deficient group receiving rosiglitazone. There is clear evidence that hypertriglyceridemia is an independent risk factor of cardiovascular diseases such as atherosclerosis [65, 151]. Furthermore, triglyceride-rich lipoproteins and free fatty acids are often elevated in patients with type II diabetes, and thus a major risk factor [152, 153].

Our data suggest that expression of the LPL gene, which is a PPAR γ target gene [154], and is also critical in the clearance of triglyceride-rich lipoproteins, was up-regulated in zinc-adequate mice upon treatment with rosiglitazone. Other researchers observed similar results in brown adipose tissue of rodents treated with this PPAR γ agonist [147]. In contrast, mRNA expression of LPL was minimally up-regulated in zinc-deficient mice as a result of rosiglitazone treatment, which may be due to compromised PPAR γ function. Because LPL is critical in clearance of triglyceride-rich lipoproteins, and is able to limit inflammation by generating endogenous PPAR α ligands (thus mediating PPAR α activation) [155], dysfunction of this gene due to zinc deficiency could further contribute to lipid risk factors of atherosclerosis.

Scavenger receptors like CD36 are important in the early pathology of atherosclerosis, which includes macrophage uptake of modified LDL and foam cell formation [156]. In fact, the absence of CD36 in the atherogenic ApoE-deficient mice maintained on a high fat diet resulted in a marked decrease in total lesion area in the aortic tree, which could be due to the decreased uptake of oxidized LDL by macrophages [156]. There is also evidence that an increase in CD36 is caused by defective insulin signaling and that administration of PPAR γ agonists can decrease CD36 protein [157]. In our study, CD36 gene expression in abdominal aorta was significantly up-regulated by rosiglitazone only in zinc-deficient mice, suggesting accelerated uptake of lipids and especially pro-oxidative and pro-inflammatory fatty acids, such as linoleic acid and arachidonic acid. In contrast, in another study, rosiglitazone up-regulated aortic CD36 mRNA in mice consuming a high-cholesterol diet [99]. There is evidence using human macrophages that CD36 up-regulation by darglitazone, another PPAR γ ligand, is modified by the presence or absence of physiological concentrations of albumin-bound oleic or linoleic acid [158]. In the present study, rosiglitazone treatment resulted in

elevated levels of plasma total cholesterol and total fatty acids in zinc deficient mice, which could increase cellular oxidative stress. This may be sufficient to activate the redox-sensitive transcription factor nuclear factor erythroid-2 related factor 2 (Nrf2) [159], which is another important transcription factor involved in the induction of CD36 besides PPAR γ [160]. Indeed oxidative stress has been found to increase the expression of CD36 in macrophages from atherosclerotic mice [161]. Therefore, the up-regulation of CD36 by rosiglitazone in zinc deficient mice could be due in part to the activation of Nrf2 caused by increased oxidative stress. Our data suggest that treatment with rosiglitazone during a nutritional state of zinc deficiency may increase, rather than decrease, hyperlipidemic risk factors.

There are some unexpected results in this study. For example, the similar effects of rosiglitazone on adiponectin levels in mice on either zinc deficient or zinc adequate diets suggest that adiponectin gene expression may be only partially regulated by a PPAR γ -dependent pathway and that rosiglitazone may also regulate the expression of adiponectin via PPAR γ -independent pathways [162]. Therefore, it is likely that some PPAR γ -independent pathway which is not zinc dependent contributed to the observed effects of rosiglitazone treatment on adiponectin levels.

In summary, we are providing *in vivo* evidence that zinc deficiency interacts with rosiglitazone treatment to induce selected proatherogenic lipid profiles in LDL-R^{-/-} mice. Our data also illustrate that adequate dietary zinc is critical for preventing or minimizing some possible side effects of antidiabetic PPAR γ agonists. For example, CD36 gene expression in abdominal aorta was significantly up-regulated by rosiglitazone only in zinc-deficient mice. Even though not statistically significant, treatment with rosiglitazone tended to increase plasma total cholesterol and fatty acids more when mice were zinc deficient. Because dietary zinc intake of certain population groups is still below intake recommendations [163], these data emphasize the importance of adequate dietary zinc in humans during treatment phases associated with diabetes and other cardiovascular risk factors.

Table 4.1. Effects of dietary zinc status and rosiglitazone on plasma glucose, insulin, and adiponectin concentrations in LDL-R^{-/-} mice ¹

	0 Zn	0 Zn + RSG	30 Zn	30 Zn + RSG	P-values ²		
					Overall	Zn	RSG
Glucose ³ <i>mmol/L</i>	15.6±1.6	13.1±0.9	17.2±0.9	16.0±1.1	0.0076	0.0319	0.1455
Insulin ⁴ <i>pmol/L</i>	118.5±18.1	78.5±16.7	176.3±18.1	110.6±16.7	0.0024	0.0176	0.0055
Adiponectin ⁴ <i>nmol/L</i>	511.2±121.5	1495.5±112.2	328.2±121.5	1056.6±121.5	0.0001	0.0149	0.0001

¹ Values are means ± SEM.

² P-values from two-way ANOVA. Zn × RSG interactions were not significant, *P* > 0.05.

³ n = 4–14.

⁴ n = 6–7.

Table 4.2. Effects of dietary zinc status and rosiglitazone on plasma total and individual fatty acid concentrations in LDL-R^{-/-} mice ¹

Fatty acid	0 Zn	0 Zn + RSG	30 Zn	30 Zn + RSG	<i>P</i> -values ²		
					Overall	Zn	RSG
<i>mmol/L</i>							
Total	9.39 ± 0.61	11.15 ± 0.56	8.67 ± 0.83	9.25 ± 0.78	0.062	0.080	0.150
16:0	1.85 ± 0.16	2.19 ± 0.13	1.69 ± 0.13	1.82 ± 0.13	0.039	0.059	0.115
18:0	1.23 ± 0.17	1.36 ± 0.14	0.95 ± 0.13	0.90 ± 0.14	0.045	0.015	0.837
18:1	1.52 ± 0.14	1.82 ± 0.12	1.10 ± 0.11	1.35 ± 0.12	< 0.001	< 0.001	0.031
18:2	3.40 ± 0.33	4.22 ± 0.28	3.38 ± 0.26	3.55 ± 0.28	0.128	0.232	0.130
20:4	1.40 ± 0.16	1.56 ± 0.14	1.55 ± 0.13	1.63 ± 0.14	0.557	0.453	0.393

¹ Values are means ± SEM, n = 5-8.

² *P*-values from two-way ANOVA. Zn × RSG interactions were not significant, *P* > 0.05.

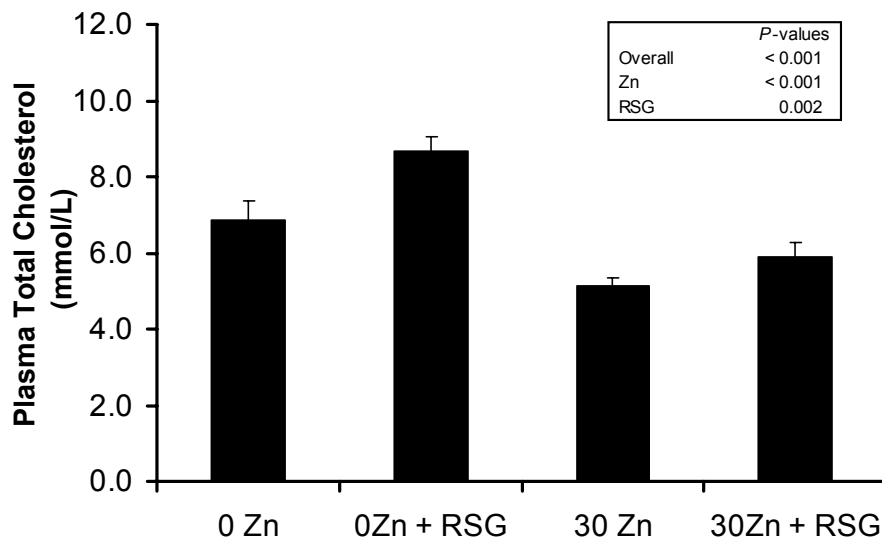


Figure 4.1. Effects of dietary zinc status and rosiglitazone on plasma total cholesterol concentration in LDL-R^{-/-} mice.

Values are means \pm SEM, n = 10-15. Zn \times RSG interaction was not significant ($P > 0.05$).

A

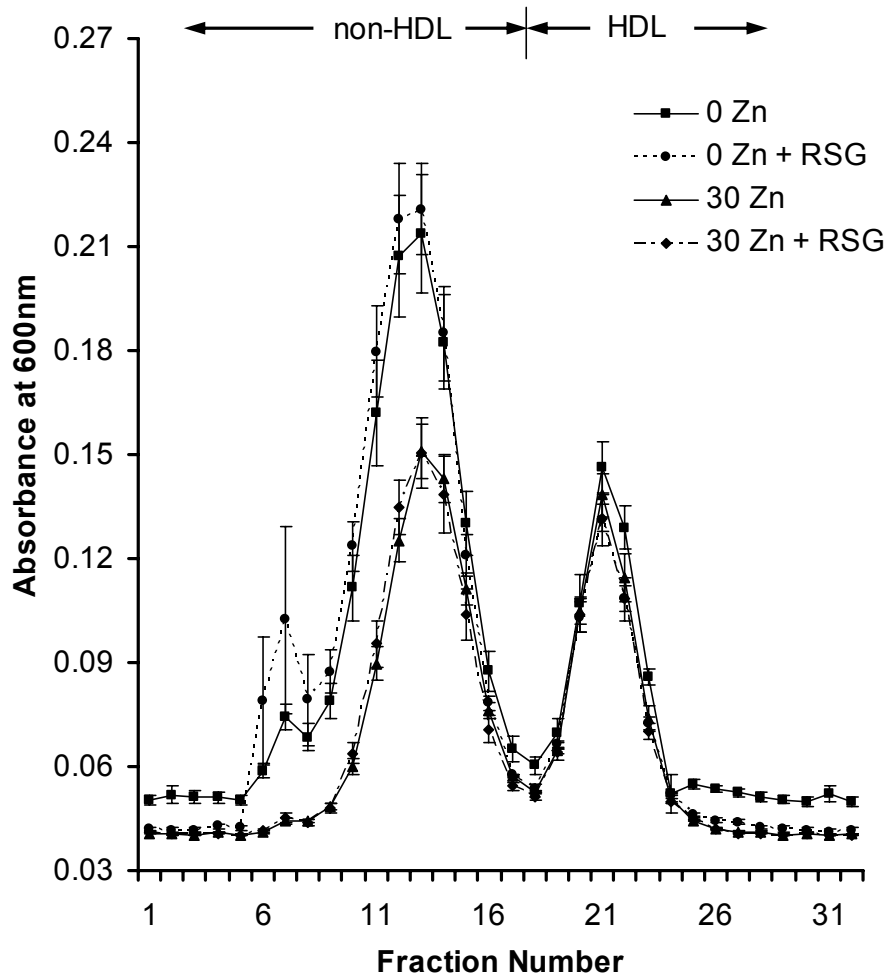


Figure 4.2. Effects of dietary zinc status and rosiglitazone on cholesterol distribution in different lipoprotein fractions in LDL-R^{-/-} mice.

A. Lipoprotein-cholesterol distribution. An equal amount (50 μ L) of individual plasma samples was applied to the FPLC column. The non-HDL includes VLDL, IDL, and LDL. B. Area under the curve. Values are means \pm SEM, n = 4. Zn \times RSG interactions were not significant ($P > 0.05$).

B

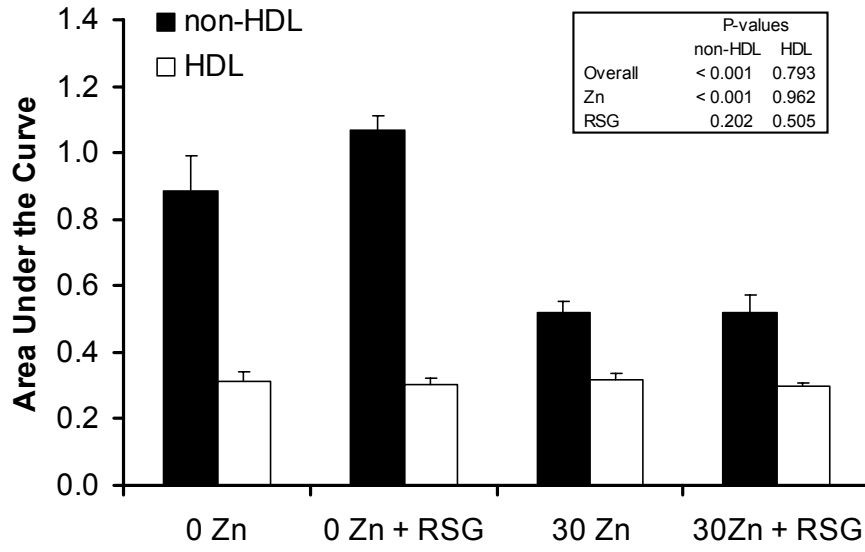


Figure 4.2 (Continued)

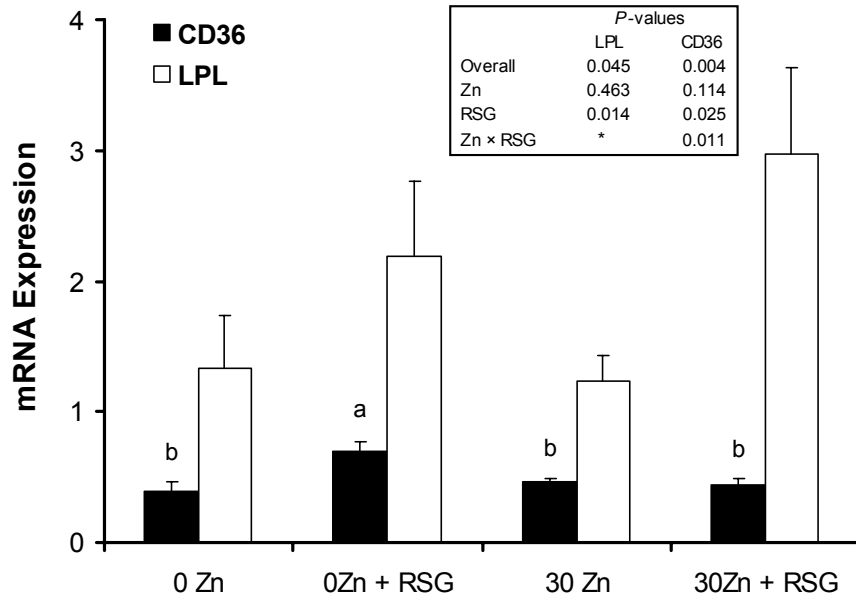


Figure 4.3. Effects of dietary zinc status and rosiglitazone on LPL and CD36 gene expression in LDL-R^{-/-} mice.

The vertical axis represents relative units, calculated as the ratio of the copy number of the target gene over the copy number of the endogenous control (18S rRNA and β -actin, respectively). Values are means \pm SEM, n =10-15 for LPL and 7-9 for CD36 mRNA expression, respectively. * Zn \times RSG interaction was not significant ($P > 0.05$).

Chaper 5. Zinc Nutritional Status Modulates Expression of AhR-Responsive P450 Enzymes in Vascular Endothelial Cells

5.1 Synopsis

Zinc has anti-inflammatory properties and is crucial for the integrity of vascular endothelial cells, and the development and homeostasis of the cardiovascular system. The aryl hydrocarbon receptor (AhR) which is expressed in the vascular endothelium also plays an important role in responses to xenobiotic exposure and cardiovascular development. We hypothesize that cellular zinc can modulate induction of AhR-responsive genes in endothelial cells. To determine if zinc deficiency can alter responses to AhR ligands, aortic endothelial cells were exposed to the AhR ligands 3, 3', 4, 4'-tetrachlorobiphenyl (PCB77) or beta-naphthoflavone (β -NF) alone or in combination with the membrane permeable zinc chelator TPEN, followed by measurements of the AhR responsive cytochrome P450 enzymes CYP1A1 and 1B1. Compared to vehicle-treated cells, both PCB77-induced CYP1A1 activity (EROD) and mRNA expression were significantly reduced during zinc deficiency. In addition, PCB77 and β -NF-mediated up-regulation of CYP1A1 and CYP1B1 protein expression was significantly reduced in zinc-deficient endothelial cells. The inhibition of CYP1A1 and CYP1B1 protein expression caused by zinc deficiency was reversible by cellular zinc supplementation. Overall, our results strongly suggest that nutrition can modulate an environmental toxicant-induced biological outcome and that adequate levels of individual nutrients such as zinc are necessary for induction of AhR-responsive genes in vascular endothelial cells.

5.2 Introduction

The aryl hydrocarbon receptor (AhR) is a ligand-activated transcription factor that is normally found in the cytoplasm and complexed with Hsp90, XAP2, Ara9 and p23. Upon activation, the AhR complex goes through a conformational change that exposes a nuclear localization signal domain and triggers translocation from the cytosol to the cell

nucleus where it forms a complex with ARNT/HIF-1 β . This complex recognizes specific enhancer domain sequences in the promoter regions of responsive genes that are known as xenobiotic response elements (XREs). The AhR/ARNT heterodimers stimulate transcription of Phase I and Phase II xenobiotic metabolizing enzymes. Cytochrome P450 genes, specifically those belonging to the CYP1 family (e.g. CYP1A1/2 and CYP1B1) are highly inducible by AhR activation, and the molecular mechanisms involved in their regulation by AhR have been well characterized [45, 50]. Although most of the research performed on AhR has focused on its role in the molecular, biochemical, and toxic responses to xenobiotic ligands, recent studies have also shown that the AhR plays a critical role in the development of various organ systems and cardiovascular homeostasis [51]. For example, mice that lack the AhR gene have been shown to suffer from cardiac fibrosis, hypertrophy, increased left ventricular mass, increased expression of the cardiac hypertrophy markers β -myosin heavy chain, and β -myosin light chain 2V, and increased plasma levels of the vasoactive agents angiotensin II and endothelin-1 [164-166]. Such findings combined with the high degree of conservation of AhR among species suggest that, in addition to orchestrating responses to exposure to xenobiotic ligands, the AhR plays an important role in systemic homeostasis and development [50]. Little is known about nutritional modulation of AhR-mediated cell signaling. The current study focuses on the micronutrient zinc, because of its importance in regulating protein structure and cell signaling [55].

Zinc has multiple roles in maintaining the physiological conditions of the cardiovascular system [55], and zinc may be critical in normal vascular development. For example, zinc deficiency leads to decreased function of transcription factors associated with cardiovascular development and homeostasis (e.g. PPARs α and γ , and GATA-4) [26, 56]. Furthermore, a threshold activity of the zinc finger transcription factors GATA4 and GATA6 is required for gene expression in the developing cardiovascular system [167]. There is also evidence that zinc may be critical for normal AhR signaling. For example, both AhR and ARNT can interact with the zinc finger domain of Sp1 via their basic HLH/PAS domains [54], and AhR can participate in induction of the zinc finger transcription factor Slug, which, in turn, regulates cellular physiology including cell adhesion and migration [168].

The objectives of the experiments described below were to determine if zinc plays a critical role in AhR function in the vascular endothelium. Our data strongly suggests that zinc is required for induction of the AhR-responsive genes CYP1A1 and CYP1B1 upon endothelial cell exposure to xenobiotic and non-toxic AhR ligands. Alterations in AhR function and transcription present a novel mechanism for understanding induction of vascular diseases associated with zinc deficiency and exposure to environmental pollutants such as AhR ligands.

5.3 Materials and Methods

Cell culture and experimental media

Endothelial cells were isolated from porcine pulmonary arteries and cultured as previously described [75]. Cells were exposed to experimental media containing the membrane-permeable zinc chelator N, N, N', N'-Tetrakis - (2-pyridylmethyl) ethylenediamine (TPEN) (Sigma-Aldrich, St. Louis, MO) with or without zinc supplementation (20 μ M) and/or the AhR ligands PCB77 or β -naphthoflavone (β -NF) (Sigma-Aldrich, St. Louis, MO) for 24 h. PCB77 was kindly provided by Dr. Larry W. Robertson (University of Iowa). The control media were composed of culture media containing 0.05 % of ethanol and up to 0.04 % of DMSO.

Measurement of CYP1A activity

Cellular cytochrome P450 1A (CYP1A) activity was measured in intact endothelial cells grown in 48 well plates (Costar, Corning Incorporated, NY) by ethoxyresorufin-o-deethylase (EROD) activity assay as previously described [169, 170]. 7-Ethoxyresorufin was used as a CYP1A substrate. CYP1A activity indicated by the fluorescence of resorufin generated was measured using a Cytofluor 4000 plate reader (PE Biosystems, Foster City, CA) with excitation and emission wave lengths at 530 nm and 590 nm, respectively.

Measurement of CYP1A1 gene expression

Total RNA was extracted with Trizol reagent (Invitrogen, Carlsbad, CA) according to the manufacturer's direction. cDNA was generated using the Reverse Transcription System (Promega, Madison, WI). Gene expression of CYP1A1 was determined by RT-PCR. β -actin was used as an endogenous control for normalizing the expression of CYP1A1. Specific primer sequences were synthesized by IDT Technologies, Inc, San Jose, CA. The primers used were: CYP1A1, forward, 5'-TGGAG AGGCA AGAGT AGTTG G-3', and reverse, 5'-GGCAC AACGG AGTAG CTCAT A-3'; β -actin, forward, 5'-GGGACCTGACCGACTACCTC-3', and reverse, 5'-GGGCGATGATCTTGATCTTC-3'. Thermocyclings were performed as previously described [169, 171]. The PCR products were separated by 1% agarose gel electrophoresis, stained with SYBR gold (Invitrogen, Carlsbad, CA) and visualized utilizing phosphoimaging technology (FLA-2000, Fuji, Stamford, CT).

Measurement of CYP1A1 and CYP1B1 protein expression

Cellular protein was extracted as previously described [62]. Protein extracts were electrophoresed on 8-10% SDS-polyacrylamide gels followed by transfer to nitrocellulose membranes. The membranes were incubated in blocking solution (5 % non-fat milk in 1 \times TBST) for 1 h followed by incubation with a 1:1000 dilution of CYP1A1 goat polyclonal IgG (Santa Cruz Biotechnology, Santa Cruz, CA) or CYP1B1 rabbit polyclonal IgG (Santa Cruz Biotechnology, Santa Cruz, CA) or a 1:4000 dilution of β -actin rabbit polyclonal IgG (Sigma, St. Louis, MO) in blocking buffer overnight at 4 °C. β -actin was used as an endogenous control to normalize the expression of proteins of interest. The membranes were then incubated with a mouse anti-goat or goat anti-rabbit secondary antibody conjugated to horseradish peroxidase. Signals of the blots were measured using the enhanced chemiluminescence (ECL) detection system (GE Healthcare, Piscataway, NJ).

Statistical analysis

Statistical analysis was performed with SPSS 12.0 (SPSS, Inc., Chicago, IL). Data were analyzed using one way ANOVA with post hoc comparisons of the means by

LSD procedure. Differences were considered significant at $P < 0.05$. Data are presented as means \pm SEM.

5.4 Results

Zinc deficiency reduces PCB77-induced CYP1A activity and CYP1A1 mRNA expression in vascular endothelial cells

To determine if zinc deficiency can alter induction of the AhR-responsive enzyme CYP1A1, we first measured PCB77 induction of CYP1A1 activity by the EROD assay. As expected, PCB77, a potent AhR agonist, significantly increased cellular CYP1A1 activity. Zinc deficiency caused by TPEN treatment did not change basal CYP1A1 activity but significantly reduced PCB77-induced CYP1A1 activity in vascular endothelial cells (Fig. 5.1A). To determine if zinc deficiency alters CYP1A1 transcription, we measured CYP1A1 mRNA expression in endothelial cells treated with PCB77 alone or in combination with TPEN. The PCB77-mediated up-regulation of CYP1A1 mRNA expression was significantly reduced during zinc deficiency (Fig. 5.1B).

Zinc deficiency compromises PCB77-induced CYP1A1 and CYP1B1 protein expression in vascular endothelial cells, which can be reversed with zinc supplementation

Western blot analysis demonstrated that the compromising effect of zinc deficiency on AhR responsive protein expression could be reversed by zinc supplementation. Specifically, PCB77 significantly increased the cellular protein levels of CYP1A1 and CYP1B1, both major PCB-inducible CYP1 enzymes. TPEN treatment alone did not affect expression of the two proteins, but co-treatment with TPEN and PCB77 led to a significant reduction in the expression of both enzymes. However, zinc supplementation of the TPEN-treated cell culture media reversed the reduction of CYP1A1 and CYP1B1 observed during zinc deficiency (Fig. 5.2).

Zinc deficiency compromises β -naphthoflavone-induced CYP1A1 protein expression in vascular endothelial cells, which can be reversed with zinc supplementation

To determine if the observations made above were specific not only to PCB77

exposure but also relevant to other AhR ligands, similar experiments were performed using the non-toxic AhR agonist β -NF. Treatment with β -NF significantly induced CYP1A1 protein expression, which was significantly reduced in TPEN-treated endothelial cells. When zinc was added back to the cell cultures, CYP1A1 protein induction by β -NF was completely reversible (Fig. 5.3).

5.5 Discussion

The results from the experiments described above suggest that induction of AhR responsive genes in the endothelium is dependent on zinc availability, i.e., our data provide evidence that zinc is required for proper induction of the AhR-CYP1 pathway. As predicted, both toxic (PCB77) and non-toxic (β -NF) AhR ligands can markedly induce both mRNA and protein of CYP1A1, as well as activity of CYP1A1. Induction of the CYP1A1 gene was markedly down-regulated during zinc deficiency. This suggests that zinc deficiency can impair enzyme function, or that zinc is critical for proper transcriptional or translational induction of gene expression. Our data also suggest that the dysfunction of the AhR pathway is zinc specific because we were able to reverse the reduction in protein of CYP1A1 (and CYP1B1) by zinc supplementation of TPEN-treated cells.

Zinc has a critical role in protein structure, enzyme activity and gene regulation. Most of the genes that are zinc regulated are involved in signal transduction, responses to stress and redox changes, growth and energy utilization [172]. Thus, zinc has a role not only in tertiary protein structure but also in the capacity of proteins to interact with DNA, RNA and other proteins. For protein-DNA and protein-RNA interactions, zinc is commonly found as a zinc finger motif in transcription factors [173]. Classical zinc fingers have also been shown to interact with RNA and DNA/RNA complexes [174]. The susceptibility of zinc fingers to zinc deprivation is not well understood. For example, certain zinc-finger transcription factors, such as 1α , 25-dihydroxyvitamin D₃ (1α , 25(OH)₂D₃) receptor (VDR) and retinoid X receptor (RXR), have been found to be inactivated due to loss of zinc as a consequence of NO-induced nitrosification of the cysteine thiols in the zinc fingers [175, 176]. Following translation, a gene is also subject

to zinc dependency during protein folding. For example, zinc is essential for certain chaperones, such as heat shock protein 40 (Hsp40) [177], and Hsp40, Hsp60, and Hsp70 mRNA expression were down-regulated during zinc deficiency [172].

One possible mechanism for our observed compromising effect of zinc deficiency on PCB77-induced CYP1A1 and CYP1B1 expression and CYP1A1 activity could have been due to changes in AhR expression. However, western blot analysis of the AhR protein expression did not show the same pattern of change (See Appendix, Fig. V). This suggests that zinc deficiency may affect cell signaling downstream of AhR. Studies from other groups also suggest that neither AhR transformation to the DNA binding form nor the AhR DNA binding is altered by depletion of metal ions, including zinc [53, 178]. However, these studies did not measure the effects of metal depletion on AhR dependent gene regulation, which may be a major target during zinc deficiency.

We provide evidence that induction of the AhR responsive P450 genes CYP1A1 and CYP1B1 is sensitive to cellular zinc depletion. The mechanism for inhibition of AhR-dependent gene up-regulation during zinc deficiency could be inhibition of zinc-dependent AhR co-factors that are necessary for transcriptional initiation and gene induction. One of these necessary interactions occurs with the transcription co-factor Sp1, which binds to GC-rich regions in the promoter of responsive genes and contains three Cys2His2 zinc fingers on its C-terminal region [179, 180]. It has been demonstrated that Sp1 expression and function is significantly reduced by cellular depletion of zinc and other metals [53, 181] and that CYP1A1 induction requires AhR/ARNT interactions with Sp1 [54]. Thus Sp1 may be a critical element in understanding the involvement of the AhR in the regulation of cardiovascular functions.

Zinc finger DNA-binding proteins such as members of the Sp1 family also contain redox-sensitive thiol groups [182]. For example, attenuation of cardiac dysfunction by PPAR- α agonists is associated with down-regulation of redox-regulated transcription factors, including Sp1, NF- κ B, and AP-1 [183]. The regulation of redox-regulated transcription factors by zinc and involvement of PPAR signaling further supports our data that zinc is also required for the anti-inflammatory properties of both PPAR- α and - γ agonists [26].

In summary, there is clear evidence that AhR function plays a critical role in the

development and homeostasis of the cardiovascular system. Our results demonstrate that zinc deficiency can inhibit AhR-dependent gene induction. Impairment of the AhR pathway presents an additional molecular mechanism by which zinc deficiency negatively alters transcription factor function and homeostasis of the vascular system.

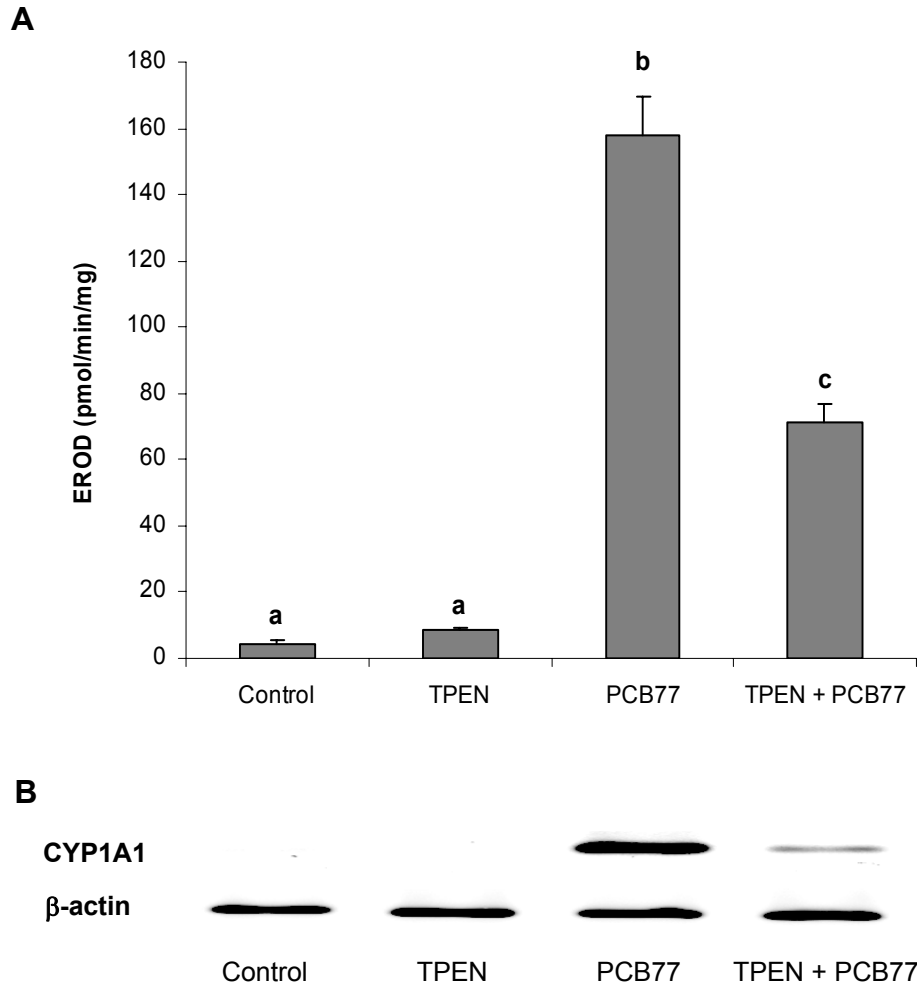


Figure 5.1. Zinc deficiency reduces PCB77-induced CYP1A activity and CYP1A1 mRNA expression in vascular endothelial cells.

A. CYP1A activity measured by EROD assay. Endothelial cells were exposed to vehicle control (0.05 % of ethanol and 0.04 % of DMSO), TPEN (1.0 μ M), PCB77 (0.04 μ M), or TPEN (1.0 μ M) plus PCB77 (0.04 μ M) for 24 hours. Bars with different letters (a, b, c) are statistically different from each other ($P < 0.05$). $n = 8$. B. CYP1A1 mRNA expression measured by RT-PCR. Cells were exposed to vehicle control, TPEN, PCB77 (3.4 μ M), or TPEN plus PCB77 for 24 hours. The gel data are a representative of the typical outcome of four repeated RT-PCR experiments.

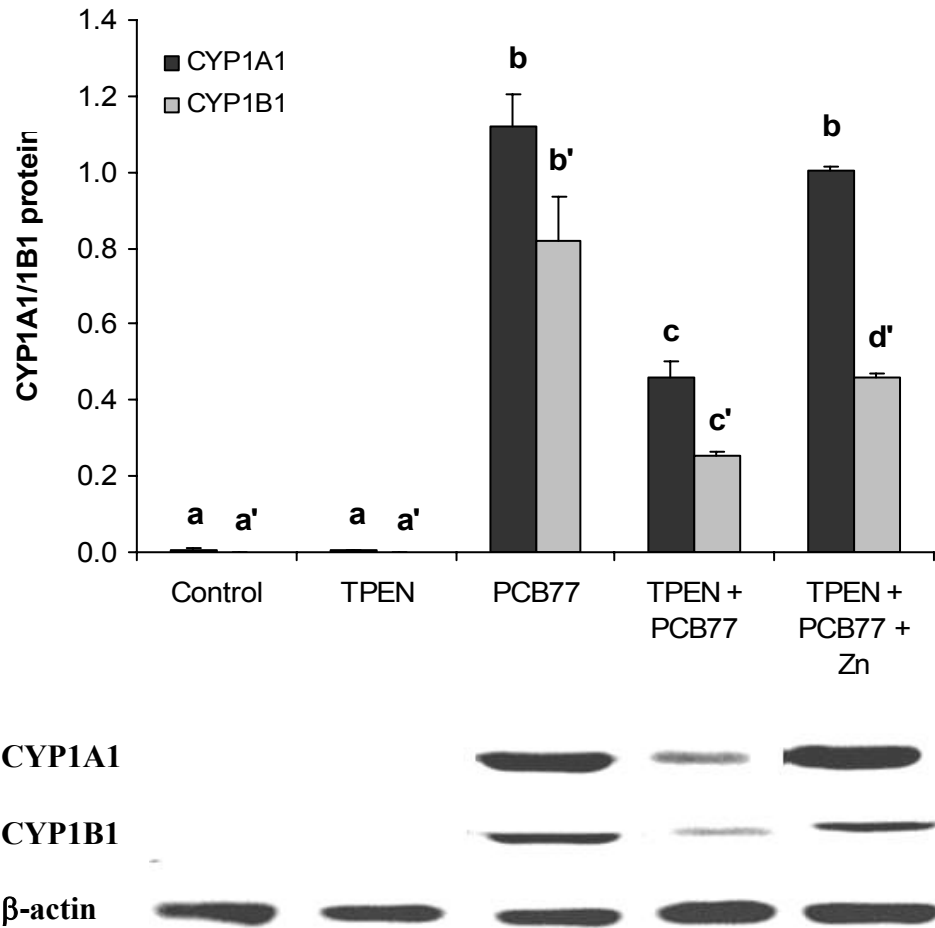


Figure 5.2. Zinc deficiency compromises PCB77-induced CYP1A1 and CYP1B1 protein expression in vascular endothelial cells

Similar to Figure 5.1, endothelial cells were exposed to vehicle control, TPEN, PCB77 (3.4 μ M), TPEN plus PCB77, or TPEN with zinc supplementation (20 μ M) plus PCB77 for 24 hours. The values are ratios of the densitometric units of CYP1A1 or CYP1B1 over those of β -actin. Bars with different letters (a, b, c for CYP1A1 and a', b', c', d' for CYP1B1) are statistically different from each other ($P < 0.05$). $n = 3$. The gel data are a representative of the typical outcome of three repeated western blot experiments.

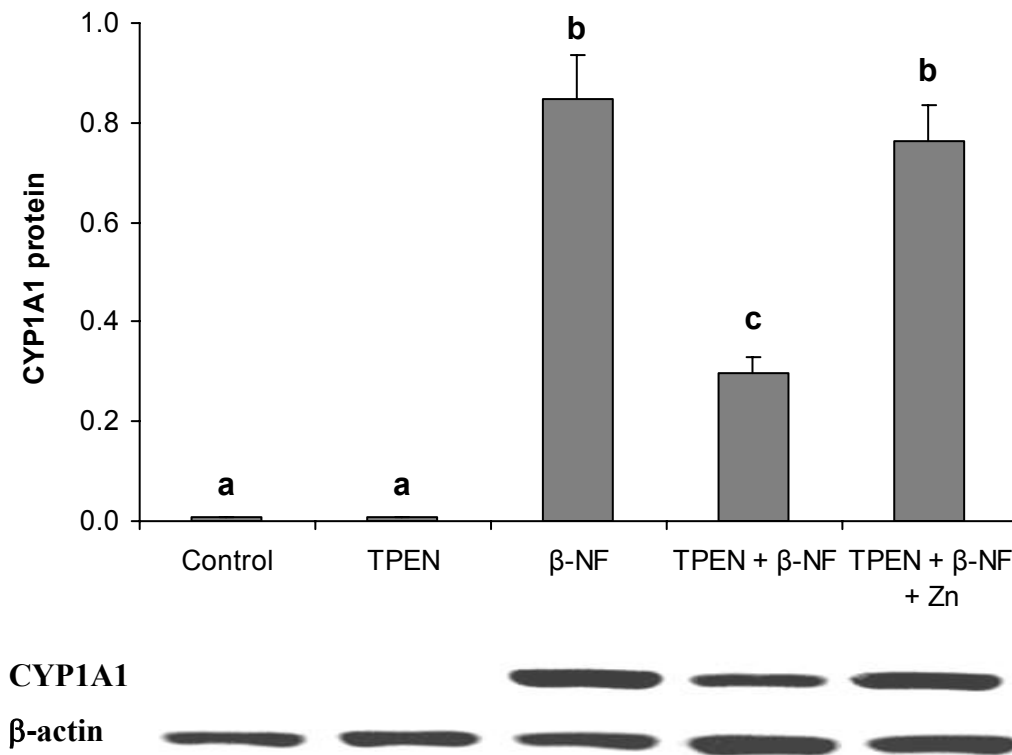


Figure 5.3. Zinc deficiency compromises β -naphthoflavone-induced CYP1A1 protein expression in vascular endothelial cells

Endothelial cells were exposed to vehicle control, TPEN, β -NF (1.0 μ M), TPEN plus β -NF, or TPEN with zinc supplementation plus β -NF for 24 hours. The values are ratios of the densitometric units of CYP1A1 over those of β -actin. Bars with different letters (a, b, c) are statistically different from each other ($P < 0.05$). $n = 3$. The gel data are a representative of the typical outcome of three repeated western blot experiments.

Chaper 6. Conclusion

Atherosclerosis is a major health issue in developed countries and has an increasing incidence in developing countries as well. The pathogenesis of atherosclerosis is thought to begin with endothelial cell dysfunction. Through increased expression of adhesion molecules, activated endothelial cells mediate monocyte attachment and migration through the endothelium into the arterial wall, where the monocytes differentiate into macrophages and by taking up modified lipids further become foam cells. In more advanced stages of atherosclerosis, formation of fibrous plaques and complex lesions will ensue, leading to an acute clinical event by plaque rupture and thrombosis [1, 2]. The development of atherosclerosis is influenced by both genetic and environmental risk factors with the later including nutritional risk factors [1, 2]. Deficiency of the micronutrient zinc can constitute a risk factor for atherosclerosis [3, 4]. Since the initial and early stages of atherosclerosis are the time points when nutrition (e.g. zinc) modulation could have the most efficient effects, the research described in this dissertation focuses on early events of atherosclerosis, including endothelial cell activation in the *in vitro* studies and a more systemic profile of early events of atherosclerosis in the *in vivo* studies.

One major link of the four chapters of this dissertation is the micronutrient zinc. In the current studies, the cells were made zinc deficient by treatment with the zinc chelators TPEN or DTPA. TPEN is a membrane permeable zinc-specific chelator that decreases intracellular zinc concentrations by depleting zinc from both a cytoplasmic free zinc pool and a nuclear pool [184-186]. The chelation of cations other than zinc by TPEN is very low with the affinities of metal to TPEN: $Zn^{2+} > Fe^{2+} > Mn^{2+} \gg Ca^{2+} = Mg^{2+}$ [187]. In a previous study of our lab, cultured endothelial cells pre-treated with TPEN (2 μ M) for 24 h were labeled with Zinquin ethyl ester, and the fluorescence that reflects biologically available labile zinc was measured, demonstrating that cellular labile zinc deficiency can be induced by exposure of endothelial cells to TPEN for 24 h [25]. In the current *in vitro* study, the same duration of TPEN treatment (i.e. 24 h) but lower concentrations of TPEN (1.0 or 1.5 μ M) were applied because 2 μ M of TPEN would cause massive cell death in the vascular endothelial cell cultures at the treatment time

point of 24 h. Therefore, the highest non-toxic concentrations of TPEN were chosen to perform these experiments on the endothelial cells. Based on the observed biological effects caused by zinc chelation and supplementation as described in Chapter Two, the TPEN treatment should have reduced the intracellular labile zinc. DTPA is a membrane impermeable chelator that decreases extracellular zinc concentrations [184]. DTPA is a potent chelator of zinc, but is not only specific for zinc [188]. A previous study has shown that in spite of the detrimental effect of DTPA on thymidine incorporation in 3T3 cells, it did not decrease the measurable cellular total zinc concentration, which may be the result of a decreased zinc concentration of only a small compartment of the cell, possibly the plasma membrane, that caused too small a change to be detected by total zinc analysis [188]. In the transient transfection-luciferase assay described in Chapter Two, the compromising effect of DTPA-induced zinc deficiency on the transactivation activity of PPAR γ was obvious despite the fact that the cellular zinc concentrations in RAVSMC were not measured. Nevertheless, one major deficiency of the present *in vitro* study is the lack of determination of the intracellular zinc concentrations. There are several ways to measure cellular zinc, with the most commonly used one being atomic absorption spectrometry, which measures total cellular zinc [189]. Fluorescence microscopy with the zinc-specific fluorescent probe FluoZin-3 can be used to quantify cellular labile zinc [190]. Recently, flow cytometry with FluoZin-3 has been employed to measure the concentrations of biologically active labile zinc in both a single cell and distinct cell populations [189]. Unlike the fluorescent probe Zinquin that was used in Hennig's laboratory before to determine intracellular labile zinc, the FluoZin-3 does not seem to interact with zinc that is bound to proteins like metallothionein [189], therefore, this method has the advantage of measuring labile zinc more accurately. Another novel way to measure intracellular exchangeable zinc is by using a fluorescence resonance energy transfer (FRET) based ratiometric zinc sensor to image and quantify zinc levels in resting eukaryotic cells [191]. In future *in vitro* zinc studies, it is important that the concentrations of intracellular labile zinc be routinely quantified using either the flow cytometric method or the ratiometric imaging method mentioned above, so that the observed biological effects caused by different cellular zinc status can be properly explained.

In the current *in vivo* study, the LDL-R^{-/-} mice were made mildly zinc deficient by feeding zinc-deficient diets that contained 0.4 mg/kg (not 0 mg/kg) of zinc for a relatively short period. Because zinc is such an important micronutrient involved in multiple life processes, it is important not to completely deplete zinc in these diets. The small amount of zinc in the zinc-deficient diets helped to keep the animals from significant weight loss, which could otherwise constitute a confounding factor in the study. It was still somewhat unexpected that the LDL-R^{-/-} mice on the zinc-deficient diets did not gain any weight (Fig. 3.2). Our previous feeding study applying the same type of diets on wild type (WT) mice showed that the zinc-deficient WT mice gained less weight than the zinc-adequate WT mice. The failure of the zinc-deficient LDL-R^{-/-} mice to gain weight in the current *in vivo* study suggests that this strain of mouse is more sensitive to zinc-depleted diets compared to the WT mice. Furthermore, our preliminary studies showed that the zinc-deficient mice always decreased their food intake compared to the zinc-adequate mice, which could partially explain their different patterns of body weight change. Some of the biological effects observed in the current *in vivo* study could be associated with the different food intake and weight change in the zinc-deficient vs. the zinc-adequate mice. In addition, the plasma zinc concentrations did not reflect the dietary zinc intake in our study. Plasma zinc concentration is not always a good indicator of body zinc levels. For example, while plasma zinc was found to be normal in elderly patients with mild zinc deficiency, the zinc levels in granulocytes and lymphocytes were decreased compared to the younger control subjects [192]. Zinc redistribution is a well recognized phenomenon during acute-phase response to injury or infection, when zinc moves into the liver with reduced plasma zinc concentration [193]. Zinc redistribution also can exist between plasma and peripheral blood mononuclear cells [194]. Determination of labile zinc in leukocytes instead of plasma zinc may be a more precise way of indicating the body zinc level, and it also allows for the correlation of leukocyte zinc levels with immunological effects [189]. The length of the *in vivo* study was based on our previous research using the same animal model and a similar dietary regimen, which has demonstrated that zinc deficiency for four weeks is sufficient to increase plasma lipids and atherosclerotic markers [118]. A longer-term study may reveal a more robust outcome revealing the pro-atherogenic effects of zinc deficiency and the anti-atherogenic properties of rosiglitazone,

and the interactions between zinc status and rosiglitazone in regulating the development of atherosclerosis as well.

Oxidative stress links all the main signaling pathways studied in this dissertation, i.e. NF- κ B, AhR, and PPAR. Oxidative stress plays a central role in atherosclerosis. ROS, the main source of oxidative stress, have a dual role in the vasculature. ROS function as homeostatic signaling molecules that regulate cell growth and adaptation responses at physiological concentrations, however, they can cause cellular injury and death at higher concentrations. The pathogenesis of atherosclerosis involves an imbalance between oxidative stress and antioxidant defense (including anti-oxidant enzymes and endogenous /exogenous anti-oxidants) that causes excessive ROS production [195]. Either inadequate or excessive cellular zinc can induce oxidative stress by altering the expression and activity of anti-oxidant enzymes and/or increasing ROS production. In the current study, zinc deficiency caused by TPEN chelation increased ROS generation in vascular endothelial cells (Fig. 2.1). In this experiment however, zinc supplementation to the chelator containing media only partially rescued the zinc-deficiency-induced cellular oxidative stress, and surprisingly, zinc supplementation alone also induced cellular oxidative stress in endothelial cells (Fig. 2.1). These observations were not in consistency with either the NF- κ B DNA binding activity data (Fig. 2.2) or the COX-2 and E-selectin mRNA expression data (Fig. 2.3). This could be due to the limitations of the DCF fluorescence method used for cellular oxidative stress measurement. The DCF assay is sensitive to ONOO⁻, H₂O₂, and [•]OH, but not to NO, hypochlorous acid (HOCl) or O₂^{•-} [196], therefore could not have reflected the whole cellular oxidative stress profile in the endothelial cells. In order to determine cellular oxidative stress more accurately, future studies should combine the DCF assay with several other methods, such as the luminol- and lucigenin-amplified chemiluminescence assays which are sensitive to HOCl and O₂^{•-}, respectively [196].

Being a redox-sensitive transcription factor, NF- κ B can be activated by oxidative stress [85]. Activation of NF- κ B leads to up-regulation of downstream target genes, such as TNF α , and COX-2 [88, 119]. Expression of these inflammatory mediators can further increase cellular oxidative stress by generating ROS [44]. This positive feedback loop amplifies the oxidative stress signaling. Activation of the AhR by certain ligands such as

2,3,7,8-tetrachlorodibenzo-*p*-dioxin (TCDD) can also lead to oxidative stress responses through induction of inflammatory mediators like TNF α and COX-2, modulation of antioxidant and prooxidant enzymes such as SOD and XO/XDH, and induction of cytochrome P450 [44]. Oxidative stress can also activate PPAR[197], which has anti-inflammatory properties and would reduce oxidative stress [198-200] and/or prevent oxidative stress induced deleterious effects [201, 202]. Cellular oxidative stress thus cross-talks with multiple signaling pathways, resulting in synergism or antagonism among signaling pathways that depend on the overall oxidative stress/antioxidant balance within a cell (Fig. 6.1).

Crosstalk between the transcription factors NF- κ B, PPAR, and AhR as influenced by zinc nutritional status also helps to integrate the studies described in this dissertation (Fig. 6.1). There is a bidirectional antagonism between the NF- κ B and PPAR signaling pathways. PPAR can repress the NF- κ B pathway by physically interacting with the p50 and p65 subunits of NF- κ B, and by inducing the expression of I κ B, the major inhibitor of NF- κ B [21]. On the other hand, NF- κ B activation can negatively regulate PPAR signaling by down-regulating the expression of PPAR mRNAs and inhibiting the transcriptional activity of PPAR proteins [203]. The interaction between PPAR and NF- κ B provides an efficient way of regulating multiple cellular events. In the current study, zinc deficiency activates the NF- κ B pathway possibly by increasing cellular oxidative stress, meanwhile, it suppresses the PPAR pathway by inhibiting PPAR expression and the transactivational activity of the PPAR proteins. When cells are zinc deficient, the activation of NF- κ B can further inhibit PPAR function and the suppressed PPAR signaling can contribute to further activation of the NF- κ B and associated downstream inflammatory events.

Similarly, physical interaction and mutual functional repression also exist between the NF- κ B and AhR signaling pathways. NF- κ B activation can inhibit AhR dependent gene expression; conversely, ligand activation of AhR can also suppress transcriptional activation by NF- κ B [204, 205]. The mutual repression is mediated by the physical interaction between the p65 subunit of NF- κ B and AhR, and may also involve the roles of nuclear receptor coactivators p300/CBP and steroid receptor coactivator-1

(SRC-1). Since both p300/CBP and SRC-1 serve as common coactivators of NF- κ B and AhR for maximum transcriptional activation, a competition for coactivator binding is possible, which will lead to activation of one pathway and repression of the other pathway [204-206]. In the present study, zinc deficiency might impair the AhR pathway either directly by affecting the AhR translocation, cofactor recruitment, and/or AhR-XRE binding, or indirectly by activating the NF- κ B pathway. Likewise, during zinc deficiency the activation of NF- κ B can further inhibit the AhR function and the compromised AhR signaling can intensify the activation of NF- κ B and inflammation, eventually contributing to the pathology of atherosclerosis.

One common finding in both the *in vitro* and the *in vivo* studies described in this dissertation is the requirement of adequate zinc for proper PPAR function. Since there are so many zinc-finger containing proteins, it is possible that zinc deficiency can also alter functions of some other zinc-finger transcription factors in addition to PPAR. However, my data demonstrate that zinc deficiency decreases the protein expression of PPAR α (Fig. 2.5B) but not of estrogen receptor (ER) α (see Appendix, Fig. VI), another zinc-finger transcription factor, in vascular endothelial cells. This observation suggests some specificity of zinc deficiency for altering PPAR function, findings which are also supported by the reversibility studies with zinc supplementation.

An interesting finding described in this dissertation is that zinc deficiency seems to protect against PCB77-induced inflammation in endothelial cells. Since both PCB77 [169] and zinc deficiency increases cellular oxidative stress, we initially thought that zinc deficiency could amplify PCB77-induced inflammatory responses. However, the current data showed the opposite. Specifically, PCB77-induced CYP1A1 activity and expression (Fig. 5.1, 5.2), and up-regulation of adhesion molecules, such as vascular cell adhesion molecule-1 (VCAM-1) and E-selectin (see Appendix, Fig. VII), were all compromised during zinc-deficiency. Since the PCB 77-induced endothelial cell inflammatory responses are mediated through the AhR-CYP1A pathway [62], one could anticipate that zinc ion could be required for some upstream events of the whole pathway, such as activation of the AhR-CYP1A1 pathway. In other words, during zinc deficiency, the AhR-CYP1A1 activation gets inhibited, leading to inactivation of the downstream inflammatory responses as a consequence. The inhibitory effect of zinc deficiency on the

non-toxic AhR ligand β -NF-induced CYP1A1 expression (Fig. 5.3) was supportive of this point.

The findings described in this dissertation foster a number of important questions that could be addressed in future studies. For example, the hitherto poorly understood upstream events in zinc deficiency-induced endothelial cell activation need to be clarified. The relevant questions include, but are not limited to, 1) how does zinc deficiency induce oxidative stress in endothelial cells and which signaling pathways are involved, and 2) how does the increased oxidative stress activate NF- κ B in endothelial cells and which kinases are involved. Another question is the detailed mechanisms involved in zinc deficiency-induced inhibition of the AhR-CYP1 pathway in vascular endothelial cells. In this aspect, future studies may address whether the translocation of AhR and/or ARNT, the coactivator recruitment, the AhR-XRE binding, and/or the transactivation activity of AhR are influenced by zinc deficiency in these cells.

In conclusion, zinc nutrition can affect the pathology of inflammatory diseases such as atherosclerosis. Zinc deficiency by itself constitutes a risk factor of atherosclerosis. In addition, zinc deficiency can modify the biological outcomes of other risk factors of atherosclerosis such as coplanar PCBs, and of certain medicines such as TZDs. The study described in this dissertation shows that zinc deficiency can intensify inflammatory events in vascular endothelial cells and the whole animal as well. The mechanisms involved include inhibition of the anti-inflammatory signaling pathways, such as the PPAR, and activation of the pro-inflammatory pathways, such as the NF- κ B, during zinc deficiency (Fig. 6.1).

In general, data presented in this dissertation are novel and important for population groups at risk of zinc deficiency and exposure to environmental pollutants such as PCBs, and patients receiving therapy with TZDs. The results shown also emphasize the importance of the micronutrient zinc in prevention of atherosclerosis and the importance of adequate dietary zinc in humans during treatment phases associated with diabetes and other cardiovascular risk factors.

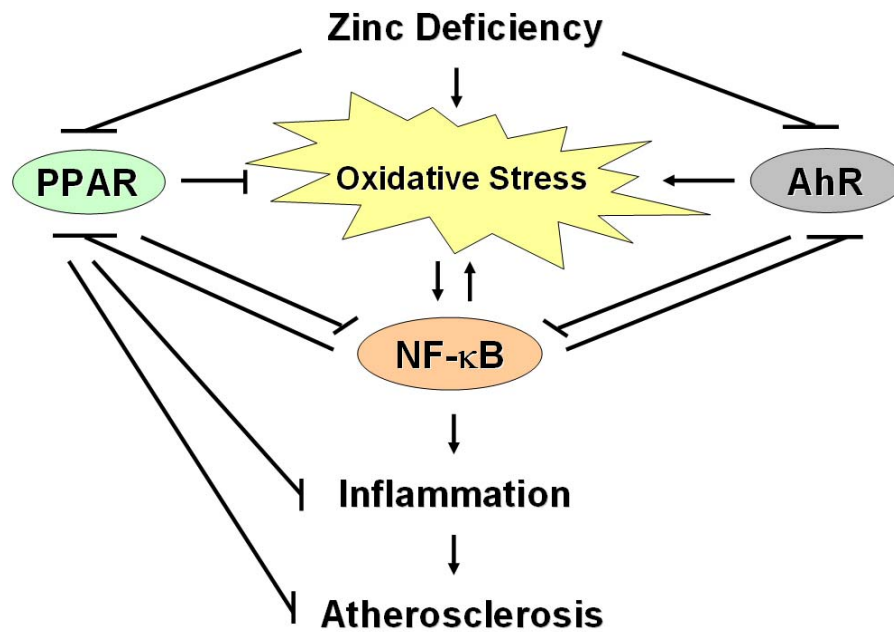


Figure 6.1. Crosstalk between the NF- κ B, PPAR, and AhR pathways during zinc deficiency.

Zinc deficiency induces oxidative stress, which activates the NF- κ B signaling pathway that leads to inflammation and atherosclerosis. Meanwhile, zinc deficiency inhibits both PPAR and AhR signaling, blocking their inhibitory effects on NF- κ B and further contributing to activation of NF- κ B and inflammation. Activation of NF- κ B can intensify the oxidative stress signaling by generating more ROS, and is able to inhibit both PPAR and AhR pathways as well. AhR activation can be pro-inflammatory by generating oxidative stress while activation of the anti-inflammatory PPAR can generally prevent the deleterious effects caused by oxidative stress.

Appendix

Methods

1. Primary endothelial cell culture

- **Establishing primary cell culture**

Endothelial cells were isolated from porcine pulmonary arteries by Dr. Bernhard Hennig at the Molecular and Cell Nutrition Laboratory, College of Agriculture, University of Kentucky, and subcultured in M-199 (Invitrogen Corporation, Carlsbad, CA) containing 10% (v/v) FBS (HyClone, Logan, UT).

- **Freezing cells**

- 1) Take one T75 cell culture flask with confluent endothelial cells. Rinse the cells with 10 mL of Hanks and then add 1 mL of trypsin (0.05 %). Place the flask in a CO₂ incubator (37 °C, 5 % CO₂) to facilitate trypsin digestion.
- 2) When the cells are detached from the bottom of the flask, add 10 mL of M199/10 % FBS, suspend the cells by repeated pipetting, and transfer the cell suspension into a 15 mL conical tube followed by centrifugation at 1,200 rpm at 37 °C for 10 min.
- 3) Gently decant supernatant, add 2 mL of freshly made freezing cocktail (M199/20 % FBS, 7 % DMSO) to resuspend the cells and transfer the cell suspension to two cryovials with 1 mL per vial. Label the cryovials with passage, date, and operator, and keep them at -20 °C for 1 h and then at -80 °C overnight. The cryovials are transferred to liquid nitrogen the next day for longtime storage.

- **Reviving cells**

- 1) Find one cryovial containing 1 mL of frozen endothelial cell suspension.
- 2) Add 0.5 mL of M199/10 % FBS (pre-warmed to 37 °C) to the cryovial, pipette repeatedly and keep transferring the thawed cells into a 15 mL conical tube.
- 3) After all cells are suspended in the 15 mL tube, centrifuge at 1,200 rpm for 10 min at 37 °C.

- 4) Gently decant supernatant, and resuspend the cells in 10 mL of M199/10 % FBS, centrifuge at 1,200 rpm for 10 min at 37 °C. Repeat this step one more time.
- 5) Gently decant supernatant, resuspend the cells in 15 mL of M199/10 % FBS and transfer the cell suspension to a T75 flask. Place the flask in a CO₂ incubator.
- 6) Change the media 3 ~ 4 h later when the cells should have attached to the bottom of the flask.
- 7) Change the media again the next day, and wait for two days until the cells are confluent.

2. Cellular oxidative stress measurement

- 1) Take one T-75 culture flask, after trypsin digestion add 60 mL of M199/10 % FBS. Distribute 0.8 mL of the endothelial cell suspension into each well of a 24 well plate.
- 2) Incubate the cells for 48 h in CO₂ incubator, then synchronize the cells (about 90 % confluent) in M199/0 % FBS overnight followed by treatment in M199/1 % FBS for 24 h.
- 3) Rinse the cells twice with HEPES buffered salt solution (HBSS) * (25 mM HEPES, 120 mM NaCl, 5.4 mM KCl, 1.8 mM CaCl₂, 25 mM NaHCO₃, 15 mM glucose, pH 7.4) and incubate with 0.5 mL of HBSS containing 10 μM of 2',7'-dichlorodihydrofluorescein diacetate (H₂DCF-DA)** at 37 °C for 30 min at dark.
- 4) Wash the cells twice with HBSS and replace with 0.5 mL of HBSS.
- 5) Measure the DCF fluorescence using a fluorescence microplate reader with excitation and emission wavelengths of 485 nm and 530 nm, respectively.

* To make 100 mL of HBSS: dissolve 0.6g HEPES, 0.7g NaCl, 40 mg KCl, 26.5 mg CaCl₂, 0.21g NaHCO₃, and 0.27g glucose in distilled H₂O, adjust pH 7.4 with NaOH, and then sterilize by filtering.

** H₂DCF-DA is added from a stock solution (10 mM): dissolve 2 mg H₂DCF-DA in 0.4 mL EtOH, store at -80 °C at dark.

3. RNA isolation

▪ RNA isolation from endothelial cells

Total RNA was isolated from endothelial cells using TRIzol Reagent (Invitrogen, Carlsbad, CA) according to the manufacturer's instruction.

▪ RNA isolation from mouse aorta

Total RNA was isolated from mouse aorta using RNeasy Fibrous Tissue Mini Kit (Qiagen, Valencia, CA) according to the manufacturer's instruction.

▪ RNA isolation from mouse liver

Total RNA was isolated from mouse liver using RNeasy Mini Kit (Qiagen, Valencia, CA) according to the manufacturer's instruction.

4. Measurement of RNA concentration

- 1) Add 3 µL of RNA sample into 600 µL of RNase-free H₂O. Mix by repeated pipetting.
- 2) Measure RNA concentration and A₂₆₀/A₂₈₀ value using a SmartSpec 3000 Spectrophotometer (Bio-Rad, Hercules, CA).

5. Reverse transcription (RT) reaction

- 1) Dilute 1 µg of RNA in RNase-free H₂O to 9.9 µL. Heat the RNA at 70 °C for 10 min in a MJ Mini 48-Well Personal Thermal Cycler (Bio-Rad, Hercules, CA) and put on ice.

- 2) Make a Master Mix using the Reverse Transcription System (Promega, Madison, WI):

MgCl ₂ (25 mM):	4.0 μL
Reverse Transcription 10 × Buffer:	2.0 μL
dNTP Mix (10 mM):	2.0 μL
RNasin Ribonuclease Inhibitor (40 u/μL):	0.5 μL
Random Primers (500 μg/mL):	1.0 μL
<u>AMV Reverse Transcriptase (10 u/μL):</u>	<u>0.6 μL</u>
Total volume	10.1 μL

- 3) Add 9.9 μL of the RNA into 10.1 μL of the Master Mix and mix well.
- 4) RT reaction in the MJ Mini 48-Well Personal Thermal Cycler: 25 °C for 10 min → 42 °C for 60 min → 95 °C for 5 min → 4 °C for 5 min.
- 5) Store the cDNA at -20 °C.

6. Polymerase chain reaction (PCR)

- 1) Prepare the PCR reaction mixture using Taq PCR Master Mix Kit (Qiagen, Valencia, CA)

Distilled H ₂ O:	10.5 μL
Target gene sense (20 pM):	0.5 μL
Target gene antisense (20 pM):	0.5 μL
cDNA:	1.0 μL
<u>Taq PCR Master Mix*:</u>	<u>12.5 μL</u>
Total volume	25.0 μL

* containing 49 u/mL of Taq DNA Polymerase

- 2) Run PCR reaction in the MJ Mini 48-Well Personal Thermal Cycler

- PCR programs for target genes:

COX-2

95 °C for 5 min, 1 cycle;

95 °C for 30 sec → 52.3 °C for 30 sec → 72 °C for 30 sec, 26 cycles;

72 °C for 7 min, 1 cycle.

E-selectin

94 °C for 5 min, 1 cycle;

94 °C for 1 min → 58.6 °C for 1 min → 72 °C for 1 min, 22 cycles;

72 °C for 7 min, 1 cycle.

CYP11A1

94 °C for 4 min, 1 cycle;

94 °C for 1 min → 58 °C for 1 min → 72 °C for 1 min, 29 cycles;

72 °C for 7 min, 1 cycle.

β-actin

94 °C for 4 min, 1 cycle;

94 °C for 1 min → 53 °C for 1 min → 72 °C for 1 min, 21 cycles;

72 °C for 7 min, 1 cycle.

7. Real-time PCR

The real-time PCR reactions were performed using the ABI Prism 7300 Real Time PCR System (Applied Biosystems, Branchburg, NJ). The quantification of PCR products was based on standard curves for the target gene and for the endogenous control, respectively. A serial dilution of cDNA was made to establish the standard curve by assigning artificial numbers (e.g. 160, 80, 40, and 20) of mRNA copy to each standard reaction.

▪ CYBR Green gene expression assay for porcine *PPARα*

1) Prepare the real-time PCR reaction mixtures:

Nuclease-free H ₂ O (Ambion, Austin, TX):	7.5 μL
PPARα / β-actin forward (100 μM):	1.5 μL
PPARα / β-actin reverse (100 μM):	1.5 μL
CYBR Green PCR Master Mix (Applied Biosystems, 2×):	12.5 μL
cDNA:	2.0 μL
<hr/>	
Total volume	25.0 μL

2) Real-time PCR:

95 °C for 10 min, 1 cycle;

95 °C for 15 sec → 60 °C for 1 min, 40 cycles.

▪ **TaqMan gene expression assays for mouse *PPAR γ* , *iNOS*, *MCP-1*, *CD36*, and *LPL***

1) Prepare the real-time PCR reaction mixtures:

Nuclease-free H ₂ O (Ambion, Austin, TX):	9.25 μ L
Probe and Primers Mix* (Applied Biosystems, 20 \times):	1.25 μ L
TaqMan Universal PCR Master Mix, No AmpErase UNG (AB, 2 \times):	12.5 μ L
<u>cDNA:</u>	<u>2.0 μL</u>
Total volume	25.0 μ L

2) Real-time PCR:

95 °C for 10 min, 1 cycle;

95 °C for 15 sec → 60 °C for 1 min, 40 cycles.

* The Probe and Primers Mixes were purchased from Applied Biosystems as TaqMan Gene Expression Assays pre-designed for different genes, i.e., mouse *PPAR γ* , *iNOS*, *MCP-1*, *CD36*, and *LPL*. Endogenous controls used were either Eukaryotic 18S rRNA or mouse ACTB, both of which are pre-developed TaqMan Assay reagents purchased from Applied Biosystems.

8. Cellular protein extraction

▪ **Cellular protein extraction from endothelial cells***

1) Rinse the endothelial monolayer twice with 5 mL of ice-cold PBS.

2) Add 3 mL of PBS and scrape the cells into a 15 mL conical tube.

3) Rinse dish with 3 mL of PBS and transfer into the same tube.

4) Centrifuge at 2,500 rpm for 10 min at 4 °C.

5) Decant the supernatant and resuspend the cells in 5 mL of PBS.

6) Centrifuge at 2,500 rpm for 5 min at 4 °C.

7) Carefully remove the supernatant and add 100 μ L of Lysis Buffer ** [20 mM Tris-HCl (pH 7.4), 150 mM NaCl, 0.5 % (v/v) Triton X-100, 1 mM EDTA,

0.05 % (w/v) NP-40, 0.1 mg/mL PMSF, 1 mM Na₃VO₄, 2.5 µg/mL leupeptin, and 10 µg/mL pepstatin].

- 8) Vortex for 30 sec then put on ice for 2 min, repeat this step for 6 ~ 8 times.
- 9) Incubate on ice for 30 ~ 60 min.
- 10) Vortex and then centrifuge at 13,000 rpm for 15 min at 4 °C.
- 11) Take the supernatant and make aliquots of it, quick freeze the aliquots on dry ice and store at -80 °C.

* All steps were carried out at 4 °C or on ice.

** Make Lysis Buffer (-) then add NP-40, PMSF, Na₃VO₄, leupeptin, and pepstatin before using:

i) To make 100 mL of Lysis Buffer (-): 2 mL Tris-HCl (1 M, pH 7.4) + 15 mL NaCl (1 M) + 5 mL Triton X-100 (10 %, v/v) + 1 mL EDTA (0.1M) + 73.75 mL distilled H₂O.

ii) To make 1 mL of Lysis Buffer: 975 µL Lysis Buffer (-) + 5 µL NP-40 (10 % w/v) + 10 µL PMSF (10 mg/mL) + 5 µL Na₃VO₄ (200 mM) + 5 µL Protease Inhibitor Cocktail (0.5 mg/mL leupeptin, 2 mg/mL pepstatin).

▪ **Cellular protein extraction from liver tissue**

- 1) Thaw the Lysis Buffer* [50 mM Tris, 150 mM NaCl, 0.05 % (v/v) Triton X-100, 0.1 mg/mL PMSF, 1 mM Na₃VO₄, 0.05 % (w/v) NP-40, 1 mM EDTA, 1 mM EGTA, 2.5 µg/mL leupeptin, 10 µg/mL pepstatin A, 10 µg/mL aprotinin, and 2 mM DTT, pH 7.4] aliquot at 37 °C and add 50 µL/sample into a glass homogenization tube on ice.
- 2) Cut frozen liver tissue on ice into approximately 2 mm³ pieces with scalpel and submerge into Lysis Buffer in the homogenizing tube immediately.
- 3) Homogenize for 10 sec on ice and let stand for 30 min on ice.
- 4) Transfer the homogenate into an eppendorf tube and centrifuge at 14,000 rpm for 30 min at 4 °C.
- 5) Obtain the supernatant, vortex for 5 sec, make aliquots, quick freeze the aliquots on dry ice, and store at -80 °C.

* To make 100 mL of Lysis Buffer: 75 mL Tris (67mM)-NaCl (200 mM) (pH 7.4) + 0.5 mL Triton X-100 (10 %, v/v) + 1 mL PMSF (10 mg/mL) + 0.5 mL Na₃VO₄ (200 mM) + 0.5 mL NP-40 (10 %, w/v) + 1 mL EDTA (100 mM) + 1 mL EGTA (100 mM) + 0.25 mL leupeptin (1 mg/mL) + 1 mL pepstatin A (1 mg/mL) + 0.1 mL aprotinin (10 mg/mL) + 2 mL DTT (100 mM) + 17.15 mL distilled H₂O.

9. Measurement of protein extract concentration

Protein concentrations were measured spectrophotometrically by Bradford Assay.

- 1) Prepare a series of protein standard, for example, 0, 2, 4, 6, 8, and 10 µg/mL of bovine serum albumin (BSA) using the Quick Start Bradford Protein Assay Kit (Bio-Rad, Hercules, CA).
- 2) Dilute each protein sample by 500 fold, i.e., 2 µL of sample + 998 µL of Bradford Dye Reagent, mix and let stand for 5 min at room temperature.
- 3) Measure A₅₉₅ using a UV-1700PC spectrophotometer (Shimadzu Scientific Instruments, Columbia, MD) and get the protein concentrations.

10. Western blot

▪ Preparing samples

- 1) Dilute protein samples with distilled H₂O to 20 µL with the total amount of protein 20 ~ 25 µg each.
- 2) Add 5 µL of 5× Sample Loading Buffer* each.
- 3) Boil the samples at 95 ~100 °C for 5 ~7 min.
- 4) Put the samples on ice until loading.

* To make 8 mL of 5× Sample Loading Buffer: 1 mL 0.5 M Tris-HCl (pH 6.8) + 0.8 mL 60 % glycerol + 1.6 mL 10 % SDS + 0.4 mL 2-mercaptoethanol + 0.4 mL 1 % (w/v) bromophenol blue + 3.8 mL distilled H₂O, make aliquots and store at -80 °C.

▪ Preparing the gel

- 1) Separating/Resolving gel: lower gel (Table I).

2) Stacking gel: upper gel (Table I).

Table I. Preparation of SDS-PAGE gels

	Stacking gel	Separating gel	Separating gel
	5 %	8 %	10 %
Distilled H ₂ O	6.09 mL	5.34 mL	4.84 mL
0.5 M Tris-HCl (pH 6.8)	2.5 mL	-	-
1.5 M Tris-HCl (pH 8.8)	-	2.5 mL	2.5 mL
40 % Acrylamide/bis	1.25 mL	2 mL	2.5 mL
10 % SDS	100 µL	100 µL	100 µL
10 % APS	50 µL	50 µL	50 µL
TEMED	10 µL	10 µL	10 µL
Total volume	10 mL	10 mL	10 mL

▪ **Running the gel**

- 1) Prepare the Running Buffer*
- 2) Put the gel in and load the samples and the protein marker (Bio-Rad, Hercules, CA).
- 3) Run at 100 V until the bromophenol blue reaches the bottom of the separating gel.

* To make 600 mL of 10 × Running Buffer: dissolve 18 g of Tris Base, 86.4 g of glycine, and 6 g of SDS in distilled H₂O. To run the gel, dilute the 10 × Running Buffer into 1 × Running Buffer with distilled H₂O.

▪ **Transfer onto nitrocellulose membrane**

- 1) Prepare the Transfer Buffer**
- 2) Make the “transfer sandwich” in ice-cold Transfer Buffer: from cathode to anode, place sponge, filter paper, gel, nitrocellulose membrane, filter paper, and sponge in turn. Close, properly put in apparatus.
- 3) Add Transfer buffer, put in ice box and cover the whole thing with ice.

4) Run at 350 mA for 2h.

** To make 800 mL of Transfer Buffer: 80 mL 10 × Running Buffer + 160 mL methanol + 560 mL distilled H₂O, cover with parafilm and leave at -20 °C for 1 h before use.

▪ **Blocking**

Block the membrane by gentle shaking in the Blocking Buffer [5 % non-fat milk in 1×TBST *** (50 mM Tris Base, 150 mM NaCl, 0.05 % Tween 20)] for 1h at room temperature.

*** To make 1L of 10 × TBS: dissolve 60.5 g Tris Base and 87.6 g NaCl in distilled H₂O, adjust pH to 7.5 with HCl, bring volume to 1L. Dilute 100 mL 10 × TBS with 900 mL distilled H₂O to get 1L 1 × TBS. To make 500 mL 1×TBST: 500 mL 1 × TBS + 250 μL Tween 20.

▪ **Binding of the primary antibody**

- 1) Add certain amount of the primary antibody into the Blocking Buffer (e.g. 1:1000 for COX-2, CYP1A1, and .1: 4000 for β-actin).
- 2) Submerge the membrane in the buffer and gently shake overnight at 4 °C.
- 3) Wash the membrane with the Blocking Buffer for 5 min, repeat 3 times.

▪ **Binding of the secondary antibody**

- 1) Add certain amount of the secondary antibody into the Blocking Buffer (usually a 1:3000 dilution).
- 2) Submerge the membrane in the buffer and gently shake for 1h 15 min at room temperature.
- 3) Wash the membrane with 1×TBST for 5 min, repeat 5 times.

▪ **Visualization**

- 1) Discard the TBST.
- 2) Mix enhanced chemiluminescence (ECL) reagents (GE Healthcare, Piscataway, NJ): 1.5 mL reagent A + 1.5 mL reagent B.
- 3) Distribute the mixture evenly by pipette on the membrane. Let sit for 1 min.

- 4) Dry the membrane gently on a Kimwipe and put the membrane into the plastic case in the cassette.
- 5) Put in a piece of Blue Basic Autorad Film (ISC BioExpress, Kaysville, UT) and expose it for 1 ~ 15 min depending on the amount of target protein on the membrane.
- 6) Develop the film.

11. Nuclear protein extraction

▪ Nuclear protein extraction from endothelial cells*

- 1) Rinse the endothelial monolayer twice with 5 mL of ice-cold PBS.
- 2) Add 3 mL of PBS and scrape the cells into a 15 mL conical tube.
- 3) Rinse dish with 3 mL of PBS and transfer into the same tube.
- 4) Centrifuge at 2,500 rpm for 10 min at 4 °C.
- 5) Resuspend the cells in 400 µL of buffer A [10 mM HEPES (pH 7.9), 10 mM KCl, 0.1 mM EDTA, 1 mM DTT, and 0.5 mM PMSF]. Incubate on ice for 15 min.
- 6) Add 25 µL of 10 % NP-40, mix, incubate on ice for about 5 min until 90 ~ 95 % of the cells were lysed.
- 7) Centrifuge at 14,000 rpm for 3 min at 4 °C.
- 8) Gently remove the supernatant and resuspend the nuclear pellet in 20 ~50 µL of buffer B [20 mM HEPES (pH 7.9), 0.4 M NaCl, 1 mM EDTA, 1 mM DTT, and 1 mM PMSF] according to the cell number.
- 9) Lyse the nuclei by shaking vigorously for 5 min at 4 °C.
- 10) Centrifuge at 14,000 rpm for 10 min at 4 °C.
- 11) Collect the supernatant, make aliquots, quick freeze the aliquots on dry ice, and store at -80 °C.

* All steps were carried out at 4 °C or on ice.

▪ Nuclear protein extraction from mouse liver

Nuclear proteins were extracted using CellLytic NuCLEAR Extraction Kit (Sigma-Aldrich, St. Louis, MO) according to the manufacturer's instruction.

12. Electrophoretic mobility shift assay (EMSA)

EMSA assays were performed using LightShift® Chemiluminescent EMSA Kit (PIERCE, Rockford, IL) according to the manufacturer's instruction.

The supershift reaction mixtures contain 10 μ L of antibodies specific for either PPAR α or NF- κ B p65 subunit.

13. Zinc quantification in plasma, liver, and rosiglitazone solution

Zinc concentrations in plasma, liver, and rosiglitazone solution were analyzed by ICP mass spectrometry by Dr. Thomas Mawhinney at the Agricultural Experiment Station Chemical Laboratories, University of Missouri.

14. Measurement of plasma cytokines/chemokines concentrations

Concentrations of plasma IL-1 α , IL-2, IL-4, IL-6, IL-10, IL-12, IL-13, IL-17, TNF α , and MCP-1 were measured using Mouse Cytokine/Chemokine LINCOplex kit (LINKO Research Inc., St. Louis, MO) according to the manufacturer's instruction. Signal detection and data analysis using Luminex 100 (Luminex Corporation, Austin, TX) and Multiplex Data Analysis Software 1.0 (Upstate USA, Inc., Chicago, IL) were performed by Jason Stevens at the Center for Oral Health Research, University of Kentucky.

15. Measurement of plasma cholesterol concentrations

Plasma total cholesterol content was measured using Wako Cholesterol E Enzymatic Kit (Wako Chemicals USA, Inc., Richmond, VA) according to the manufacturer's instruction.

16. Fast-performance liquid chromatography (FPLC)

Plasma cholesterol distribution in different lipoprotein fractions was measured using FPLC by Jessica Moorleghen at the Cardiovascular Research Center, University of Kentucky.

17. Analysis of plasma fatty acids

- 1) Prepare butylated hydroxytoluene* (BHT, 100 µg/mL) in Folch Extraction Mixture (chloroform: methanol = 2:1):
 - * To make 420 mL of BHT (100 µg/mL): 280 mL of chloroform + 140 mL of methanol + 42 mg of BHT.
- 2) Prepare Standard [heptadecanoic acid (17:0, 5 mg/mL)]: dissolve 11.8 mg of 17:0 in 2.36 mL of methanol.
- 3) 50 µL plasma sample + 5 µL Standard (5 mg/mL) + 1 mL BHT (100 µg/mL), vortex.
- 4) Move to a glass tube, add 1 mL of distilled H₂O, vortex.
- 5) Centrifuge at 2,000 rpm for 10 min at room temperature.
- 6) Take chloroform (bottom) phase to a reaction tube.
- 7) Dry with N₂.
- 8) Add 100 µL of chloroform to dissolve sample.
- 9) Add 1 mL of boron trifluoride-methanol solution (BF₃).
- 10) Incubate at 55 °C overnight.
- 11) Move to a glass tube and add 1mL of distilled H₂O and 1mL of chloroform, vortex.
- 12) Centrifuge at 2,000 rpm for 10 min at room temperature.
- 13) Take chloroform (bottom) phase to a fresh glass tube.
- 14) Dry with N₂.
- 15) Add 500 µL of chloroform, shake, and transfer to a brown glass bottle, seal.
- 16) Plasma fatty acids profile was determined by gas chromatography by Dr. Xiang-an Li at the Department of Pediatrics, University of Kentucky.

18. Ethoxyresorufin-o-deethylase (EROD) assay

▪ Preparing stock solutions

- 1) Resorufin (RR, 50 µM) in methanol.
 - Dissolve 0.0587 g of RR in 5 mL of methanol to get 50 mM of RR.
 - Make a 1:1000 dilution of the RR (50 mM) with methanol to get 50 µM of RR.

- Store at -20 °C in brown bottle with lid wrapped in parafilm.
- 2) Fluorescamine (0.6 mg/mL) in acetone.
- Dissolve 30 mg of fluorescamine in 50 mL of acetone.
 - Store at -20 °C in brown bottle with lid wrapped in parafilm
- 3) 7-ethoxyresorufin (7ER, saturated) in methanol.
- Add a few crystals of 7ER to 2 mL of methanol, warm with hot water, vortex and settle. A saturated methanol solution of 7ER is around 400 μM .
 - Make triplicate 1:100 dilutions in PBS (e.g. 10 μL 7ER + 990 μL of PBS); read absorbance of each dilution at 482 nm (A_{482}).
 - Determine the concentration of 7ER using the equation: $\text{Con}_{7\text{ER}} (\text{mM}) = A_{482} \times 100 / E^*$.
* E (excitation coefficient) = $22.5 \text{ mM}^{-1} \text{ cm}^{-1}$.
 - Store at -20 °C in brown bottle with lid wrapped in parafilm.
- 4) BSA (2 mg/mL) in PBS.
- Dissolve 20 mg of BSA in 10 mL of PBS.
 - Make aliquots and store at -20 °C.
- **Preparing working solutions**
- 1) RR (15 μM): 150 μL of 50 μM RR + 350 μL of PBS.
 - 2) 7ER (9.4 μM): make a working solution using methanol according the concentration of the stock solution.
 - 3) Warm up the PBS to 37 °C.
- **Preparing the 48-well standard plate**
- Pipette the following to the standard wells (Table II):
- 1) PBS: 135, 124, 114, 93, 71, 50 μL per well.
 - 2) BSA (2 mg/mL): 0, 10, 20, 40, 60, 80 μL per well, corresponding to 0, 20, 40, 80, 120, 160 μg per well.
 - 3) RR (15 μM): 0, 0.5, 1, 2, 4, 5 μL per well, corresponding to 0, 7.5, 15, 30, 60, 75 pmol per well.

Table II. Preparation of 48-well standard plate for EROD assay

PBS 135µl BSA 0µl RR 0µl	PBS 135µl BSA 0µl RR 0µl	PBS 135µl BSA 0µl RR 0µl	PBS 135µl BSA 0µl RR 0µl	PBS 135µl BSA 0µl RR 0µl	PBS 135µl BSA 0µl RR 0µl	PBS 135µl BSA 0µl RR 0µl	PBS 135µl BSA 0µl RR 0µl
PBS 124µl BSA 10µl RR 0.5µl	PBS 124µl BSA 10µl RR 0.5µl	PBS 124µl BSA 10µl RR 0.5µl	PBS 124µl BSA 10µl RR 0.5µl	PBS 124µl BSA 10µl RR 0.5µl	PBS 124µl BSA 10µl RR 0.5µl	PBS 124µl BSA 10µl RR 0.5µl	PBS 124µl BSA 10µl RR 0.5µl
PBS 114µl BSA 20µl RR 1µl	PBS 114µl BSA 20µl RR 1µl	PBS 114µl BSA 20µl RR 1µl	PBS 114µl BSA 20µl RR 1µl	PBS 114µl BSA 20µl RR 1µl	PBS 114µl BSA 20µl RR 1µl	PBS 114µl BSA 20µl RR 1µl	PBS 114µl BSA 20µl RR 1µl
PBS 93µl BSA 40µl RR 2µl	PBS 93µl BSA 40µl RR 2µl	PBS 93µl BSA 40µl RR 2µl	PBS 93µl BSA 40µl RR 2µl	PBS 93µl BSA 40µl RR 2µl	PBS 93µl BSA 40µl RR 2µl	PBS 93µl BSA 40µl RR 2µl	PBS 93µl BSA 40µl RR 2µl
PBS 71µl BSA 60µl RR 4µl	PBS 71µl BSA 60µl RR 4µl	PBS 71µl BSA 60µl RR 4µl	PBS 71µl BSA 60µl RR 4µl	PBS 71µl BSA 60µl RR 4µl	PBS 71µl BSA 60µl RR 4µl	PBS 71µl BSA 60µl RR 4µl	PBS 71µl BSA 60µl RR 4µl
PBS 50µl BSA 80µl RR 5µl	PBS 50µl BSA 80µl RR 5µl	PBS 50µl BSA 80µl RR 5µl	PBS 50µl BSA 80µl RR 5µl	PBS 50µl BSA 80µl RR 5µl	PBS 50µl BSA 80µl RR 5µl	PBS 50µl BSA 80µl RR 5µl	PBS 50µl BSA 80µl RR 5µl

- **Preparing the 48-well cell plates**

- 1) Remove exposure media from the cells.
- 2) Rinse the cells with 300 µL of PBS, and replace with 135 µL of PBS.

- **Reaction and Reading**

- 1) Add 50 µL of 7ER working solution to all standard and cells wells
- 2) Place plate immediately into a Cytofluor 4000 plate reader (PE Biosystems, Foster City, CA) and start reading (measuring EROD).

- Program for the plate reader:

Excitation: 530 nm; Emission: 590 nm.

Run 10 cycles

Sensitivity: choose 15 or 16.

On the Cytofluor choose 2 scans/cycle, gains of 50 and 60, and 3 reads/well.

- 3) Go to kinetics menu on Cytofluor and check for a linear rate. The reaction should be linear for the first 10 to 15 minutes. Save files to Excel.
- 4) Remove the plate from the plate reader and add 100 μL of fluorescamine (0.6 mg/mL) to all wells. This will stop the reaction and develops the protein signal.
- 5) Create a new file for the protein measurements
 - Program for the plate reader:
Excitation: 409 nm; Emission: 460 nm.
Sensitivity: same as used for measuring EROD

▪ **Calculations**

- 1) Get the following parameters for each well:
 - Slope of EROD
 - Protein amount
 - Slope/Protein
- 2) Average of replicate wells = AFU*/min/mg
*AFU, absorbance fluorescence units
- 3) Convert to mole numbers of RR:
 $(\text{AFU}/\text{min}/\text{mg})/(\text{AFU}/\text{pmoles RR}) = \text{pmol}/\text{min}/\text{mg}$

Additional data

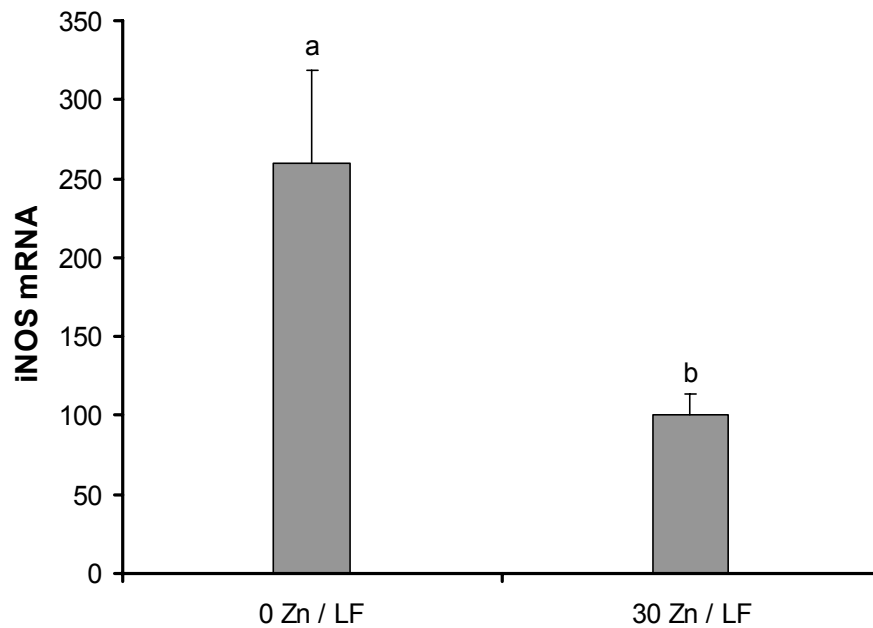


Figure I. Effect of zinc status on iNOS gene expression in abdominal aorta of low-fat diet fed LDL-R^{-/-} mice.

The vertical axis represents relative units, calculated as the ratio of the copy number of iNOS over the copy number of 18S rRNA, the endogenous control. Values are means \pm SEM, n = 6-7. Means without a common letter differ (a > b), P < 0.05.

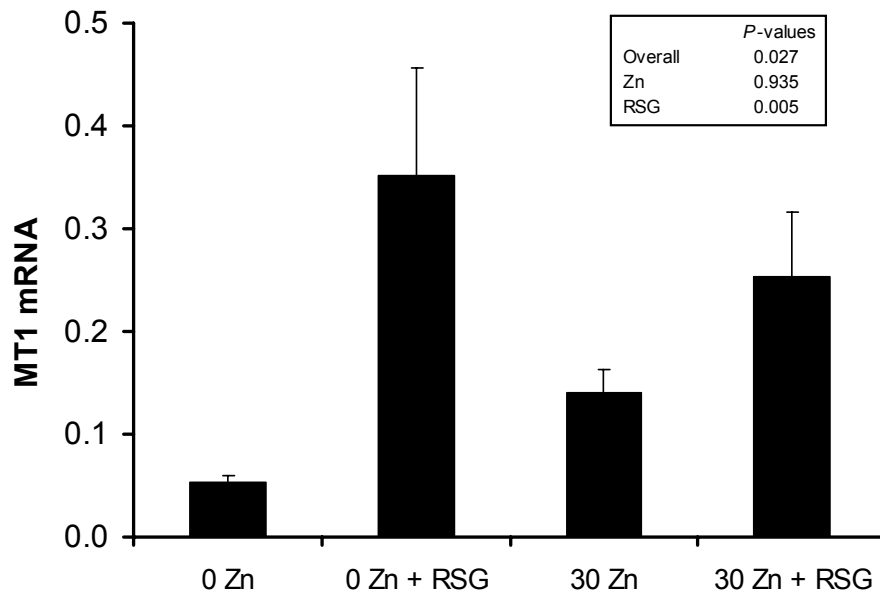


Figure II. Effects of dietary zinc status and rosiglitazone on MT1 mRNA expression in LDL-R^{-/-} mice.

The vertical axis represents relative units, calculated as the ratio of the copy number of MT1 over the copy number of β -actin, the endogenous control. Values are means \pm SEM, n = 7-10. Zn \times RSG interaction was not significant ($P > 0.05$).

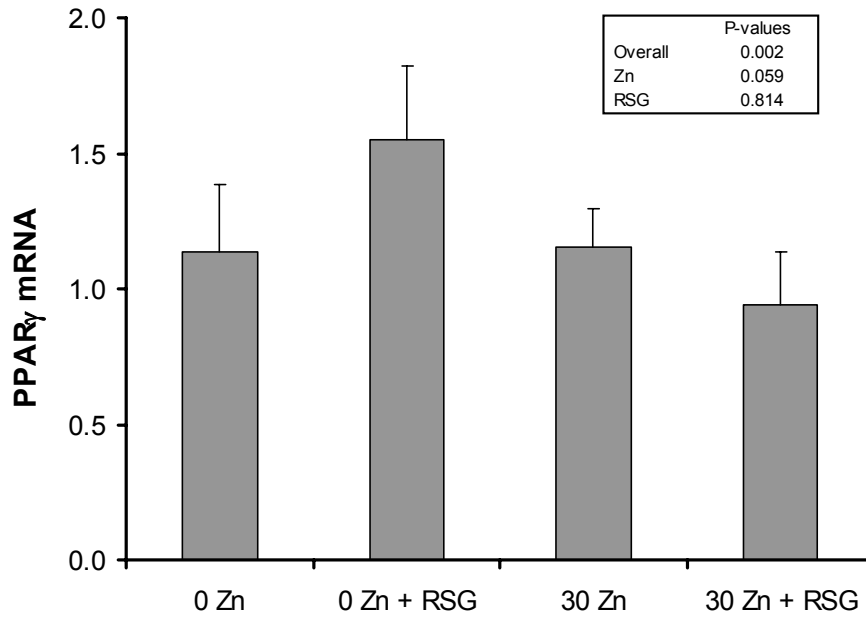


Figure III. Effects of dietary zinc status and rosiglitazone on PPAR γ gene expression in LDL-R^{-/-} mice.

The vertical axis represents relative units, calculated as the ratio of the copy number of PPAR γ over the copy number of β -actin, the endogenous control. Values are means \pm SEM, n = 7-9. Zn \times RSG interaction was not significant ($P > 0.05$).

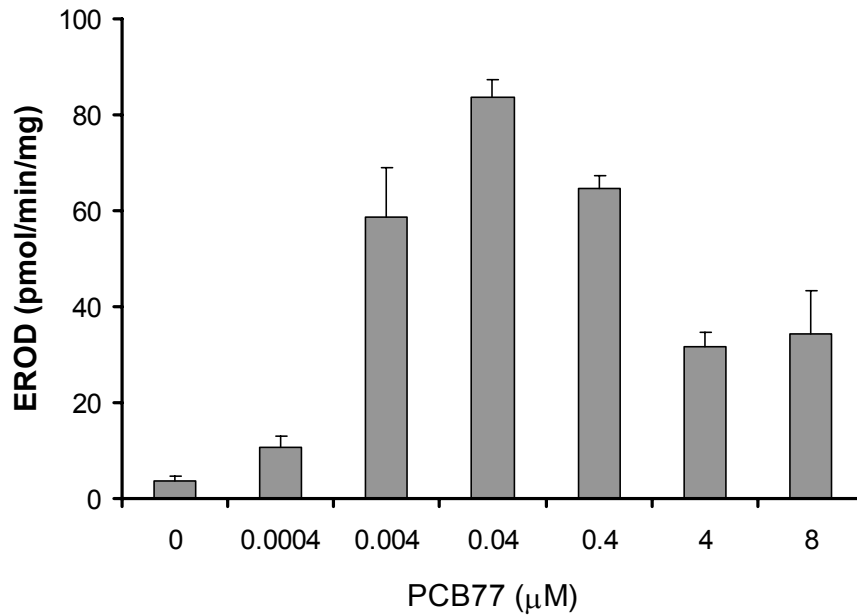


Figure IV. Dose-response relationship between PCB77 and CYP1A activity in vascular endothelial cells*.

CYP1A activity was measured by EROD assay. Endothelial cells were exposed to increasing concentrations of PCB77 (0, 0.0004, 0.004, 0.04, 0.4, 4, and 8 μM) for 24 hours. $n = 8$.

* The data were contributed by Dr. Xabier Arzuaga at the University of Kentucky Molecular and Cell Nutrition Laboratory (Hennig's laboratory).

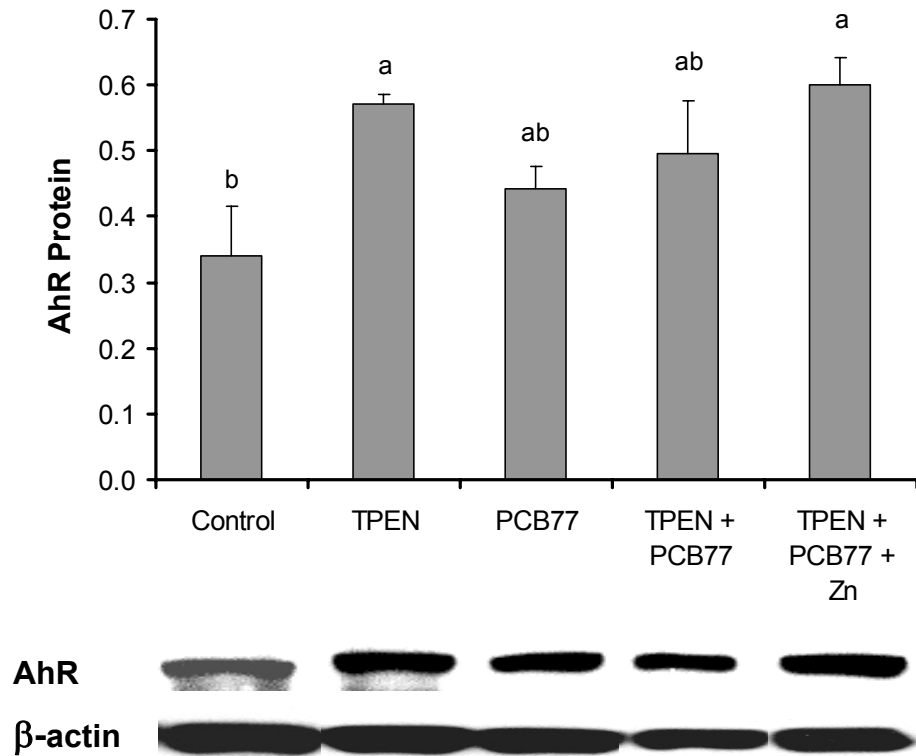


Figure V. Effects of cellular zinc status and PCB77 on the AhR protein expression in vascular endothelial cells.

Similar to Figure 5.1, endothelial cells were exposed to vehicle control, TPEN, PCB77 (3.4 μ M), TPEN plus PCB77, or TPEN with zinc supplementation (20 μ M) plus PCB77 for 24 hours. The values are ratios of the densitometric units of AhR over those of β -Actin. Bars with different letters (a, b) are statistically different from each other ($P < 0.05$). $n = 3$. The gel data are a representative of the typical outcome of three repeated western blot experiments.

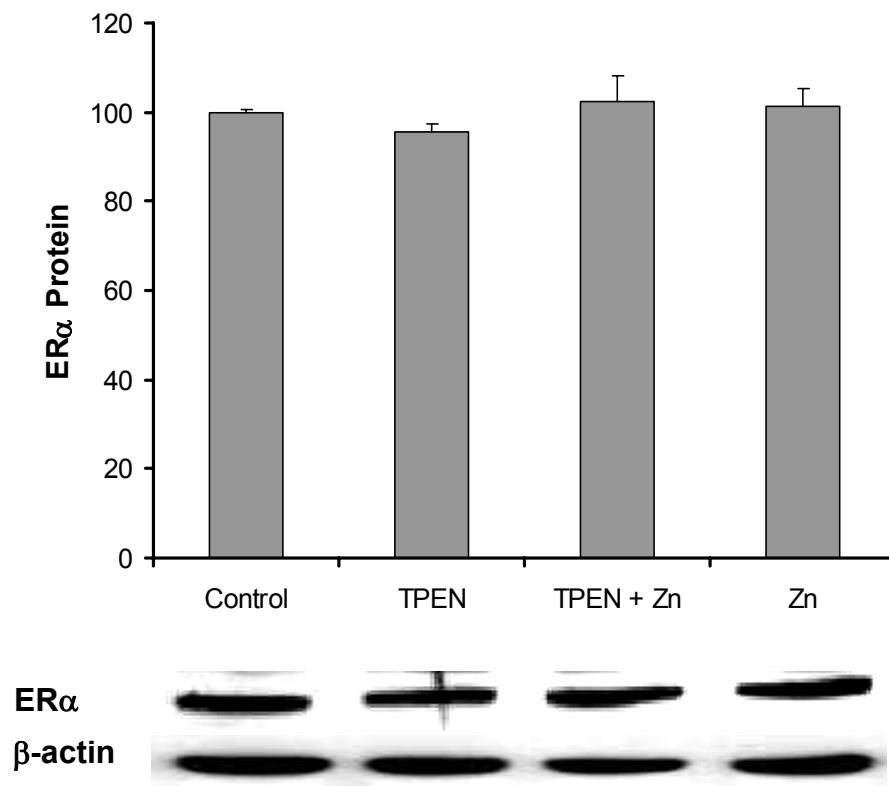


Figure VI. Zinc deficiency does not affect estrogen receptor (ER) α protein expression in vascular endothelial cells.

Endothelial cells were exposed to vehicle control (ethanol, 0.075 %), TPEN (1.5 μ M), TPEN (1.5 μ M) plus Zn (20 μ M), or Zn (20 μ M) for 24 h. ER α protein expression was measured by Western blot. The values are ratios of the densitometric units of ER α over those of β -actin, the endogenous control, expressed as percentage of control. Values are means \pm SEM, n = 4. The gel data are a representative of the typical outcome of four repeated Western Blot experiments.

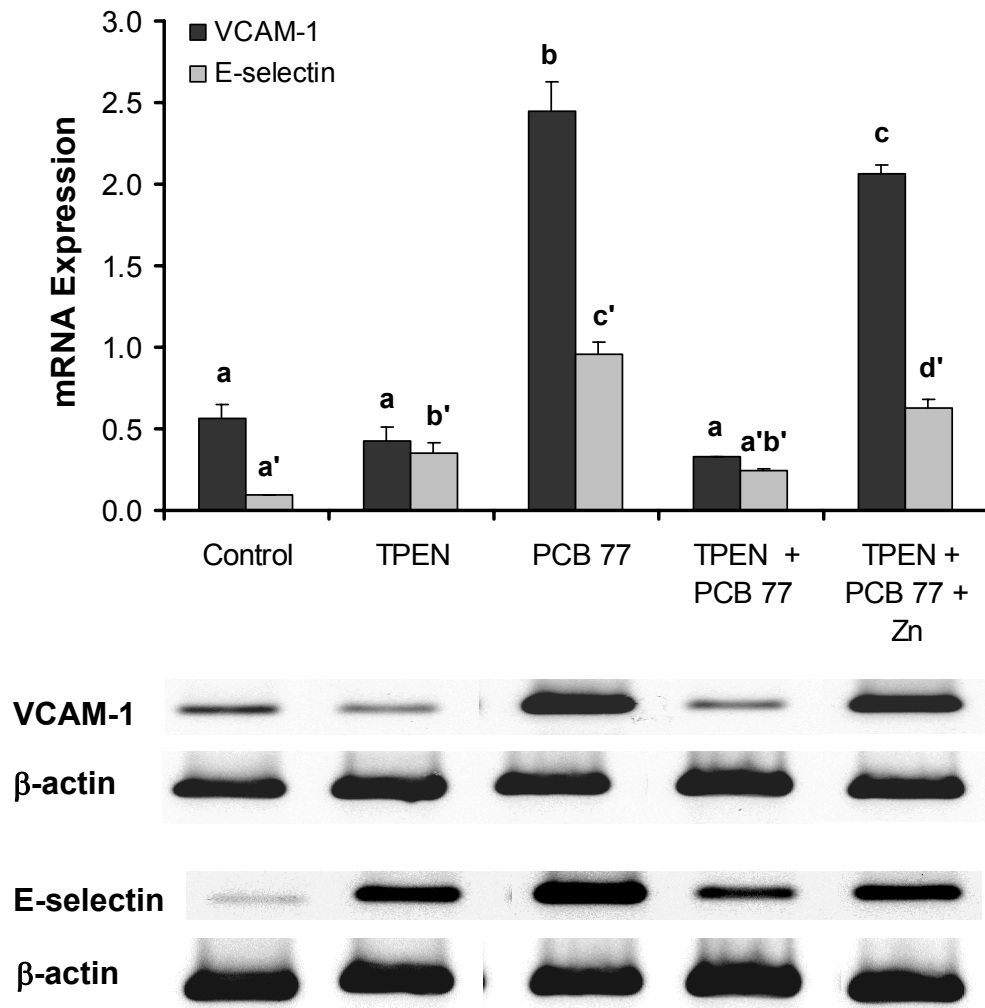


Figure VII. Zinc deficiency compromises PCB77-induced VCAM-1 and E-selectin mRNA expression in vascular endothelial cells

Similar to Figure 5.1, endothelial cells were exposed to vehicle control, TPEN, PCB77 (3.4 μ M), TPEN plus PCB77, or TPEN with zinc supplementation (20 μ M) plus PCB77 for 24 hours. The values are ratios of the densitometric units of VCAM-1 or E-selectin over those of β -actin. Bars with different letters (a, b, c for VCAM-1 and a', b', c', d' for E-selectin) are statistically different from each other ($P < 0.05$). $n = 3$. The gel data are a representative of the typical outcome of three repeated RT-PCR experiments.

References

1. Glass, C.K. and J.L. Witztum, *Atherosclerosis. the road ahead*. Cell, 2001. **104**(4): p. 503-16.
2. Lusis, A.J., *Atherosclerosis*. Nature, 2000. **407**(6801): p. 233-41.
3. Beattie, J.H. and I.S. Kwun, *Is zinc deficiency a risk factor for atherosclerosis?* Br J Nutr, 2004. **91**(2): p. 177-81.
4. Oteiza, P.I. and G.G. Mackenzie, *Zinc, oxidant-triggered cell signaling, and human health*. Mol Aspects Med, 2005. **26**(4-5): p. 245-55.
5. Lonnerdal, B., *Dietary factors influencing zinc absorption*. J Nutr, 2000. **130**(5S Suppl): p. 1378S-83S.
6. Kinlaw, W.B., et al., *Abnormal zinc metabolism in type II diabetes mellitus*. Am J Med, 1983. **75**(2): p. 273-7.
7. Milanino, R., et al., *Copper and zinc status during acute inflammation: studies on blood, liver and kidneys metal levels in normal and inflamed rats*. Agents Actions, 1986. **19**(3-4): p. 215-23.
8. Hambidge, K.M. and N.F. Krebs, *Zinc deficiency: a special challenge*. J Nutr, 2007. **137**(4): p. 1101-5.
9. Bettger, W.J. and B.L. O'Dell, *A critical physiological role of zinc in the structure and function of biomembranes*. Life Sci, 1981. **28**(13): p. 1425-38.
10. Hennig, B., et al., *Antioxidant-like properties of zinc in activated endothelial cells*. J Am Coll Nutr, 1999. **18**(2): p. 152-8.
11. Maret, W., *Zinc coordination environments in proteins determine zinc functions*. J Trace Elem Med Biol, 2005. **19**(1): p. 7-12.
12. Prasad, A.S. and O. Kucuk, *Zinc in cancer prevention*. Cancer Metastasis Rev, 2002. **21**(3-4): p. 291-5.
13. Lee, D.H., A.R. Folsom, and D.R. Jacobs, Jr., *Iron, zinc, and alcohol consumption and mortality from cardiovascular diseases: the Iowa Women's Health Study*. Am J Clin Nutr, 2005. **81**(4): p. 787-91.
14. Korichneva, I., *Zinc dynamics in the myocardial redox signaling network*. Antioxid Redox Signal, 2006. **8**(9-10): p. 1707-21.
15. Liuzzi, J.P. and R.J. Cousins, *Mammalian zinc transporters*. Annu Rev Nutr, 2004. **24**: p. 151-72.
16. Cousins, R.J., J.P. Liuzzi, and L.A. Lichten, *Mammalian zinc transport, trafficking, and signals*. J Biol Chem, 2006. **281**(34): p. 24085-9.
17. Kang, Y.J., *Metallothionein redox cycle and function*. Exp Biol Med (Maywood), 2006. **231**(9): p. 1459-67.
18. Maret, W., *Zinc coordination environments in proteins as redox sensors and signal transducers*. Antioxid Redox Signal, 2006. **8**(9-10): p. 1419-41.

19. Li, X., H. Chen, and P.N. Epstein, *Metallothionein protects islets from hypoxia and extends islet graft survival by scavenging most kinds of reactive oxygen species*. J Biol Chem, 2004. **279**(1): p. 765-71.
20. Thornalley, P.J. and M. Vasak, *Possible role for metallothionein in protection against radiation-induced oxidative stress. Kinetics and mechanism of its reaction with superoxide and hydroxyl radicals*. Biochim Biophys Acta, 1985. **827**(1): p. 36-44.
21. Blanquart, C., et al., *Peroxisome proliferator-activated receptors: regulation of transcriptional activities and roles in inflammation*. J Steroid Biochem Mol Biol, 2003. **85**(2-5): p. 267-73.
22. Hihi, A.K., L. Michalik, and W. Wahli, *PPARs: transcriptional effectors of fatty acids and their derivatives*. Cell Mol Life Sci, 2002. **59**(5): p. 790-8.
23. Torra, I.P., et al., *Peroxisome proliferator-activated receptors: from transcriptional control to clinical practice*. Curr Opin Lipidol, 2001. **12**(3): p. 245-54.
24. Lee, M.S., et al., *Structure of the retinoid X receptor alpha DNA binding domain: a helix required for homodimeric DNA binding*. Science, 1993. **260**(5111): p. 1117-21.
25. Meerarani, P., et al., *Zinc modulates PPARgamma signaling and activation of porcine endothelial cells*. J Nutr, 2003. **133**(10): p. 3058-64.
26. Reiterer, G., M. Toborek, and B. Hennig, *Peroxisome proliferator activated receptors alpha and gamma require zinc for their anti-inflammatory properties in porcine vascular endothelial cells*. J Nutr, 2004. **134**(7): p. 1711-5.
27. Ho, L.H., et al., *Labile zinc and zinc transporter ZnT4 in mast cell granules: role in regulation of caspase activation and NF-kappaB translocation*. J Immunol, 2004. **172**(12): p. 7750-60.
28. Prasad, A.S., et al., *Antioxidant effect of zinc in humans*. Free Radic Biol Med, 2004. **37**(8): p. 1182-90.
29. Prasad, A.S., et al., *Zinc enhances the expression of interleukin-2 and interleukin-2 receptors in HUT-78 cells by way of NF-kappaB activation*. J Lab Clin Med, 2002. **140**(4): p. 272-89.
30. Mackenzie, G.G., et al., *Low intracellular zinc impairs the translocation of activated NF-kappa B to the nuclei in human neuroblastoma IMR-32 cells*. J Biol Chem, 2002. **277**(37): p. 34610-7.
31. Oteiza, P.I., et al., *Zinc deficiency induces oxidative stress and AP-1 activation in 3T3 cells*. Free Radic Biol Med, 2000. **28**(7): p. 1091-9.
32. Ho, E. and B.N. Ames, *Low intracellular zinc induces oxidative DNA damage, disrupts p53, NFkappa B, and AP1 DNA binding, and affects DNA repair in a rat glioma cell line*. Proc Natl Acad Sci U S A, 2002. **99**(26): p. 16770-5.

33. De Martin, R., et al., *The transcription factor NF-kappa B and the regulation of vascular cell function*. *Arterioscler Thromb Vasc Biol*, 2000. **20**(11): p. E83-8.
34. Delerive, P., et al., *Peroxisome proliferator-activated receptor alpha negatively regulates the vascular inflammatory gene response by negative cross-talk with transcription factors NF-kappaB and AP-1*. *J Biol Chem*, 1999. **274**(45): p. 32048-54.
35. Chung, S.W., et al., *Oxidized low density lipoprotein inhibits interleukin-12 production in lipopolysaccharide-activated mouse macrophages via direct interactions between peroxisome proliferator-activated receptor-gamma and nuclear factor-kappa B*. *J Biol Chem*, 2000. **275**(42): p. 32681-7.
36. Delerive, P., et al., *Induction of IkappaBalpha expression as a mechanism contributing to the anti-inflammatory activities of peroxisome proliferator-activated receptor-alpha activators*. *J Biol Chem*, 2000. **275**(47): p. 36703-7.
37. Law, R.E., et al., *Troglitazone inhibits vascular smooth muscle cell growth and intimal hyperplasia*. *J Clin Invest*, 1996. **98**(8): p. 1897-905.
38. Qayyum, R. and P. Schulman, *Cardiovascular effects of the thiazolidinediones*. *Diabetes Metab Res Rev*, 2006. **22**(2): p. 88-97.
39. van Wijk, J.P. and T.J. Rabelink, *Impact of thiazolidinedione therapy on atherogenesis*. *Curr Atheroscler Rep*, 2005. **7**(5): p. 369-74.
40. Irons, B.K., et al., *Implications of rosiglitazone and pioglitazone on cardiovascular risk in patients with type 2 diabetes mellitus*. *Pharmacotherapy*, 2006. **26**(2): p. 168-81.
41. Granberry, M.C., J.B. Hawkins, and A.M. Franks, *Thiazolidinediones in patients with type 2 diabetes mellitus and heart failure*. *Am J Health Syst Pharm*, 2007. **64**(9): p. 931-6.
42. Lago, R.M., P.P. Singh, and R.W. Nesto, *Congestive heart failure and cardiovascular death in patients with prediabetes and type 2 diabetes given thiazolidinediones: a meta-analysis of randomised clinical trials*. *Lancet*, 2007. **370**(9593): p. 1129-36.
43. Swanson, H.I. and C.A. Bradfield, *The AH-receptor: genetics, structure and function*. *Pharmacogenetics*, 1993. **3**(5): p. 213-30.
44. Dalton, T.P., A. Puga, and H.G. Shertzer, *Induction of cellular oxidative stress by aryl hydrocarbon receptor activation*. *Chem Biol Interact*, 2002. **141**(1-2): p. 77-95.
45. Puga, A., C.R. Tomlinson, and Y. Xia, *Ah receptor signals cross-talk with multiple developmental pathways*. *Biochem Pharmacol*, 2005. **69**(2): p. 199-207.
46. Hankinson, O., *The aryl hydrocarbon receptor complex*. *Annu Rev Pharmacol Toxicol*, 1995. **35**: p. 307-40.

47. Barouki, R., X. Coumoul, and P.M. Fernandez-Salguero, *The aryl hydrocarbon receptor, more than a xenobiotic-interacting protein*. FEBS Lett, 2007. **581**(19): p. 3608-15.
48. Nebert, D.W., et al., *Role of the aromatic hydrocarbon receptor and [Ah] gene battery in the oxidative stress response, cell cycle control, and apoptosis*. Biochem Pharmacol, 2000. **59**(1): p. 65-85.
49. Zangar, R.C., D.R. Davydov, and S. Verma, *Mechanisms that regulate production of reactive oxygen species by cytochrome P450*. Toxicol Appl Pharmacol, 2004. **199**(3): p. 316-31.
50. Fujii-Kuriyama, Y. and J. Mimura, *Molecular mechanisms of AhR functions in the regulation of cytochrome P450 genes*. Biochem Biophys Res Commun, 2005. **338**(1): p. 311-7.
51. Savouret, J.F., A. Berdeaux, and R.F. Casper, *The aryl hydrocarbon receptor and its xenobiotic ligands: a fundamental trigger for cardiovascular diseases*. Nutr Metab Cardiovasc Dis, 2003. **13**(2): p. 104-13.
52. Kawajiri, K. and Y. Fujii-Kuriyama, *Cytochrome P450 gene regulation and physiological functions mediated by the aryl hydrocarbon receptor*. Arch Biochem Biophys, 2007. **464**(2): p. 207-12.
53. Denison, M.S. and R.M. Deal, *The binding of transformed aromatic hydrocarbon (Ah) receptor to its DNA recognition site is not affected by metal depletion*. Mol Cell Endocrinol, 1990. **69**(1): p. 51-7.
54. Kobayashi, A., K. Sogawa, and Y. Fujii-Kuriyama, *Cooperative interaction between AhR.Arnt and Sp1 for the drug-inducible expression of CYP1A1 gene*. J Biol Chem, 1996. **271**(21): p. 12310-6.
55. Reiterer, G., M. Toborek, and B. Hennig, *Zinc and cell signaling during inflammation: implications in atherosclerosis*. Current Nutrition and Food Science, 2006. **2**: p. 23-28.
56. Duffy, J.Y., et al., *Cardiac abnormalities induced by zinc deficiency are associated with alterations in the expression of genes regulated by the zinc-finger transcription factor GATA-4*. Birth Defects Res B Dev Reprod Toxicol, 2004. **71**(2): p. 102-9.
57. Pocar, P., et al., *Cellular and molecular mechanisms mediating the effect of polychlorinated biphenyls on oocyte in vitro maturation*. Reprod Toxicol, 2006. **22**(2): p. 242-9.
58. Fonnum, F., E. Mariussen, and T. Reistad, *Molecular mechanisms involved in the toxic effects of polychlorinated biphenyls (PCBs) and brominated flame retardants (BFRs)*. J Toxicol Environ Health A, 2006. **69**(1-2): p. 21-35.
59. Schlezinger, J.J., R.D. White, and J.J. Stegeman, *Oxidative inactivation of cytochrome P-450 1A (CYP1A) stimulated by 3,3',4,4'-tetrachlorobiphenyl: production of reactive oxygen by vertebrate CYP1As*. Mol Pharmacol, 1999. **56**(3): p. 588-97.

60. La Rocca, C. and A. Mantovani, *From environment to food: the case of PCB*. Ann Ist Super Sanita, 2006. **42**(4): p. 410-6.
61. Hennig, B., et al., *Modification of environmental toxicity by nutrients: implications in atherosclerosis*. Cardiovasc Toxicol, 2005. **5**(2): p. 153-60.
62. Slim, R., et al., *Antioxidant protection against PCB-mediated endothelial cell activation*. Toxicol Sci, 1999. **52**(2): p. 232-9.
63. Vasto, S., et al., *Inflammation, genes and zinc in ageing and age-related diseases*. Biogerontology, 2006. **7**(5-6): p. 315-27.
64. Kettler, S.I., et al., *Zinc deficiency and the activities of lipoprotein lipase in plasma and tissues of rats force-fed diets with coconut oil or fish oil*. J Nutr Biochem, 2000. **11**(3): p. 132-8.
65. Malloy, M.J. and J.P. Kane, *A risk factor for atherosclerosis: triglyceride-rich lipoproteins*. Adv Intern Med, 2001. **47**: p. 111-36.
66. Tubek, S., *Role of zinc in regulation of arterial blood pressure and in the etiopathogenesis of arterial hypertension*. Biol Trace Elem Res, 2007. **117**(1-3): p. 39-51.
67. Singh, R.B., et al., *Epidemiologic study of trace elements and magnesium on risk of coronary artery disease in rural and urban Indian populations*. J Am Coll Nutr, 1997. **16**(1): p. 62-7.
68. Singh, R.B., et al., *Current zinc intake and risk of diabetes and coronary artery disease and factors associated with insulin resistance in rural and urban populations of North India*. J Am Coll Nutr, 1998. **17**(6): p. 564-70.
69. Vlad, M., et al., *Concentration of copper, zinc, chromium, iron and nickel in the abdominal aorta of patients deceased with coronary heart disease*. J Trace Elem Electrolytes Health Dis, 1994. **8**(2): p. 111-4.
70. Hennig, B., et al., *Zinc nutrition and apoptosis of vascular endothelial cells: implications in atherosclerosis*. Nutrition, 1999. **15**(10): p. 744-8.
71. Cousins, R.J., *A role of zinc in the regulation of gene expression*. Proc Nutr Soc, 1998. **57**(2): p. 307-11.
72. O'Dell, B.L., *Role of zinc in plasma membrane function*. J Nutr, 2000. **130**(5S Suppl): p. 1432S-6S.
73. Shen, H., et al., *Zinc Deficiency Alters Lipid Metabolism in LDL Receptor Deficient Mice Treated with Rosiglitazone*. J Nutr, 2007. **137**(11): p. 2339-2345.
74. Li, A.C., et al., *Differential inhibition of macrophage foam-cell formation and atherosclerosis in mice by PPARalpha, beta/delta, and gamma*. J Clin Invest, 2004. **114**(11): p. 1564-76.
75. Hennig, B., et al., *Exposure to free fatty acid increases the transfer of albumin across cultured endothelial monolayers*. Arteriosclerosis, 1984. **4**(5): p. 489-97.
76. Toborek, M., et al., *Unsaturated fatty acids selectively induce an inflammatory environment in human endothelial cells*. Am J Clin Nutr, 2002. **75**(1): p. 119-25.

77. Choi, W., et al., *PCB 104-induced proinflammatory reactions in human vascular endothelial cells: relationship to cancer metastasis and atherogenesis*. Toxicol Sci, 2003. **75**(1): p. 47-56.
78. Lim, E.J. and C.W. Kim, *Functional characterization of the promoter region of the chicken elongation factor-2 gene*. Gene, 2007. **386**(1-2): p. 183-90.
79. Bruemmer, D., et al., *A non-thiazolidinedione partial peroxisome proliferator-activated receptor gamma ligand inhibits vascular smooth muscle cell growth*. Eur J Pharmacol, 2003. **466**(3): p. 225-34.
80. Chung, H.Y., et al., *The molecular inflammatory process in aging*. Antioxid Redox Signal, 2006. **8**(3-4): p. 572-81.
81. Vasto, S., et al., *Zinc and inflammatory/immune response in aging*. Ann N Y Acad Sci, 2007. **1100**: p. 111-22.
82. Prasad, A.S., *Zinc: mechanisms of host defense*. J Nutr, 2007. **137**(5): p. 1345-9.
83. Griendling, K.K. and G.A. FitzGerald, *Oxidative stress and cardiovascular injury: Part I: basic mechanisms and in vivo monitoring of ROS*. Circulation, 2003. **108**(16): p. 1912-6.
84. Griendling, K.K. and G.A. FitzGerald, *Oxidative stress and cardiovascular injury: Part II: animal and human studies*. Circulation, 2003. **108**(17): p. 2034-40.
85. Li, N. and M. Karin, *Is NF-kappaB the sensor of oxidative stress?* Faseb J, 1999. **13**(10): p. 1137-43.
86. Monaco, C. and E. Paleolog, *Nuclear factor kappaB: a potential therapeutic target in atherosclerosis and thrombosis*. Cardiovasc Res, 2004. **61**(4): p. 671-82.
87. Connell, P., et al., *Zinc attenuates tumor necrosis factor-mediated activation of transcription factors in endothelial cells*. J Am Coll Nutr, 1997. **16**(5): p. 411-7.
88. Baldwin, A.S., Jr., *Series introduction: the transcription factor NF-kappaB and human disease*. J Clin Invest, 2001. **107**(1): p. 3-6.
89. Brostjan, C., et al., *Glucocorticoids inhibit E-selectin expression by targeting NF-kappaB and not ATF/c-Jun*. J Immunol, 1997. **158**(8): p. 3836-44.
90. Bishop-Bailey, D., J.A. Mitchell, and T.D. Warner, *COX-2 in cardiovascular disease*. Arterioscler Thromb Vasc Biol, 2006. **26**(5): p. 956-8.
91. Kaneko, M., et al., *Probucol downregulates E-selectin expression on cultured human vascular endothelial cells*. Arterioscler Thromb Vasc Biol, 1996. **16**(8): p. 1047-51.
92. Natarajan, K., et al., *Caffeic acid phenethyl ester is a potent and specific inhibitor of activation of nuclear transcription factor NF-kappa B*. Proc Natl Acad Sci U S A, 1996. **93**(17): p. 9090-5.
93. Rattazzi, M., et al., *C-reactive protein and interleukin-6 in vascular disease: culprits or passive bystanders?* J Hypertens, 2003. **21**(10): p. 1787-803.

94. Schwartz, S.M., *Perspectives series: cell adhesion in vascular biology. Smooth muscle migration in atherosclerosis and restenosis.* J Clin Invest, 1997. **99**(12): p. 2814-6.
95. Hennig, B., M. Toborek, and C.J. McClain, *Antiatherogenic properties of zinc: implications in endothelial cell metabolism.* Nutrition, 1996. **12**(10): p. 711-7.
96. Lebovitz, H.E., et al., *Rosiglitazone monotherapy is effective in patients with type 2 diabetes.* J Clin Endocrinol Metab, 2001. **86**(1): p. 280-8.
97. Mohanty, P., et al., *Evidence for a potent antiinflammatory effect of rosiglitazone.* J Clin Endocrinol Metab, 2004. **89**(6): p. 2728-35.
98. Cuzzocrea, S., et al., *Rosiglitazone, a ligand of the peroxisome proliferator-activated receptor-gamma, reduces acute inflammation.* Eur J Pharmacol, 2004. **483**(1): p. 79-93.
99. Li, A.C., et al., *Peroxisome proliferator-activated receptor gamma ligands inhibit development of atherosclerosis in LDL receptor-deficient mice.* J Clin Invest, 2000. **106**(4): p. 523-31.
100. Levi, Z., et al., *Rosiglitazone (PPARgamma-agonist) attenuates atherogenesis with no effect on hyperglycaemia in a combined diabetes-atherosclerosis mouse model.* Diabetes Obes Metab, 2003. **5**(1): p. 45-50.
101. Haffner, S.M., et al., *Effect of rosiglitazone treatment on nontraditional markers of cardiovascular disease in patients with type 2 diabetes mellitus.* Circulation, 2002. **106**(6): p. 679-84.
102. Meisner, F., et al., *Effect of rosiglitazone treatment on plaque inflammation and collagen content in nondiabetic patients: data from a randomized placebo-controlled trial.* Arterioscler Thromb Vasc Biol, 2006. **26**(4): p. 845-50.
103. Samaha, F.F., et al., *Effects of rosiglitazone on lipids, adipokines, and inflammatory markers in nondiabetic patients with low high-density lipoprotein cholesterol and metabolic syndrome.* Arterioscler Thromb Vasc Biol, 2006. **26**(3): p. 624-30.
104. Ishibashi, S., et al., *Massive xanthomatosis and atherosclerosis in cholesterol-fed low density lipoprotein receptor-negative mice.* J Clin Invest, 1994. **93**(5): p. 1885-93.
105. Reeves, P.G., K.L. Rossow, and J. Lindlauf, *Development and testing of the AIN-93 purified diets for rodents: results on growth, kidney calcification and bone mineralization in rats and mice.* J Nutr, 1993. **123**(11): p. 1923-31.
106. Emery, M.P., J.D. Browning, and B.L. O'Dell, *Impaired hemostasis and platelet function in rats fed low zinc diets based on egg white protein.* J Nutr, 1990. **120**(9): p. 1062-7.
107. Browning, J.D., et al., *Reduced food intake in zinc deficient rats is normalized by megestrol acetate but not by insulin-like growth factor-I.* J Nutr, 1998. **128**(1): p. 136-42.

108. Canton, M.C. and F.M. Cremin, *The effect of dietary zinc depletion and repletion on rats: Zn concentration in various tissues and activity of pancreatic gamma-glutamyl hydrolase (EC 3.4.22.12) as indices of Zn status*. Br J Nutr, 1990. **64**(1): p. 201-9.
109. Lucas, A.D. and D.R. Greaves, *Atherosclerosis: role of chemokines and macrophages*. Expert Rev Mol Med, 2001. **3**(25): p. 1-18.
110. Maret, W. and A. Krezel, *Cellular zinc and redox buffering capacity of metallothionein/thionein in health and disease*. Mol Med, 2007. **13**(7-8): p. 371-5.
111. Giacconi, R., et al., *+647 A/C and +1245 MT1A polymorphisms in the susceptibility of diabetes mellitus and cardiovascular complications*. Mol Genet Metab, 2008.
112. Kaul, D., *Molecular link between cholesterol, cytokines and atherosclerosis*. Mol Cell Biochem, 2001. **219**(1-2): p. 65-71.
113. Dinarello, C.A., *Proinflammatory cytokines*. Chest, 2000. **118**(2): p. 503-8.
114. Opal, S.M. and V.A. DePalo, *Anti-inflammatory cytokines*. Chest, 2000. **117**(4): p. 1162-72.
115. Signorelli, S.S., et al., *Proinflammatory circulating molecules in peripheral arterial disease*. Int J Mol Med, 2007. **20**(3): p. 279-86.
116. Hauer, A.D., et al., *Blockade of interleukin-12 function by protein vaccination attenuates atherosclerosis*. Circulation, 2005. **112**(7): p. 1054-62.
117. Ito, T. and U. Ikeda, *Inflammatory cytokines and cardiovascular disease*. Curr Drug Targets Inflamm Allergy, 2003. **2**(3): p. 257-65.
118. Reiterer, G., et al., *Zinc deficiency increases plasma lipids and atherosclerotic markers in LDL-receptor-deficient mice*. J Nutr, 2005. **135**(9): p. 2114-8.
119. Siebenlist, U., G. Franzoso, and K. Brown, *Structure, regulation and function of NF-kappa B*. Annu Rev Cell Biol, 1994. **10**: p. 405-55.
120. Baldwin, A.S., Jr., *The NF-kappa B and I kappa B proteins: new discoveries and insights*. Annu Rev Immunol, 1996. **14**: p. 649-83.
121. Basu, A., S. Devaraj, and I. Jialal, *Dietary factors that promote or retard inflammation*. Arterioscler Thromb Vasc Biol, 2006. **26**(5): p. 995-1001.
122. Perona, J.S., R. Cabello-Moruno, and V. Ruiz-Gutierrez, *The role of virgin olive oil components in the modulation of endothelial function*. J Nutr Biochem, 2006. **17**(7): p. 429-45.
123. Menuet, R., C.J. Lavie, and R.V. Milani, *Importance and management of dyslipidemia in the metabolic syndrome*. Am J Med Sci, 2005. **330**(6): p. 295-302.
124. Taylor, C.G., *Zinc, the pancreas, and diabetes: insights from rodent studies and future directions*. Biometals, 2005. **18**(4): p. 305-12.

125. Haase, H. and W. Maret, *Protein tyrosine phosphatases as targets of the combined insulinomimetic effects of zinc and oxidants*. *Biometals*, 2005. **18**(4): p. 333-8.
126. Sidhu, J.S., et al., *Effect of rosiglitazone on common carotid intima-media thickness progression in coronary artery disease patients without diabetes mellitus*. *Arterioscler Thromb Vasc Biol*, 2004. **24**(5): p. 930-4.
127. Dormandy, J.A., et al., *Secondary prevention of macrovascular events in patients with type 2 diabetes in the PROactive Study (PROspective pioglitAzone Clinical Trial In macroVascular Events): a randomised controlled trial*. *Lancet*, 2005. **366**(9493): p. 1279-89.
128. Phillips, L.S., et al., *Once- and twice-daily dosing with rosiglitazone improves glycemic control in patients with type 2 diabetes*. *Diabetes Care*, 2001. **24**(2): p. 308-15.
129. Van Wijk, J.P., et al., *Rosiglitazone improves postprandial triglyceride and free fatty acid metabolism in type 2 diabetes*. *Diabetes Care*, 2005. **28**(4): p. 844-9.
130. Sidhu, J.S., D. Cowan, and J.C. Kaski, *Effects of rosiglitazone on endothelial function in men with coronary artery disease without diabetes mellitus*. *Am J Cardiol*, 2004. **94**(2): p. 151-6.
131. Barish, G.D., *Peroxisome proliferator-activated receptors and liver X receptors in atherosclerosis and immunity*. *J Nutr*, 2006. **136**(3): p. 690-4.
132. Hsu, M.H., et al., *A carboxyl-terminal extension of the zinc finger domain contributes to the specificity and polarity of peroxisome proliferator-activated receptor DNA binding*. *J Biol Chem*, 1998. **273**(43): p. 27988-97.
133. Staels, B., *PPARgamma and atherosclerosis*. *Curr Med Res Opin*, 2005. **21 Suppl 1**: p. S13-20.
134. Gillooly, D.J., A. Simonsen, and H. Stenmark, *Cellular functions of phosphatidylinositol 3-phosphate and FYVE domain proteins*. *Biochem J*, 2001. **355**(Pt 2): p. 249-58.
135. Daugherty, A., et al., *The effects of total lymphocyte deficiency on the extent of atherosclerosis in apolipoprotein E^{-/-} mice*. *J Clin Invest*, 1997. **100**(6): p. 1575-80.
136. Folch, J., M. Lees, and G.H. Sloane Stanley, *A simple method for the isolation and purification of total lipides from animal tissues*. *J Biol Chem*, 1957. **226**(1): p. 497-509.
137. Shirai, N., H. Suzuki, and S. Wada, *Direct methylation from mouse plasma and from liver and brain homogenates*. *Anal Biochem*, 2005. **343**(1): p. 48-53.
138. Li, A.C. and C.K. Glass, *PPAR- and LXR-dependent pathways controlling lipid metabolism and the development of atherosclerosis*. *J Lipid Res*, 2004. **45**(12): p. 2161-73.

139. Iwaki, M., et al., *Induction of adiponectin, a fat-derived antidiabetic and antiatherogenic factor, by nuclear receptors*. Diabetes, 2003. **52**(7): p. 1655-63.
140. Evans, R.M., G.D. Barish, and Y.X. Wang, *PPARs and the complex journey to obesity*. Nat Med, 2004. **10**(4): p. 355-61.
141. Semple, R.K., V.K. Chatterjee, and S. O'Rahilly, *PPAR gamma and human metabolic disease*. J Clin Invest, 2006. **116**(3): p. 581-9.
142. Samman, S. and D.C. Roberts, *The effect of zinc supplements on lipoproteins and copper status*. Atherosclerosis, 1988. **70**(3): p. 247-52.
143. Partida-Hernandez, G., et al., *Effect of zinc replacement on lipids and lipoproteins in type 2-diabetic patients*. Biomed Pharmacother, 2006. **60**(4): p. 161-8.
144. Gatto, L.M. and S. Samman, *The effect of zinc supplementation on plasma lipids and low-density lipoprotein oxidation in males*. Free Radic Biol Med, 1995. **19**(4): p. 517-21.
145. Hooper, P.L., et al., *Zinc lowers high-density lipoprotein-cholesterol levels*. Jama, 1980. **244**(17): p. 1960-1.
146. Black, M.R., et al., *Zinc supplements and serum lipids in young adult white males*. Am J Clin Nutr, 1988. **47**(6): p. 970-5.
147. Teruel, T., et al., *Rosiglitazone up-regulates lipoprotein lipase, hormone-sensitive lipase and uncoupling protein-1, and down-regulates insulin-induced fatty acid synthase gene expression in brown adipocytes of Wistar rats*. Diabetologia, 2005. **48**(6): p. 1180-8.
148. Tan, G.D., et al., *The effects of rosiglitazone on fatty acid and triglyceride metabolism in type 2 diabetes*. Diabetologia, 2005. **48**(1): p. 83-95.
149. Ovalle, F. and D.S. Bell, *Lipoprotein effects of different thiazolidinediones in clinical practice*. Endocr Pract, 2002. **8**(6): p. 406-10.
150. Goldberg, R.B., et al., *A comparison of lipid and glycemic effects of pioglitazone and rosiglitazone in patients with type 2 diabetes and dyslipidemia*. Diabetes Care, 2005. **28**(7): p. 1547-54.
151. Austin, M.A., et al., *Cardiovascular disease mortality in familial forms of hypertriglyceridemia: A 20-year prospective study*. Circulation, 2000. **101**(24): p. 2777-82.
152. Woodman, R.J., G.T. Chew, and G.F. Watts, *Mechanisms, significance and treatment of vascular dysfunction in type 2 diabetes mellitus: focus on lipid-regulating therapy*. Drugs, 2005. **65**(1): p. 31-74.
153. Krauss, R.M., *Lipids and lipoproteins in patients with type 2 diabetes*. Diabetes Care, 2004. **27**(6): p. 1496-504.
154. Michalik, L., et al., *International Union of Pharmacology. LXI. Peroxisome proliferator-activated receptors*. Pharmacol Rev, 2006. **58**(4): p. 726-41.

155. Ziouzenkova, O., et al., *Dual roles for lipolysis and oxidation in peroxisome proliferation-activator receptor responses to electronegative low density lipoprotein*. J Biol Chem, 2003. **278**(41): p. 39874-81.
156. Nicholson, A.C., et al., *Role of CD36, the macrophage class B scavenger receptor, in atherosclerosis*. Ann N Y Acad Sci, 2001. **947**: p. 224-8.
157. Liang, C.P., et al., *Increased CD36 protein as a response to defective insulin signaling in macrophages*. J Clin Invest, 2004. **113**(5): p. 764-73.
158. Svensson, L., et al., *Fatty acids modulate the effect of darglitazone on macrophage CD36 expression*. Eur J Clin Invest, 2003. **33**(6): p. 464-71.
159. Zhang, D.D., *Mechanistic studies of the Nrf2-Keap1 signaling pathway*. Drug Metab Rev, 2006. **38**(4): p. 769-89.
160. Ishii, T., et al., *Role of Nrf2 in the regulation of CD36 and stress protein expression in murine macrophages: activation by oxidatively modified LDL and 4-hydroxynonenal*. Circ Res, 2004. **94**(5): p. 609-16.
161. Fuhrman, B., N. Volkova, and M. Aviram, *Oxidative stress increases the expression of the CD36 scavenger receptor and the cellular uptake of oxidized low-density lipoprotein in macrophages from atherosclerotic mice: protective role of antioxidants and of paraoxonase*. Atherosclerosis, 2002. **161**(2): p. 307-16.
162. Kim, K.Y., et al., *c-Jun N-terminal kinase is involved in the suppression of adiponectin expression by TNF-alpha in 3T3-L1 adipocytes*. Biochem Biophys Res Commun, 2005. **327**(2): p. 460-7.
163. Tapiero, H. and K.D. Tew, *Trace elements in human physiology and pathology: zinc and metallothioneins*. Biomed Pharmacother, 2003. **57**(9): p. 399-411.
164. Lund, A.K., et al., *Characterizing the role of endothelin-1 in the progression of cardiac hypertrophy in aryl hydrocarbon receptor (AhR) null mice*. Toxicol Appl Pharmacol, 2006. **212**(2): p. 127-35.
165. Fernandez-Salguero, P.M., et al., *Lesions of aryl-hydrocarbon receptor-deficient mice*. Vet Pathol, 1997. **34**(6): p. 605-14.
166. Lund, A.K., et al., *Cardiac hypertrophy in aryl hydrocarbon receptor null mice is correlated with elevated angiotensin II, endothelin-1, and mean arterial blood pressure*. Toxicol Appl Pharmacol, 2003. **193**(2): p. 177-87.
167. Xin, M., et al., *A threshold of GATA4 and GATA6 expression is required for cardiovascular development*. Proc Natl Acad Sci U S A, 2006. **103**(30): p. 11189-94.
168. Ikuta, T. and K. Kawajiri, *Zinc finger transcription factor Slug is a novel target gene of aryl hydrocarbon receptor*. Exp Cell Res, 2006. **312**(18): p. 3585-94.
169. Ramadass, P., et al., *Dietary flavonoids modulate PCB-induced oxidative stress, CYP1A1 induction, and AhR-DNA binding activity in vascular endothelial cells*. Toxicol Sci, 2003. **76**(1): p. 212-9.

170. Stegeman, J.J., et al., *Induction of cytochrome P4501A1 by aryl hydrocarbon receptor agonists in porcine aorta endothelial cells in culture and cytochrome P4501A1 activity in intact cells*. Mol Pharmacol, 1995. **47**(2): p. 296-306.
171. Barchowsky, A., et al., *Expression and activity of urokinase and its receptor in endothelial and pulmonary epithelial cells exposed to asbestos*. Toxicol Appl Pharmacol, 1998. **152**(2): p. 388-96.
172. Cousins, R.J., et al., *Regulation of zinc metabolism and genomic outcomes*. J Nutr, 2003. **133**(5 Suppl 1): p. 1521S-6S.
173. Klug, A. and J.W. Schwabe, *Protein motifs 5. Zinc fingers*. Faseb J, 1995. **9**(8): p. 597-604.
174. Shi, Y. and J.M. Berg, *Specific DNA-RNA hybrid binding by zinc finger proteins*. Science, 1995. **268**(5208): p. 282-4.
175. Kroncke, K.D. and C. Carlberg, *Inactivation of zinc finger transcription factors provides a mechanism for a gene regulatory role of nitric oxide*. Faseb J, 2000. **14**(1): p. 166-73.
176. Kroncke, K.D., et al., *Comparing nitrosative versus oxidative stress toward zinc finger-dependent transcription. Unique role for NO*. J Biol Chem, 2002. **277**(15): p. 13294-301.
177. Linke, K., et al., *The roles of the two zinc binding sites in DnaJ*. J Biol Chem, 2003. **278**(45): p. 44457-66.
178. Mahon, M.J. and T.A. Gasiewicz, *Chelatable metal ions are not required for aryl hydrocarbon receptor transformation to a DNA binding form: phenanthrolines are possible competitive antagonists of 2,3,7,8-tetrachlorodibenzo-p-dioxin*. Arch Biochem Biophys, 1992. **297**(1): p. 1-8.
179. Li, L., et al., *Gene regulation by Sp1 and Sp3*. Biochem Cell Biol, 2004. **82**(4): p. 460-71.
180. Suske, G., *The Sp-family of transcription factors*. Gene, 1999. **238**(2): p. 291-300.
181. Thiesen, H.J. and C. Bach, *Transition metals modulate DNA-protein interactions of SP1 zinc finger domains with its cognate target site*. Biochem Biophys Res Commun, 1991. **176**(2): p. 551-7.
182. Wu, X., et al., *Physical and functional sensitivity of zinc finger transcription factors to redox change*. Mol Cell Biol, 1996. **16**(3): p. 1035-46.
183. Ichihara, S., et al., *Attenuation of cardiac dysfunction by a PPAR-alpha agonist is associated with down-regulation of redox-regulated transcription factors*. J Mol Cell Cardiol, 2006. **41**(2): p. 318-29.
184. Hashemi, M., et al., *Cytotoxic effects of intra and extracellular zinc chelation on human breast cancer cells*. Eur J Pharmacol, 2007. **557**(1): p. 9-19.
185. Hyun, H.J., et al., *Depletion of intracellular zinc and copper with TPEN results in apoptosis of cultured human retinal pigment epithelial cells*. Invest Ophthalmol Vis Sci, 2001. **42**(2): p. 460-5.

186. Cao, J., et al., *Effects of intracellular zinc depletion on metallothionein and ZIP2 transporter expression and apoptosis*. J Leukoc Biol, 2001. **70**(4): p. 559-66.
187. Arslan, P., et al., *Cytosolic Ca²⁺ homeostasis in Ehrlich and Yoshida carcinomas. A new, membrane-permeant chelator of heavy metals reveals that these ascites tumor cell lines have normal cytosolic free Ca²⁺*. J Biol Chem, 1985. **260**(5): p. 2719-27.
188. MacDonald, R.S., et al., *Zinc deprivation of murine 3T3 cells by use of diethylenetri-nitropentaacetate impairs DNA synthesis upon stimulation with insulin-like growth factor-1 (IGF-1)*. J Nutr, 1998. **128**(10): p. 1600-5.
189. Haase, H., et al., *Flow cytometric measurement of labile zinc in peripheral blood mononuclear cells*. Anal Biochem, 2006. **352**(2): p. 222-30.
190. Haase, H. and W. Maret, *Intracellular zinc fluctuations modulate protein tyrosine phosphatase activity in insulin/insulin-like growth factor-1 signaling*. Exp Cell Res, 2003. **291**(2): p. 289-98.
191. Bozym, R.A., et al., *Measuring picomolar intracellular exchangeable zinc in PC-12 cells using a ratiometric fluorescence biosensor*. ACS Chem Biol, 2006. **1**(2): p. 103-11.
192. Prasad, A.S., et al., *Zinc deficiency in elderly patients*. Nutrition, 1993. **9**(3): p. 218-24.
193. Shenkin, A., *Trace elements and inflammatory response: implications for nutritional support*. Nutrition, 1995. **11**(1 Suppl): p. 100-5.
194. Wanchu, A., et al., *Plasma and peripheral blood mononuclear cells levels of Zn and Cu among Indian patients with RA*. Ann Rheum Dis, 2002. **61**(1): p. 88.
195. Thomson, M.J., V. Puntmann, and J.C. Kaski, *Atherosclerosis and oxidant stress: the end of the road for antioxidant vitamin treatment?* Cardiovasc Drugs Ther, 2007. **21**(3): p. 195-210.
196. Myhre, O., et al., *Evaluation of the probes 2',7'-dichlorofluorescein diacetate, luminol, and lucigenin as indicators of reactive species formation*. Biochem Pharmacol, 2003. **65**(10): p. 1575-82.
197. Zhang, Q., et al., *Involvement of PPAR γ in oxidative stress-mediated prostaglandin E(2) production in SZ95 human sebaceous gland cells*. J Invest Dermatol, 2006. **126**(1): p. 42-8.
198. Riserus, U., et al., *Activation of PPAR δ promotes reversal of multiple metabolic abnormalities, reduces oxidative stress and increases fatty acid oxidation in moderately obese men*. Diabetes, 2007.
199. Collino, M., et al., *Modulation of the oxidative stress and inflammatory response by PPAR- γ agonists in the hippocampus of rats exposed to cerebral ischemia/reperfusion*. Eur J Pharmacol, 2006. **530**(1-2): p. 70-80.

200. Bagi, Z., A. Koller, and G. Kaley, *PPARgamma activation, by reducing oxidative stress, increases NO bioavailability in coronary arterioles of mice with Type 2 diabetes*. *Am J Physiol Heart Circ Physiol*, 2004. **286**(2): p. H742-8.
201. Fuenzalida, K., et al., *PPAR gamma up-regulates the Bcl-2 anti-apoptotic protein in neurons and induces mitochondrial stabilization and protection against oxidative stress and apoptosis*. *J Biol Chem*, 2007.
202. Guellich, A., et al., *Role of oxidative stress in cardiac dysfunction of PPARalpha-/- mice*. *Am J Physiol Heart Circ Physiol*, 2007. **293**(1): p. H93-H102.
203. Remels, A.H., et al., *Systemic inflammation and skeletal muscle dysfunction in chronic obstructive pulmonary disease: state of the art and novel insights in regulation of muscle plasticity*. *Clin Chest Med*, 2007. **28**(3): p. 537-52, vi.
204. Ke, S., et al., *Mechanism of suppression of cytochrome P-450 1A1 expression by tumor necrosis factor-alpha and lipopolysaccharide*. *J Biol Chem*, 2001. **276**(43): p. 39638-44.
205. Tian, Y., et al., *Ah receptor and NF-kappaB interactions, a potential mechanism for dioxin toxicity*. *J Biol Chem*, 1999. **274**(1): p. 510-5.
206. Tian, Y., A.B. Rabson, and M.A. Gallo, *Ah receptor and NF-kappaB interactions: mechanisms and physiological implications*. *Chem Biol Interact*, 2002. **141**(1-2): p. 97-115.

Vita

Huiyun Shen

Date and Place of Birth: 10/29/1973, Chengdu, Sichuan, P. R. China

Education

1. **B.M.** West China University of Medical Sciences. 08/1992 – 06/1997.
Major: Preventive Medicine
2. **M.S.** Sichuan University. 08/1999 – 06/2002.
Major: Toxicology
Advisor: Prof. Yuqing Liu

Research and Professional Experience

1. Research and Teaching Assistant in the Department of Hygiene Toxicology, School of Public Health, West China Center of Medical Sciences, Sichuan University, Chengdu, Sichuan, P. R. China. 08/1999 – 06/2002.
2. Research Project Administrator Assistant in the General Office, Sichuan Provincial Center for Disease Control and Prevention, Chengdu, Sichuan, P. R. China. 7/1997 – 08/1999.

Academic Honors

1. Member of the Delta Epsilon Iota Academic Honor Society. 01/2008.
2. University of Kentucky Superfund Basic Research Program Traineeship. 07/2005 – 06/2006.
3. Kentucky Opportunity Fellowship from University of Kentucky. 07/2004 – 06/2005.
4. Research Challenge Trust Fund I Fellowship from University of Kentucky. 08/2002 – 06/2003.
5. Honored Student of the Year from West China University of Medical Sciences. 06/1997.

Publications

1. **Shen H**, Oesterling E, Stromberg A, Toborek M, MacDonald R, and Hennig B. Zinc deficiency induces vascular pro-inflammatory parameters associated with NF- κ B and PPAR signaling. *J Am Coll Nutr* (In Press).
2. **Shen H**, Arzuaga X, Toborek M, and Hennig B. (2008) Zinc nutritional status modulates expression of AhR-responsive P450 enzymes in vascular endothelial cells. *Environ Toxicol Pharmacol* 25: 197-201.
3. **Shen H**, MacDonald R, Bruemmer D, Stromberg A, Daugherty A, Li X, Toborek M, and Hennig B. (2007) Zinc deficiency alters lipid metabolism in LDL-receptor-deficient mice treated with rosiglitazone. *J. Nutr.* 137: 2339-2345.
4. Xie Z, Zhang Y, Guliaev AB, **Shen H**, Hang B, Singer B, and Wang, Z. (2005) The p-benzoquinone DNA adducts derived from benzene are highly mutagenic. *DNA Repair* 4: 1399-1409.
5. Zhao B, Xie Z, **Shen H**, and Wang Z. (2004) Role of DNA polymerase η in the bypass of abasic sites in yeast cells. *Nucleic Acids Res.* 32: 3984-3994.
6. Guo D, Xie Z, **Shen H**, Zhao B, and Wang Z. (2004) Translesion synthesis of acetylaminofluorene-dG adducts by DNA polymerase ζ is stimulated by yeast Rev1 protein. *Nucleic Acids Res.* 32: 1122-1130.